



Intensification of multiphase processes

Matthew Tailby
MPhil project 2018/2019
Supervised by Prof. Wirth



Ysgoloriaethau Sgiliau Economi Gwybodaeth
Knowledge Economy Skills Scholarships



Acknowledgements

I would first like to express my deepest thanks to Professor Thomas Wirth, for giving me the opportunity to work on this exciting project and providing guidance and help whenever I needed it. I have very much enjoyed my time in the Wirth lab.

I would also like to sincerest gratitude to everyone at Bioextractions, especially to Dr. Aled Finniear for allowing me to use their HPCCC whenever I needed it, and for giving me helpful ideas throughout the year.

I would like to extend my thanks to everyone working for KESS2, for funding my project and allowing this all to happen.

Finally, I would like to thank everyone in the Wirth Group for making the lab a fun and enjoyable environment to be in, as well as helping me whenever I needed any help.

Special thanks to Micol, Toby, Marina, Harry, Ziyue, Beth, Simon, Shaun, Donya, Nasim, Katsunori, Jakob, Nasser and Haifa. I will miss sharing a lab with you all.

Abbreviations

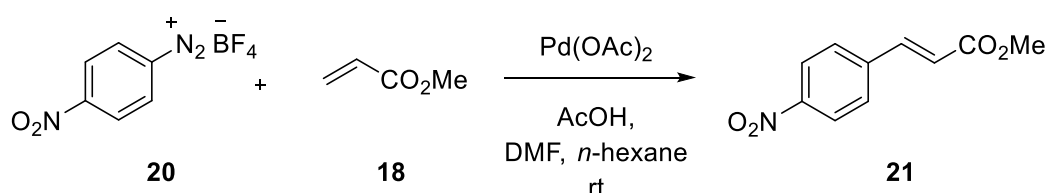
°C	Degrees Centigrade
AcOH	Acetic Acid
aq.	aqueous
Ar	Aryl
Bn	Benzyl
BPR	Back Pressure Regulator
Cat.	Catalyst
CCC	Counter Current Chromatography
ee	Enantiomeric Excess
eq.	Equivalent
EtOAc	Ethyl acetate
G	G-force
g	Gram
GC	Gas Chromatography
h	Hour
HPCCC	High Performance Counter Current Chromatography
HPLC	High Performance Liquid Chromatography
ID	Internal Diameter
IR	Infrared
L	Litre
m	Metre
MeOH	Methanol

Me	Methyl
mg	Milligrams
mmol	Millimoles
Min	Minute
M	Molar (mol/dm ³)
mol%	Mole percentage
NMR	Nuclear magnetic resonance
OAc	Acetoxy group
P	Partition coefficient
psi	Pounds per square inch
PTC	Phase transfer catalyst
PTFE	Polytetrafluoroethylene
RP	Reverse phase
rpm	Revolutions per minute
rt	Room temperature
TBAB	tetrabutylammonium bromide
<i>t</i> -Bu	<i>tert</i> -Butyl group
TLC	Thin-layer chromatography
UV	Ultraviolet
w/v	Weight/volume
X _s	Segregation Index

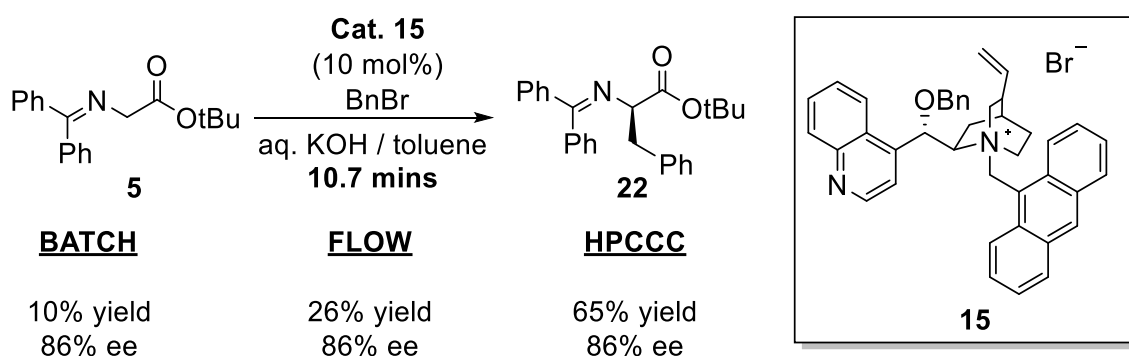
Abstract

High Performance Counter Current Chromatography (HPCCC) is a form of liquid-liquid chromatography that employs a biphasic stationary/mobile phase solvent system. The HPCCC machine consists of leads and tubing of either analytical or preparative sizes, which are spun at speeds up to 2100 revolutions per minute (rpm). The resulting velocity and acceleration caused by the spinning creates alternating zones of intense mixing and settling. Up until now, this intense mixing has only been utilised for purification purposes. In this research, biphasic reactions that have previously been limited to batch and flow chemistry, have now successfully been translated into the HPCCC machine, giving accelerated reaction times and superior yields.

A monophasic Heck reaction was successfully intensified inside the HPCCC machine, by the introduction of *n*-hexane as an inert “mixing” phase. The target product was obtained in a 69% yield after 12.5 minutes, outperforming segmented flow (64% after 27 minutes). The increase in yield and decrease in reaction time suggested a much greater mixing efficiency inside the HPCCC machine.



The phase transfer catalysed asymmetric alkylation of *N*-(diphenylmethylene)glycine *tert*-butyl ester (**5**) with benzyl bromide, using chiral catalyst (**15**) as the phase transfer catalyst was successfully intensified in the HPCCC machine.



The target product was obtained in a 65% yield after 10.7 minutes reaction time, with no reduction in enantioselectivity when compared to batch methods (86% ee). The results obtained from the HPCCC were much higher in yield than that obtained in batch (10%) and flow (26%) for the same reaction time. This clearly confirmed the superior mixing efficiency inside the HPCCC machine.

Table of contents

Abstract	v
1. Introduction	1
1.1. Counter Current Chromatography	1
1.1.1 Choosing a suitable biphasic solvent system	2
1.1.2. The HPCCC in action	4
1.2. Phase transfer catalysis	6
1.2.1. Asymmetric alkylation using chiral PTCs	6
1.2.2. Asymmetric epoxidations using chiral PTCs	9
1.2.3. Phase transfer catalysis in microreactors	11
1.3. The Heck reaction in segmented flow	13
1.4. Quantification of mixing efficiency	17
1.5. Objectives for this research project	19
2. Results and discussion	21
2.1. Phase transfer catalysis	21
2.1.1. Optimising the asymmetric alkylation reaction in flow	21
2.1.2. Preliminary attempts of optimisation in the HPCCC machine: asymmetric alkylation	24
2.1.3. Troubleshooting issues with stationary phase retention	25
2.1.4. Utilising the “premix” method in the HPCCC machine	27
2.1.5. Evaluation of a new chinchonine derived catalyst	29
2.1.6. Evaluation of the asymmetric alkylation in the HPCCC machine with the chiral catalyst (15)	32
2.1.7. Investigation of the asymmetric epoxidation of chalcone	37
2.2. The Heck reaction	40
2.2.1. Finding a suitable Heck reaction to intensify in the HPCCC machine	40

2.2.2. Investigating the diazonium Heck reaction.....	43
2.3. Quantification of the mixing efficiency inside the HPCCC.....	45
3. Conclusion	47
4. Experimental.....	49
4.1. General.....	49
4.2. Asymmetric alkylation	50
4.2.1. General batch procedure for the asymmetric alkylation of <i>N</i> - (diphenylmethylene)glycine <i>tert</i> -butyl ester.....	50
4.2.2. Flow setup and general flow procedure for the asymmetric alkylation of <i>N</i> - (diphenylmethylene)glycine <i>tert</i> -butyl ester.....	51
4.2.3. HPCCC setup and general procedure for the asymmetric alkylation of <i>N</i> - (diphenylmethylene)glycine <i>tert</i> -butyl ester.....	52
4.2.4. Characterisation of alkylation products	53
4.2.5 Synthesis of the chiral catalyst (10)	60
4.3. Heck reaction.....	62
4.3.1. HPCCC setup and general procedure for the diazonium Heck reaction	62
4.3.2. Characterisation of Heck reaction products	63
4.4. Calculation of Segregation index	64
4.4.1. Calculation of X_s - flow rate = 0.5 mL/min	64
5. References	66
6. Appendix.....	70

1. Introduction

1.1. Counter Current Chromatography

Solid-liquid chromatographic techniques, such as high performance liquid chromatography (HPLC) and flash chromatography, are well established separation techniques that are the first choice for many organic chemists. Counter current chromatography (CCC) is a form of liquid-liquid chromatography that employs a biphasic stationary/mobile phase solvent system. Despite having the words “counter current” in its name, this technique does not necessarily involve the counter current flow of two phases. CCC is a liquid chromatography technique with a support-free liquid stationary phase.¹ The use of a liquid stationary phase instead of a classic solid stationary phase such as silica has many advantages. With a liquid stationary phase, there is total recovery of sample as there is no chance of adsorption onto a solid support. Other advantages include high injection loadings, improved sample solubility (sample can be dissolved in mobile phase or stationary phase), and ease of scale up.² The main obstacle to overcome with CCC is obtaining a stable support-free stationary phase. Centrifugal forces (expressed as a multiple of gravitational force, G) are used to hold the liquid stationary phase in the column when the liquid mobile phase is pumped through it. The development of HPCCC instruments in the 1980s meant G-levels of 240 G were achievable instead of 60 G to 80 G achievable in the older machines.² This allowed for better retention of the stationary phase and faster separation times.



Figure 1: The HPCCC machine (right) connected to two HPLC pumps and a UV detector (left).

The HPCCC instrument consists of polytetrafluoroethylene (PTFE) tubes wrapped around a bobbin on a planetary gear (Figure 1). The stationary phase is pumped into these tubes until the column is full, before being spun at speeds of up to 2100 rpm. Due to the high rpm of the column and the inevitable heat production, the temperature is kept constant using a chiller unit connected to the machine. The temperature inside the machine is monitored with an inbuilt temperature probe. Upon pumping of the mobile phase, a certain amount of stationary phase is displaced (dependent on flow rate and solvent system), with the rest of the stationary phase being retained in the column due to high levels of G force present. When the mobile phase containing the analyte is pumped through the column, the velocity and acceleration caused by the spinning (2100 rpm) creates alternating zones of intense mixing and settling (Figure 2).³ Separation of the sample will occur based on an analytes partition coefficient with the stationary phase and the mobile phase. The partition coefficient is defined by the concentration of the target compound in the upper phase, divided by the concentration of the target compound in the lower phase.⁴

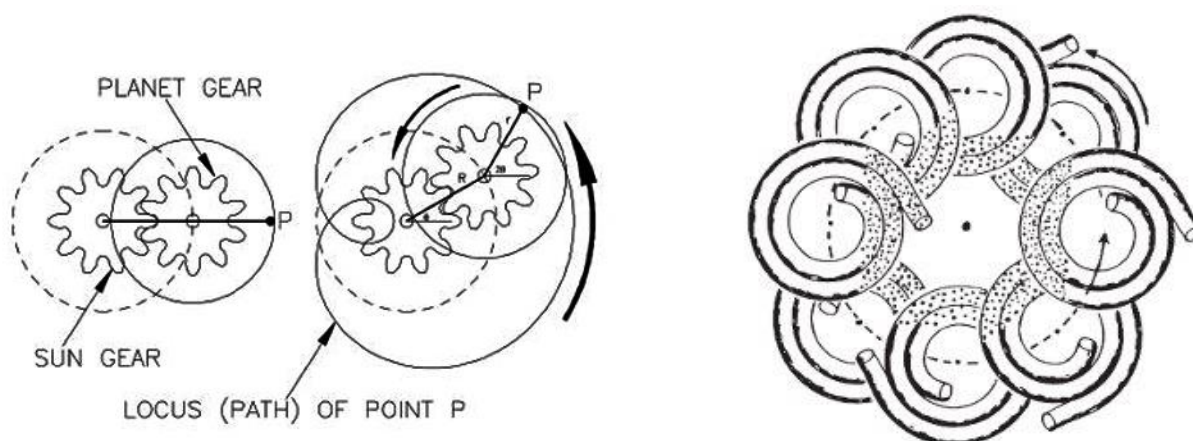


Figure 2: The planetary motion of the column (left), and the mixing (dots) and settling (clear) zones in the column (right).³

1.1.1 Choosing a suitable biphasic solvent system

The great advantage of CCC is that, in theory, any liquid mixture that forms two phases can be used. However, there are certain criteria that need to be met. For successful retention of the stationary phase in the HPCCC, it is important that both the mobile and the stationary phase have the correct physio-chemical properties.⁵ The three important physio-chemical properties that need to be considered of the pure liquids are; viscosity,

interfacial tension, and density difference between the two solvents. It has been shown that the less viscous the solvent system, the more the stationary phase is likely to be retained. This is due to a large correlation between high viscosity and long settling times. A high interfacial tension and large density difference between the two phases is also desirable for stationary phase retention.⁶

A good way of screening suitable biphasic solvent systems is to measure the settling time of the two solvent phases. This is defined as the time required for a vigorously hand-shaken solvent mixture to be completely separated into two layers. This provides a reliable numerical index for the hydrodynamic behavior of the system in the HPLCC.⁶ Solvent systems with low interfacial tension between the two phases tend to form emulsions, leading to long settling times. For stationary phase retention, a settling time of less than 30 seconds is required for mixing and separation to take place.⁴

After consideration of all these factors, the most important criteria for the solvent system is whether separation can be achieved. It is also important that the crude mixture is soluble in one of the phases. The HEMWat method (based on a progression of *n*-hexane / ethyl acetate / methanol / water solvent systems) was designed to provide a systematic process of choosing an HPLCC solvent system for separation of a wide range of organic compounds, from medium lipophilic to slightly polar.⁴

Table 1: The HEMWat volume ratios for CCC separations.

HEMWat system #	<i>n</i> -Hexane	EtOAc	Methanol	Water
-7	9	1	9	1
-6	8	2	8	2
-5	7	3	7	3
-4	7	3	6	4
-3	6	4	6	4
-2	7	3	5	5
-1	6	4	5	5
0	5	5	5	5
+1	4	6	5	5
+2	3	7	5	5
+3	4	6	4	6
+4	3	7	4	6
+5	3	7	3	7
+6	2	8	2	8
+7	1	9	1	9
+8	0	10	0	10

Solvent systems composed of *n*-hexane / ethyl acetate / methanol / water have been used to separate a variety of natural products.⁷ A helpful method for solvent system selection is known as the “shake-flask” method. This method involves dissolving a small amount of purified product / crude mixture in a biphasic system, vigorously shaking the biphasic system, and allowing equilibration to occur. The concentration of the target compounds in each layer can then be measured by UV, HPLC or GC, which can then be used to work out the partition coefficient (P). For successful HPCCC separations, the value of P should be greater than 0.4, but less than 2.5, with a P value of 1 being the optimum value for separation. A P value less than 0.4 results in a loss of peak resolution, whilst a value larger than 2.5 results in band broadening.^{4, 8}

1.1.2. The HPCCC in action

Over recent years, HPCCC has been widely used as a device for natural product isolation and separation. Koziol *et al.* were able to isolate lucidafuranocoumarin A (**1**) and bergamottin (**2**) from a crude dichloromethane extract of the plant *Peucedanum alsaticum* L.⁹ The genus *Peucedanum* is a proven source of neuroactive, drug like metabolites, that could potentially be used in the treatment of neurodegenerative disorders such as Alzheimer's or Parkinson's disease.¹⁰

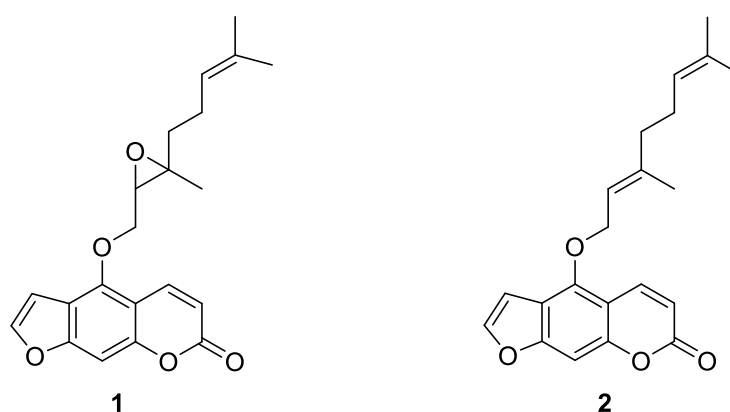


Figure 3: Structures of the natural products lucidafuranocoumarin A (**1**) and bergamottin (**2**).

The two natural products were isolated using HPCCC. A HEMwat solvent system was employed for the separation, with the most effective ratio of solvents being 3:1:3:1 (v:v:v:v heptane/EtOAc/MeOH/water). In this solvent system, the P value of compound **1** was

1.13, which falls into the optimum range of P values for successful separation. The value of compound **2** was 3.36, which falls just outside of the optimum range, however this did not affect the separation in this case. The separation of the crude extract was run on a preparative scale (400 mg - 600 mg), with compound **1** eluting between 19 and 23 minutes (2.63 mg, purity 98%) and compound **2** eluting between 46 and 54 minutes (8.82 mg, purity 96%). Lucidafuranocoumarin A (**1**) and bergamottin (**2**) both exhibited strong inhibiting effects of butyrylcholinesterase (BChE), with Lucidafuranocoumarin A (**1**) showing strong anti-seizure activity.⁹

The use of HPLCC to purify natural products has also been proven in some cases to be much more efficient and sustainable than other separation techniques. Spinosyn A (**3**) and spinosyn D (**4**) are natural products that have successfully been isolated from Spinosad, a fermentation-derived insecticide produced by the bacterium, *Saccharopolyspora spinosa*. The two natural products were isolated using HPLCC. A HEMwat solvent system was employed for the separation, with the most effective ratio of solvents being 5:2:5:2 (v:v:v:v, heptane/EtOAc/MeOH/water). The P values for spinosyn A (**3**) and spinosyn D (**4**) were 3.65 and 3.97 respectively. The separation was performed in reverse phase mode, where the aqueous solvent system acted as the mobile phase. The separation was performed on an analytical (83 mg injections), preparative (500 mg injections) and pilot scale (67 g injections). For the pilot separation, spinosyn A was collected after 90 - 120 mins (348 g, >99% purity), whilst spinosyn D was collected after 130 - 150 minutes (62.5 g, >99% purity).

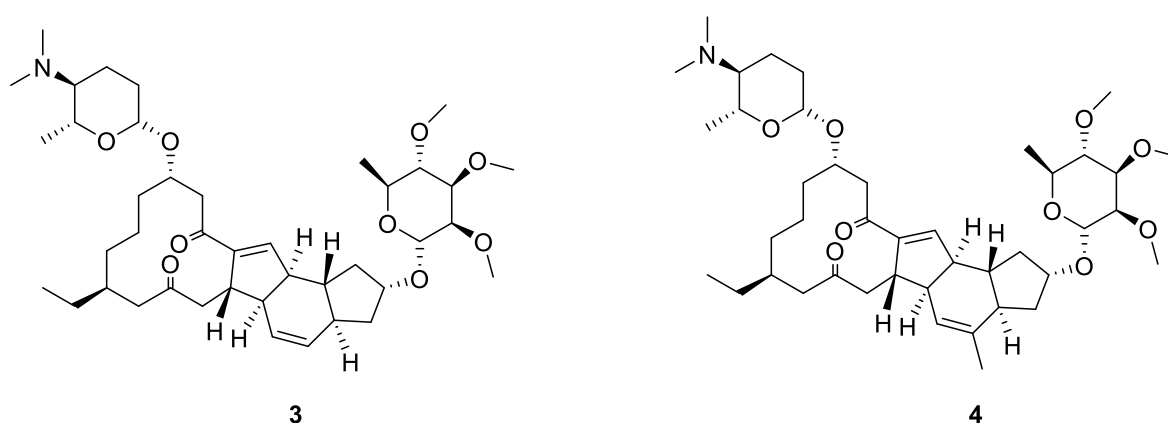


Figure 4: Structures of the natural products spinosyn A (**3**) and spinosyn D (**4**).

This separation was also performed using reverse phase HPLC and the results were compared with the results obtained with the HPLCC. On a pilot scale, the HPLCC gave

a 96% reduction on the stationary phase cost. This was attributed to the stationary phase loading, which was 11 times higher for the HPCCC in comparison to HPLC. Solvent usage was also 42% less compared to reverse phase (RP) HPLC.¹¹

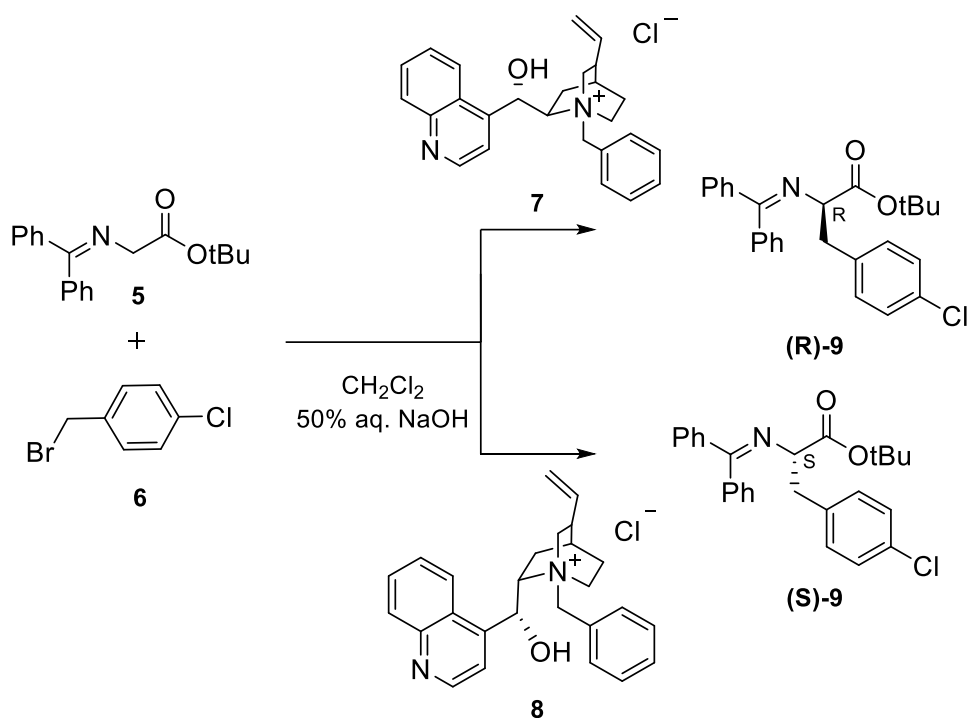
1.2. Phase transfer catalysis

Ever since its discovery in the late 1960s, phase transfer catalysis has become a well established synthetic technique used widely in both academia and industry.^{12, 13} In a biphasic reaction where the two reactants are in separate immiscible phases, the role of a phase transfer catalyst (typically a tetraalkylammonium salt or a phosphonium salt) is to facilitate the movement of the reactant into the other phase so the reaction can take place. The use of a phase transfer catalyst can increase the rate of reaction substantially. The catalytic addition of hexadecyltributylphosphonium bromide to the reaction of 1-chlorooctane with aqueous sodium cyanide was shown to increase the reaction rate by over a thousandfold.¹⁴

Due to the ease of synthesising structurally and stereochemically modifiable tetraalkylammonium ions, asymmetric phase transfer catalyst has become of great interest over the past 30 years.¹⁵ For reactions where stereocenters are formed from achiral reactants, the classical achiral PTCs (such as tetrabutylammonium bromide, TBAB) can be replaced with chiral PTCs, forming chiral products in high selectivity.¹⁵

1.2.1. Asymmetric alkylation using chiral PTCs

In 1989, *N*-(benzyl)cinchoninium chloride (**7**) was used as the chiral PTC in the asymmetric alkylation of *N*-(diphenylmethylene)glycine *tert*-butyl ester (**5**), using 4-chlorobenzyl bromide (**6**) as the electrophile and 50% aqueous KOH (w/v) as the base (Scheme 1). The alkylated product was obtained in a good yield (81%) and moderate enantioselectivity (66% ee).¹⁶



Scheme 1: The asymmetric alkylation reaction using chiral catalysts (7) and (8) - affording the R-isomer (66% ee) and the S-isomer (62% ee) respectively.

Switching the cinchonine-derived catalyst (7) to the cinchonidine-derived catalyst (8) afforded the *S*-enantiomer in a similar yield (82%) and enantioselectivity (62% ee). The mechanism for this asymmetric phase transfer catalysis reaction is well understood. The first step of the alkylation is the interfacial deprotonation of the Schiff base (5), using KOH to form the metal enolate. This metal enolate stays at the interface of the two layers. Ion-exchange of the anion with the chiral catalyst then generates a lipophilic chiral onium enolate. This step results in the enolate migrating from the interface into the organic phase, where it reacts with benzyl bromide to afford the optically active monoalkylation product (Figure 5). For high enantioselectivity, it is important that the chiral onium enolate is rapidly formed and that one of the two enantiotopic faces of the enolate are blocked. This prevents the progress of the metal enolate alkylation reaction, limiting the amount of racemic product formed. Effectively blocking one face of the chiral onium enolate will reduce the chances of the alkylation occurring at that face, controlling the stereochemistry.^{15, 17}

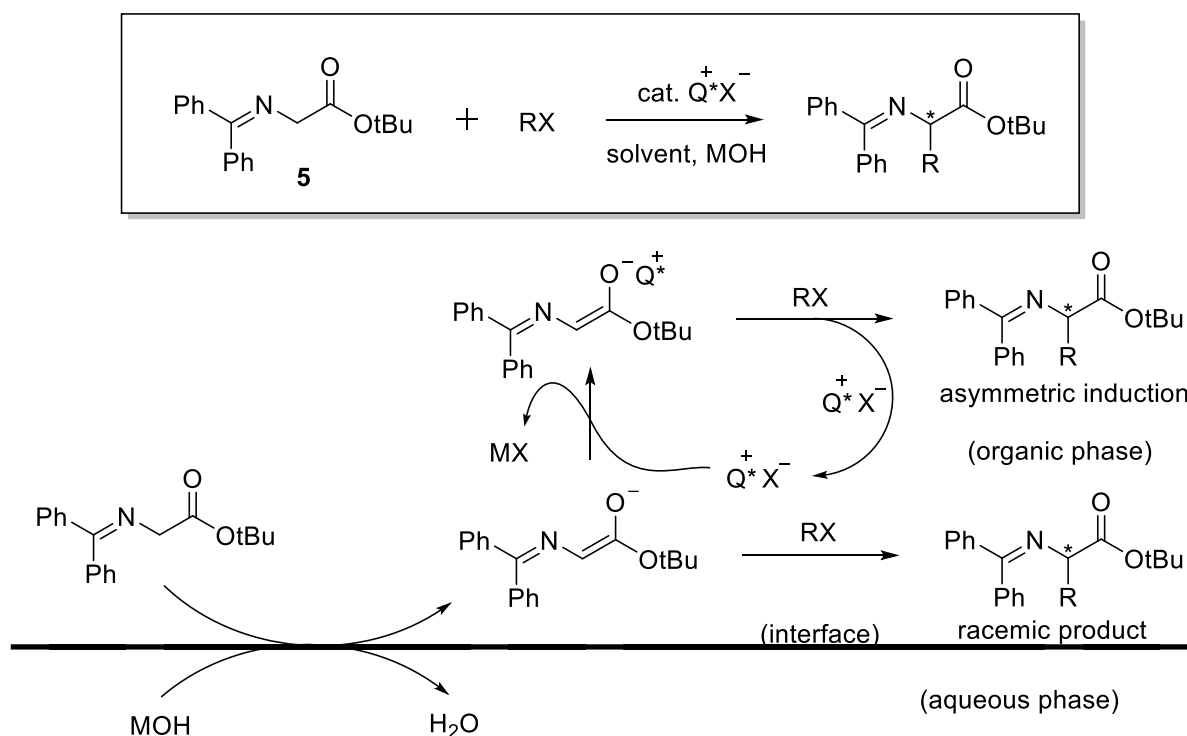


Figure 5: The interfacial mechanism for the biphasic phase transfer catalyzed asymmetric alkylation reaction.¹⁵

The asymmetric alkylation of α -amino acids using benzyl bromide as the electrophile has become the benchmark reaction for testing the enantioselectivity of new chiral PTCs. Careful fine tuning to the functional groups of the relatively inexpensive, commercially available cinchona alkaloids led to increase in enantioselectivity. Catalysts containing an *N*-anthracenylmethyl group (**10**) instead of a benzyl group increased the enantioselectivity from 62 - 66% to 89 - 91%.¹⁸ The enantioselectivity was further increased with the use of *O*-allyl-*N*-anthracenylmethyl cinchonidinium salts (**11**), decreasing the temperature (0 °C), and using aqueous CsOH as the base (94% ee).¹⁹

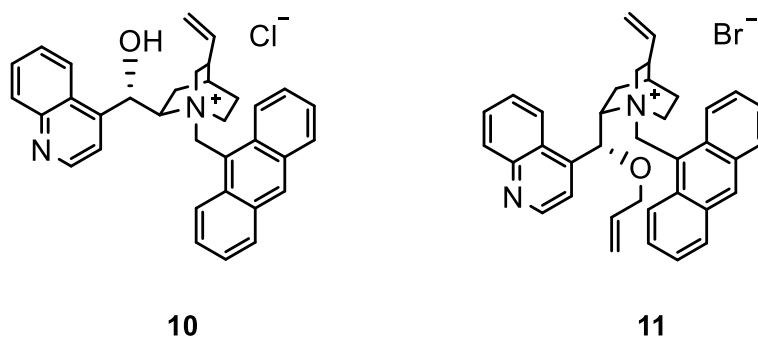


Figure 6: Cinchona-derived catalysts (**10**) and (**11**), both giving high enantioselectivities in the asymmetric alkylation reaction.

In 1999, a new class of PTC, structurally rigid, chiral spiroammonium salts (**12**) were discovered.²⁰ These bulky C_2 -symmetric phase-transfer catalysts were successfully used in the asymmetric alkylation reaction, obtaining the target product in a good yield (90%) and excellent selectivity (99% ee). It was discovered that the enantioselectivity of these catalysts was influenced heavily by the aromatic substituent shown in Figure 7. Changing the Ar group from a phenyl to a 3,4,5-trifluorophenyl (**12e**) increased the enantioselectivity from 89% to 99% ee.²⁰

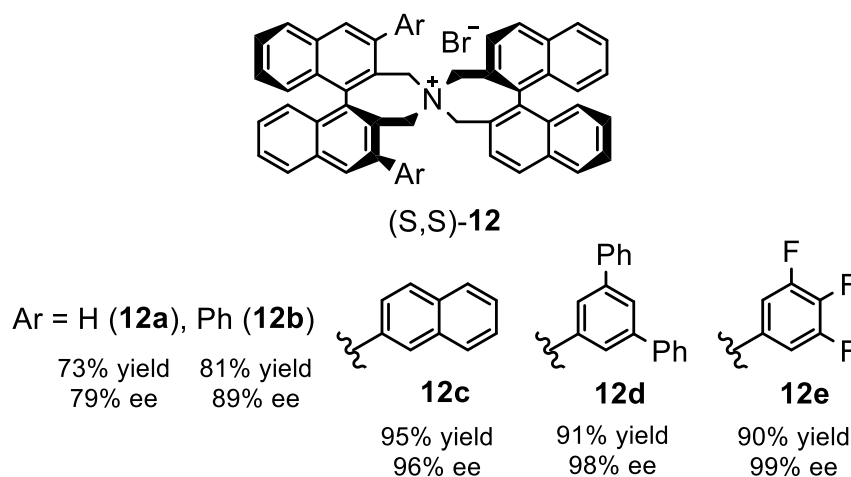
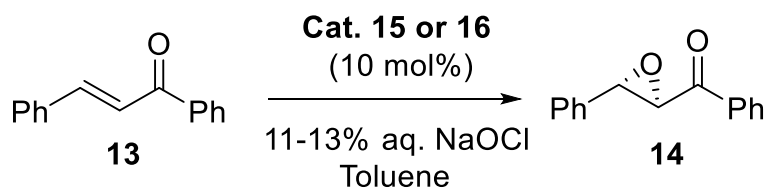


Figure 7: Chiral spiroammonium salts (**12**), providing very high enantioselectivities for the asymmetric alkylation reaction.

1.2.2. Asymmetric epoxidations using chiral PTCs

Another well established phase transfer catalysis transformation is the asymmetric epoxidation of α,β unsaturated ketones, using aqueous NaOCl as the oxidant. Common PTCs used for these reactions are also cinchona derived or binaphthyl based.²¹



Scheme 2: Asymmetric epoxidation of chalcone, using phase transfer catalysis.

In 1998, the cinchona-derived catalyst (**15**) was used for the asymmetric epoxidation of chalcone (**13**), using aqueous NaOCl as the oxidant and toluene as the solvent (Scheme

2). Using the cinchonine-derived catalyst gave a good yield (90%) with good enantioselectivity (81% ee). Switching to the cinchonidine-derived catalyst also gave a good yield (90%), and slightly enhanced enantioselectivity (86% ee).²² Axially chiral binaphthyl based PTCs (Maruoka catalysts) were designed to provide higher stereocontrol than the cinchona derived PTCs. These binaphthyl based PTCs (**16**) contain an important diarylmethanol group that is essential for catalytic ability and enantioselectivity.

The first catalyst tested (**16a**) gave a moderate yield (69%) with good enantioselectivity (66% ee). The removal of both hydroxy groups from catalyst (**16a**) proved detrimental to the reaction, giving a poor yield (3%) and a significant decrease in enantioselectivity (46% ee). Fine-tuning the electronic and steric properties of this diarylmethanol group led to the optimal catalyst (**16b**), which gave an excellent yield (99%) and excellent enantioselectivity (96% ee).²³

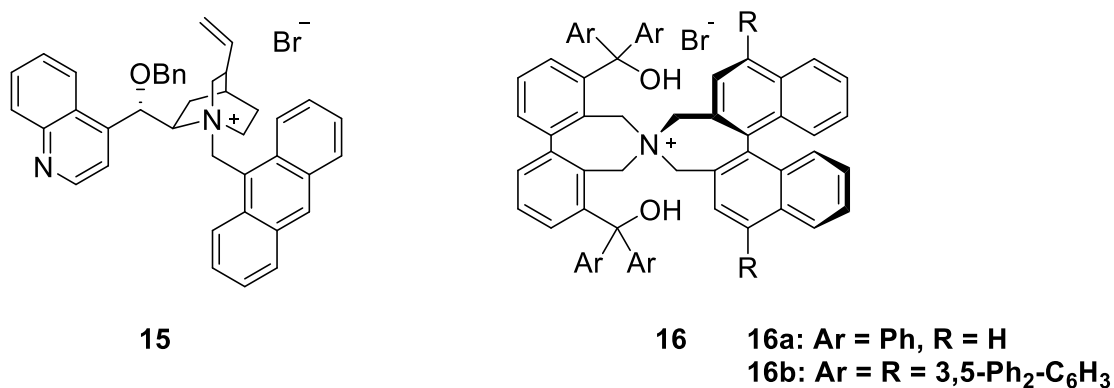


*Figure 8: Cinchona derived catalyst (**15**) and the chiral spiroammonium salts (**16**) used in the asymmetric epoxidation reactions.*

The asymmetric epoxidation of α,β -unsaturated ketones follows an extraction mechanism.¹⁴ The OCl anion migrates into the organic phase as a chiral ion pair by ion exchange with the chiral catalyst. The chiral ion pair then attacks the α,β unsaturated ketone, forming a new stereogenic center. The α,β -epoxyketone is then formed and the catalyst is regenerated, ready to re-enter the catalytic cycle. The chiral onium hypochlorite is responsible for the enantioselectivity of the final product.^{14, 15}

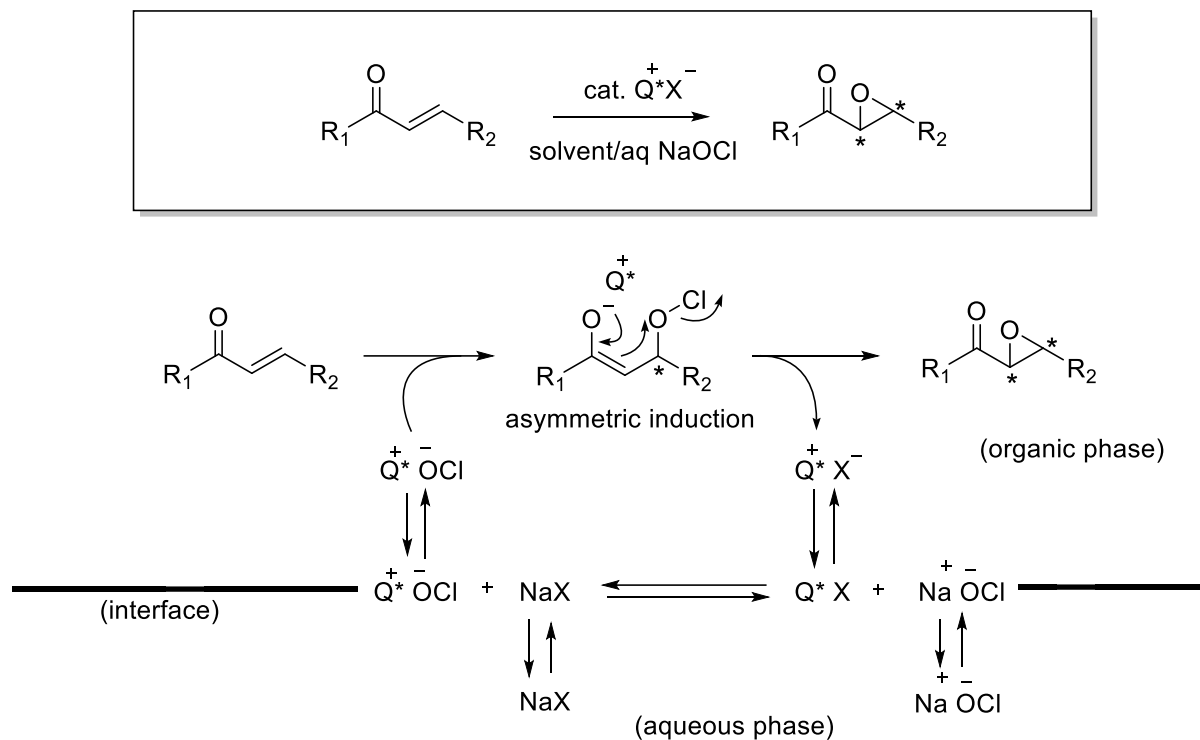


Figure 9: The extraction mechanism for the asymmetric epoxidation of α,β -unsaturated ketones.¹⁵

1.2.3. Phase transfer catalysis in microreactors

Reactions performed in microreactors have higher surface area/volume ratio, leading to a much more efficient heat and mass transfer. The efficiency of mixing is also increased, and there is the possibility of heating the reaction to temperatures that exceed the boiling point of the solvent. All these factors lead to an increase in the rate of reaction.²⁴ The use of microreactors for biphasic phase transfer catalysis has been an area of great interest in the past few decades.²⁵ This is mainly because of the potential to increase the rate of reaction using a technique known as “segmented flow”. When two immiscible phases are introduced to each other through a “T junction”, segments of alternating organic and aqueous phases are formed. One phase moves into the channel whilst the other phase is forced into the junction, cutting the flow of the first phase due to the high interfacial forces between the phases. Upon the build up of pressure, the flow is switched to the other phase. This then continues to repeat, forming a regular segmented flow stream in the process.²⁶ An internal vortex is generated in each segment by interaction of the liquid with the channel wall that allows rapid internal mixing and a continuous refreshing of the interface.²⁷

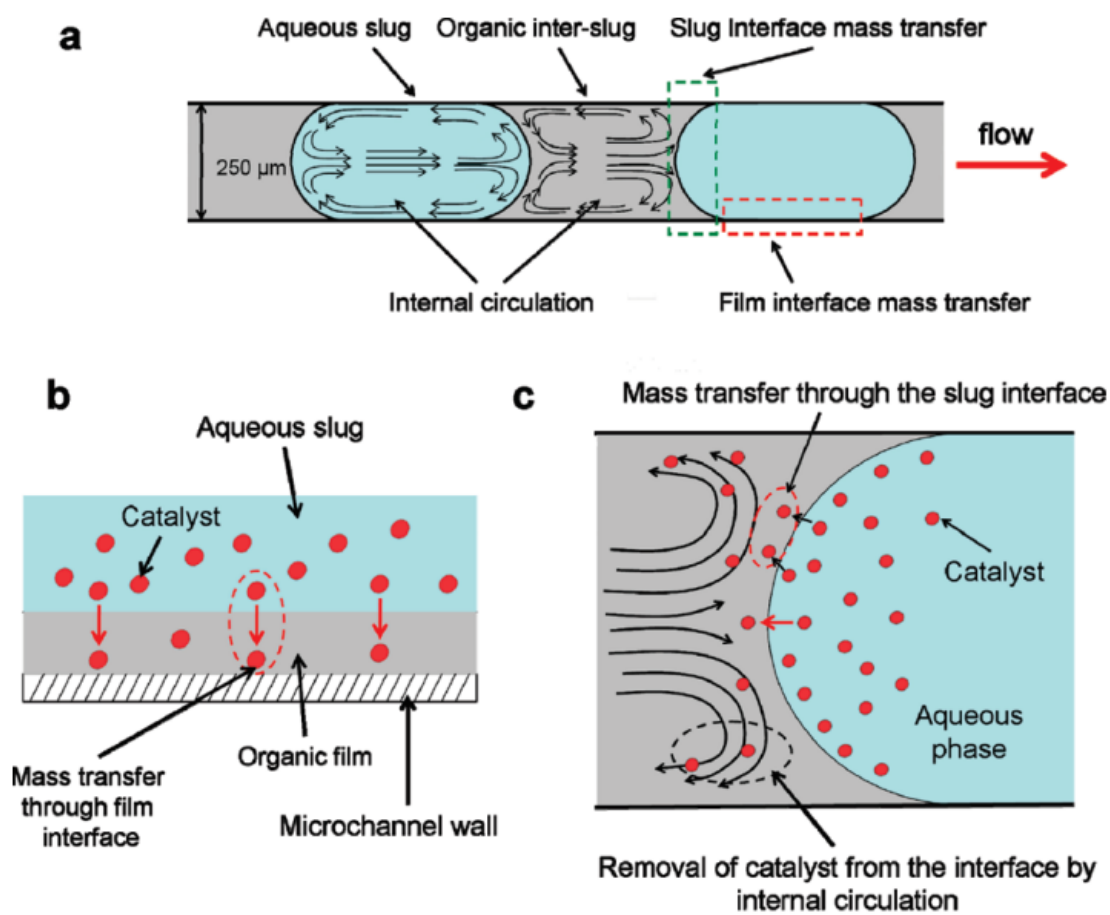


Figure 10: How phase transfer catalysis is intensified in segmented flow.²⁷

A rate limiting step in a phase transfer catalysed reaction is the ability of the catalyst to penetrate the interface between two immiscible liquid phases to be transferred into the phase where the reaction takes place. This rapid internal mixing and continuous refreshing of the interface associated with segmented flow allows quicker transfer of the PTC to the reaction phase and increases the rate of reaction.²⁸

The first example of a phase transfer catalysis reaction being intensified in a microchannel under segmented flow conditions was the alkylation of β -keto esters, using TBAB as the PTC. The reaction was performed in batch and in the microreactor (0.2 mm ID), and the results were compared. It was found that for the same reaction time (60 seconds), there was a 20% yield increase in the microreactor (57%) compared to the yield obtained in batch with vigorous stirring (37%). In all reactions performed, the microreactor gave higher yields than reactions performed in a round-bottomed flask with vigorous stirring at the same residence time.²⁹

Further highlighting the advantage of using segmented flow for phase transfer catalysis was the research performed by De Zani *et al.*³⁰ The phase transfer catalysed *O*-alkylation of substituted phenols with alkyl halides was performed in continuous segmented flow. After a 5 minute residence time (1 mm ID), the target product was obtained with full conversion of starting material. The reaction was repeated in a round bottom flask under the same conditions, and after a 5 minute reaction time, only 30% conversion was observed.³⁰

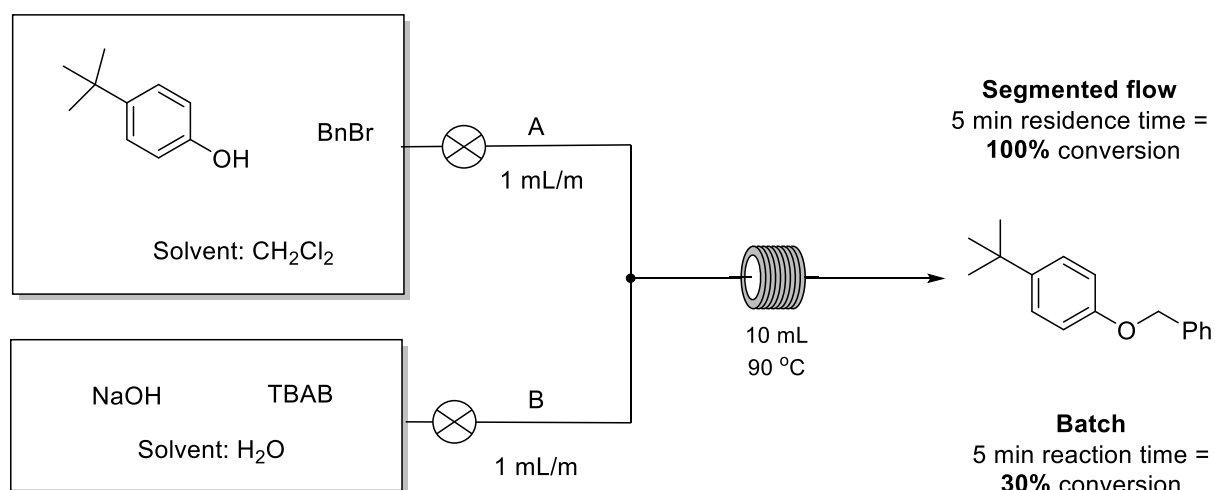


Figure 11: Segmented flow set-up for the phase transfer catalysed *O*-alkylation of substituted phenols.²⁹

There are many more examples in literature of successful intensification of biphasic phase transfer catalysis reactions in microreactors.³¹ However, as of 2019 asymmetric transformations employing chiral PTCs have not been investigated inside a microreactor.

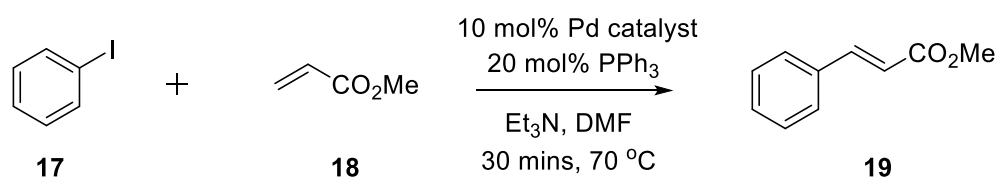
1.3. The Heck reaction in segmented flow

The Heck reaction, discovered in the early 1970s by Richard Heck, is one of the most important and widely known metal-catalysed reactions in organic synthesis.³² Due to its versatility and applicability to a wide range of substrates, the cross coupling reaction has been used in the synthesis of various natural products, such as morphine, taxol, and conidiogenone.^{33, 34, 35} The Heck reaction is generally performed using an aryl or vinyl

halide and an alkene, in the presence of a palladium catalyst. For the classical Heck reaction, a base and phosphine ligand source are also required. The general mechanism for the Heck reaction starts off with the formation of the active Pd (0) species. This undergoes oxidative addition with the aryl halide to form the organopalladium species, which coordinates to the alkene and undergoes migratory insertion. A β -hydride elimination yields the arylated alkene, which then dissociates from the palladium catalyst. Finally, the hydridopalladium catalyst undergoes reductive elimination to reform the active catalyst.³⁶

The Heck reaction is widely known as a homogeneous reaction, however a few examples of liquid-liquid biphasic Heck reactions can be found in literature. Bhanage *et al.* performed a Heck reaction using a toluene/ethylene glycol solvent mixture.³⁷ The toluene phase contained the reactants and products and the ethylene glycol phase contained the catalyst and the base, keeping the catalyst ($\text{Pd}(\text{OAc})_2$) separate from the reactant phase and the product phase. This is advantageous when it comes to catalyst recycling, as the ethylene glycol phase containing the catalyst can be reused in another reaction.³⁷

In 2008, Ahmed-Omer *et al.* discovered that the homogeneous Heck reaction between iodobenzene (**17**) and methyl acrylate (**18**), could be intensified using segmented flow conditions.³⁸ Segmentation was achieved by the introduction of an inert “mixing” face, such as decane. Although no reactants enter the inert phase, the introduction of decane creates small pockets of intense mixing in the reaction phase, in the same way discussed in section 1.2.3. This intense mixing was shown to increase the rate of the reaction of the monophasic Heck reaction.³⁸



Scheme 3: The cross coupling reaction intensified by segmented flow.

The reaction was performed in batch and laminar flow, using a variety of different palladium catalysts. For all catalysts tested, laminar flow showed an increase in percentage yield compared to the batch reaction with identical conditions. When using Pd catalysts, a black particulate was observed as a result of catalyst decomposition. Performing the reaction in batch using $\text{Pd}(\text{OAc})_2$ as the catalyst, methyl cinnamate (**19**)

was obtained in a 26% yield. This yield was increased to 53% using laminar flow. It was discovered that under laminar flow conditions, Pd(PPh₃)₄ was the best performing catalyst, forming the least amount of black particulate and obtaining the target product (**19**) in a 62% yield. Using Pd(PPh₃)₄, the reaction was performed in segmented flow, using perfluorodecalin as the inert “mixing” phase. Decane was originally used, however at higher temperatures the decane homogenised with the reaction phase (DMF), losing the segmented flow regime. Segmentation was achieved using a four way cross junction: syringe A contained a solution of iodobenzene (**17**), methyl acrylate (**18**) and triethylamine in DMF, syringe B contained a solution of metal catalyst and PPh₃ in DMF, and syringe C contained perfluorodecalin (Figure 12). Under segmented flow conditions, methyl cinnamate (**19**) was obtained in a 76% yield, an increase of 14% when compared with laminar flow.³⁸

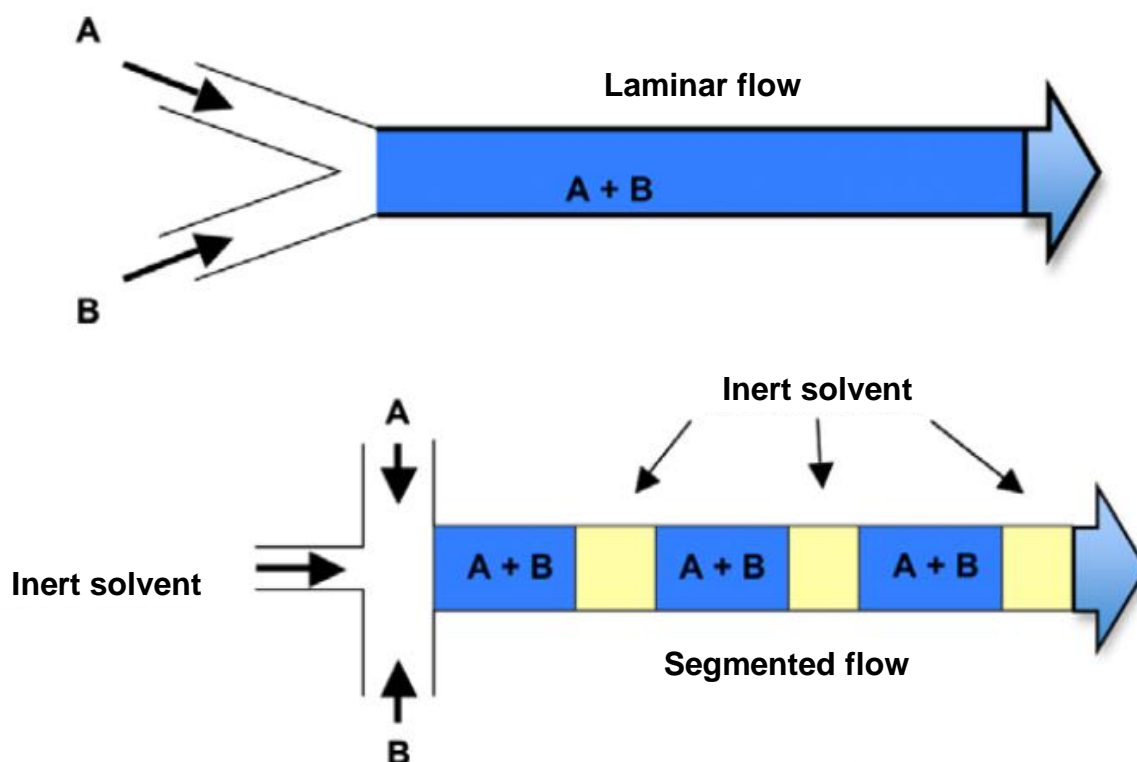


Figure 12: Laminar (top) and segmented flow (bottom) set-ups for the biphasic Heck reaction: Syringe A – iodobenzene (**17**), methyl acrylate (**18**) and triethylamine in DMF; Syringe B - metal catalyst and PPh₃ in DMF; inert solvent - perfluorodecalin.³⁷

Another homogenous reaction that was successfully intensified in segmented flow was the tandem diazonium Heck reaction between aniline and methyl acrylate (**18**). The first reaction was the *in situ* formation of the diazonium salt under acidic conditions. The

second reaction was the cross coupling reaction between the diazonium salt and methyl acrylate (**18**). The inert “mixing” phase used for this reaction was *n*-hexane.³⁸

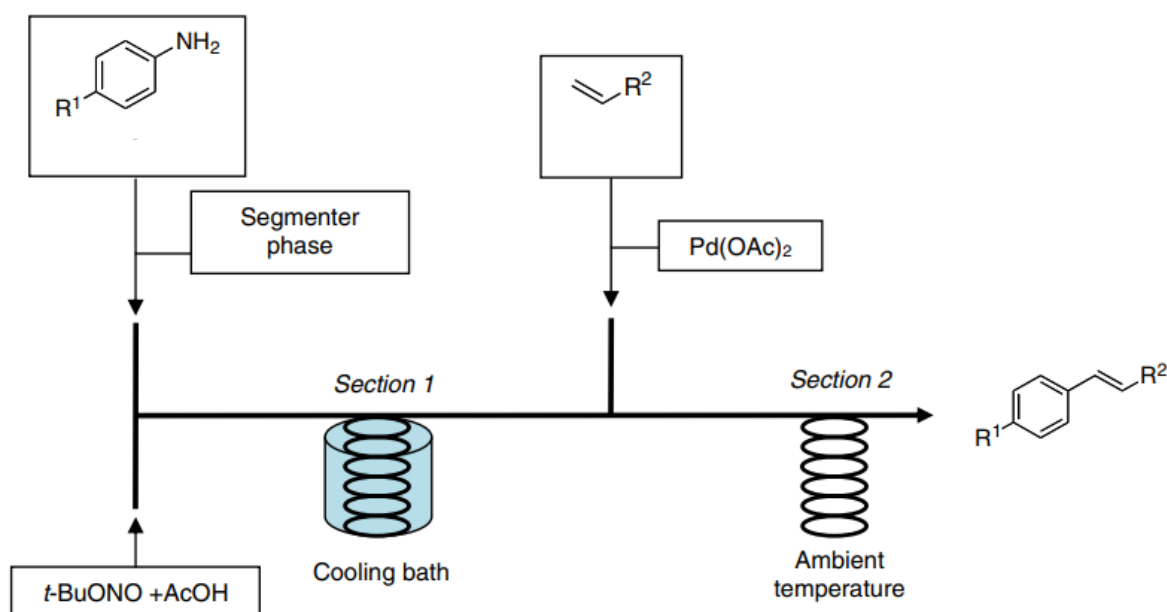
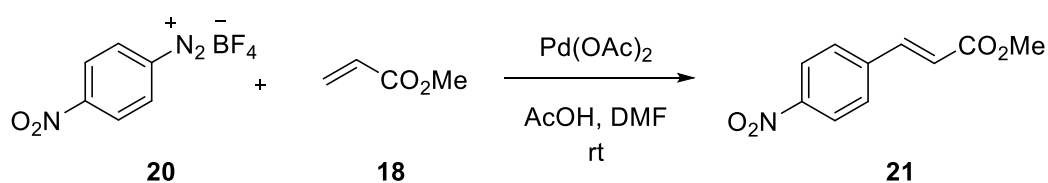


Figure 13: Segmented flow set-up for the tandem diazonium Heck reaction, using *n*-hexane as the inert “mixing” phase (segmenter phase).³⁷

Methyl cinnamate (**19**) was obtained in a moderate yield (54%). Various alkenes and aniline derivatives were tested under the same segmented flow conditions, giving good to excellent yields (62 - 90%). However, when using an aniline derivative such as *p*-methoxyaniline, the yield significantly dropped (18 - 33%). This could be rationalised by the presence of the electron donating group, which deactivated the substrate and lowered reactivity.³⁸

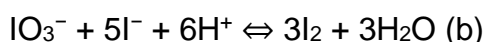
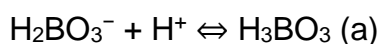
This reaction was also performed using commercially available *p*-nitrobenzenediazonium tetrafluoroborate (**20**), a stable diazonium salt that can undergo the Heck reaction in the presence of an acid. The reaction yielded similar results (64%) to those obtained using aniline (54%), meaning the *in situ* diazonium formation step in the microchannel was working efficiently.



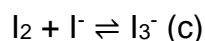
Scheme 4: Heck coupling of diazonium salt (**20**) with methyl acrylate (**18**).

1.4. Quantification of mixing efficiency

Choosing to perform reactions in flow microreactors instead of in batch has been shown to decrease reaction times significantly. This is due to many factors, one of which being an increase in mixing efficiency. The mixing efficiency of a system can be characterized and quantified using various techniques.³⁹ The most widely used characterization technique is the Villermaux-Dushman reaction.⁴⁰ The Villermaux-Dushman reaction is based on two competing reactions:



Upon the addition of aqueous acid to a premixed solution of aqueous I^- and IO_3^- in a $\text{H}_2\text{BO}_3^-/\text{H}_3\text{BO}_3$ buffer, two reactions can occur. A quasi-instantaneous protonation of H_2BO_3^- (a), and a quick (but relatively slower) redox reaction between IO_3^- , I^- and H^+ (b). In perfect mixing conditions, the acid is instantaneously consumed by the neutralisation reaction, so that no I_2 can be formed. However, if the mixing is inefficient, unreacted acid can react to form I_2 , which then is quasi instantaneously converted to I_3^- (c).



Of which the equilibrium constant K_B [L/mol] is related to the operating temperature T [K]:

$$K_B = \frac{[\text{I}_3^-]}{[\text{I}_2][\text{I}^-]} \quad \text{(eq. 1)}$$

$$\text{Log}_{10}(K_B) = \frac{555}{T} + 7.355 - 2.575 \log_{10}T \quad \text{(eq. 2)}$$

The I_3^- concentration can be measured by UV-vis spectroscopy at 353 nm, using the Beer Lambert law:

$$A = \epsilon \cdot c \cdot l \quad \text{(eq. 3)}$$

A = absorbance, c = concentration (M), ϵ = extinction coefficient (L/mol/cm), l = path length (cm).

The extinction coefficient of triiodide at 353 nm ($\epsilon_{353 \text{ nm}}$) is 26,047 L/mol/cm, whilst the path length of the cuvette was 1 cm. In order to quantify the mixing performance, the segregation index (X_s , a ratio of I_2 and I_3^- yield to the theoretical yield of $\text{I}_2 + \text{I}_3^-$ when

mixing is infinitely slow) can be calculated. X_s is equal to 0 when efficiency of mixing is perfect, and is equal to 1 in a totally segregated medium.^{40, 41}

$$X_s = \frac{Y}{Y_{ST}} \quad (\text{eq. 4})$$

$$\text{Where: } Y = \frac{4([I_2] + [I_3^-])}{[H^+]_0} \quad (\text{eq. 5})$$

$$Y_{ST} = \frac{6[IO_3^-]_0}{6[IO_3^-]_0 + [H_2BO_3^-]_0} \quad (\text{eq. 6})$$

Where Y denotes the ratio of the number of acid moles consumed by reaction (b) to the total number of acid moles, and Y_{ST} denotes the value of Y when mixing is infinitely slow. Subscript 0 denotes the initial concentration of the component in the respective solution. The Villermaux-Dushman reaction has been successfully used to evaluate the mixing efficiency in a variety of microreactors.⁴² Baccar *et al.* obtained the segregation index for a hollow fiber device over a variety of flow rates.⁴¹ Increasing the flow rate led to a decrease in X_s , proving quantitatively that mixing efficiency increased with increasing flow rate. For comparison, the segregation index was obtained for a stirred vessel (batch). The results obtained in batch ($X_s = 0.1 - 0.3$) were much larger than the results obtained in the hollow fibre device ($X_s = 0.01 - 0.001$), showing that much more efficient mixing was present inside the hollow fiber device.⁴¹

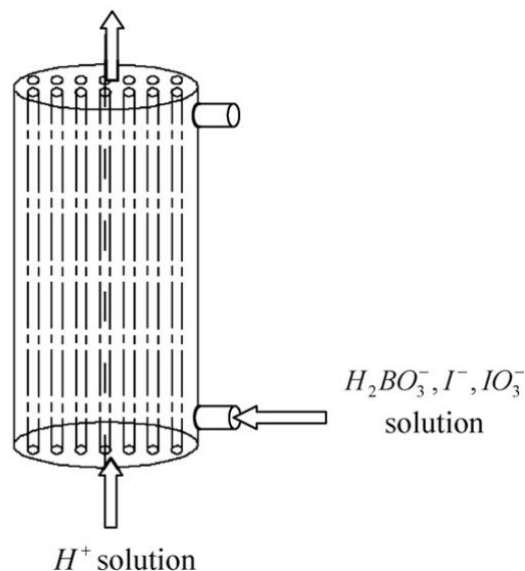


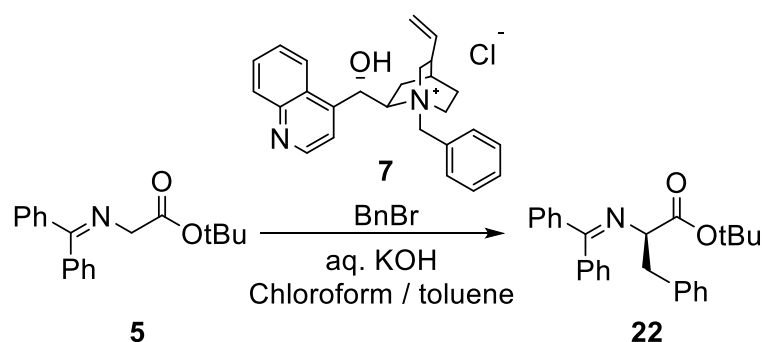
Figure 14: Setup for the Villermaux-Dushman reaction in a hollow fiber membrane device.⁴¹

1.5. Objectives for this research project

The rate of reaction for liquid-liquid biphasic reactions is directly correlated to the mixing efficiency of the system. Phase transfer catalysis has benefited greatly from flow chemistry; segmented flow has been shown to drastically reduce reaction times by increasing the mixing efficiency compared to batch.^{25, 38}

As previously discussed, inside the HPCCC machine velocity and acceleration caused by the spinning (up to 2100 rpm) creates alternating zones of very intense mixing and settling. This “mixing” characteristic has only been utilised for the separation of compounds due to their partition coefficients with the stationary phase. The aim of this research is to take known biphasic reactions and intensify these reactions in the HPCCC. It was hypothesised that due to the intense mixing present in the machine, that reaction times could be reduced further than what could be achieved in both batch and segmented flow.

Chiral phase transfer catalysis reactions will be investigated inside the HPCCC machine. The asymmetric alkylation of *N*-(diphenylmethylene)glycine *tert*-butyl ester (**5**), using benzyl bromide as the electrophile and *N*-(benzyl)cinchoninium chloride (**7**) as the chiral PTC, was chosen as the benchmark reaction to intensify (Scheme 5).

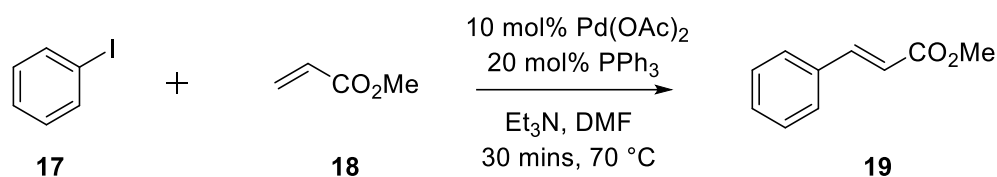


Scheme 5: The asymmetric alkylation reaction to be investigated in the HPCCC machine, using N-(benzyl)cinchoninium chloride (7) as the chiral PTC.

The reaction will first be optimised in segmented flow. Performing chiral phase transfer catalysis reactions in segmental flow has not yet been investigated. The effect of segmented flow on the enantioselectivity and yield of the reactions will be investigated as part of this novel research proposal. After optimisation in flow, the reaction will be

evaluated inside the HPCCC machine. A direct comparison between batch, segmented flow and HPCCC can then be made.

The biphasic Heck reaction will also be investigated inside the HPCCC machine. The cross coupling between iodobenzene (**17**) and methyl acrylate (**18**) will be the initial reaction of interest (Scheme 6). The reaction generally proceeds at 70 °C, however the optimum operating temperature of the HPCCC is only 30 °C. The reaction will be performed at lower operating temperatures inside the HPCCC machine to investigate whether high yields can still be obtained. The reaction will be optimised in segmented flow, and then translated to the HPCCC where a suitable method will be developed. A direct comparison between batch, segmented flow and HPCCC can then be made.



Scheme 6: The Heck reaction to be investigated inside the HPCCC machine.

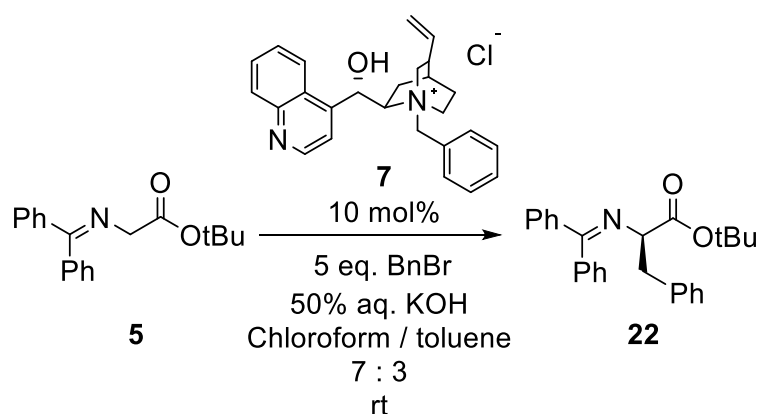
The tandem diazonium Heck reaction mentioned in **Section 1.3.1** is a Heck reaction that only requires ambient temperatures and very mild conditions. Therefore, this reaction is a suitable candidate to be investigated in the HPCCC.

2. Results and discussion

2.1. Phase transfer catalysis

2.1.1. Optimising the asymmetric alkylation reaction in flow

The general procedure for the asymmetric alkylation of *N*-(diphenylmethylene)glycine *tert*-butyl ester (**5**) employed the use of 50% aqueous KOH (w/v), a chiral PTC, and 5 equivalents of benzyl bromide (Scheme 7).⁴³ The catalyst chosen for this reaction was *N*-benzylcinchoninium chloride (**7**). The reaction was successfully performed in batch, obtaining the target product in a 62% yield, with moderate enantioselectivity (66% ee).



Scheme 7: Asymmetric alkylation of N-(diphenylmethylene)glycine tert-butyl ester (5).

The biphasic alkylation reaction was then optimised in segmented flow. Syringe A was 50% aqueous KOH solution was loaded into Syringe A, whilst a solution of the *tert*-butyl ester (**5**), benzyl bromide and the PTC (**7**) in an organic solvent was loaded into Syringe B. These two solutions were then introduced at identical flow rates (0.1 - 0.5 mL/min) using a T junction (Figure 15).

To transfer this reaction from batch to flow, it was essential that the catalyst was fully dissolved in either the organic or aqueous phase. The chiral catalyst (**7**) showed no solubility in the aqueous phase and was only sparingly soluble in the solvent system chosen for the batch reaction. This led to very low yielding results in segmented flow as sedimentation of the catalyst was visible inside the syringe (Table 2, entries 1 - 2).

The solubility of the chiral catalyst (**7**) was evaluated in a variety of solvents, with dichloromethane, chloroform and water being the only three solvents capable of fully dissolving the catalyst (**7**). The use of pure dichloromethane in biphasic asymmetric alkylation reactions was also well established.¹⁶ Switching the reaction solvent to dichloromethane led to a significant increase in the reaction yield (Table 2, entry 3). There was a small drop in enantioselectivity going from batch to flow (66% to 58%).

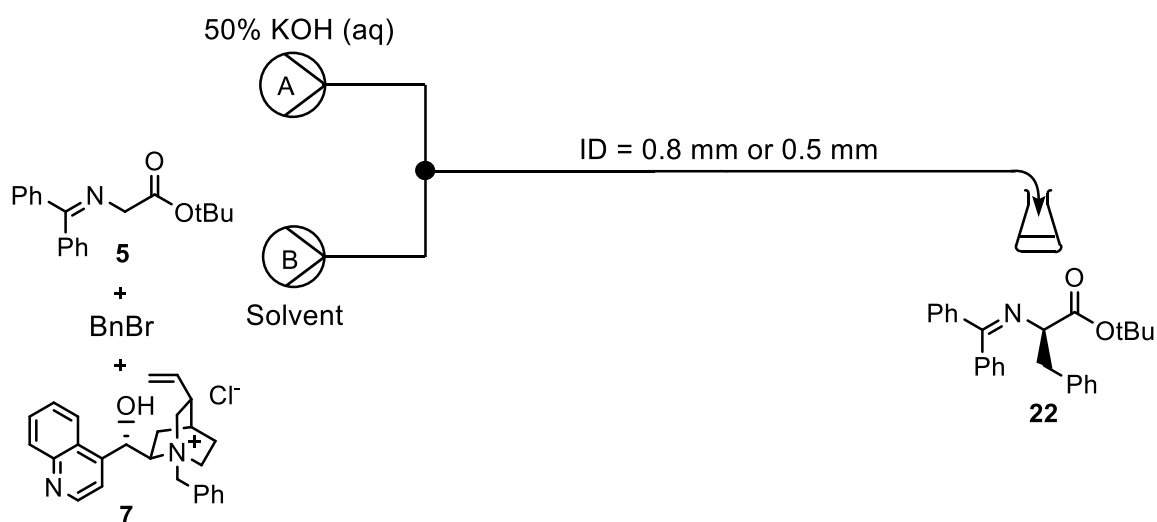


Figure 15: Segmented flow setup for the asymmetric alkylation reaction.

The effect of the internal diameter size of the PTFE tubing was also evaluated. Changing the ID from 0.8 mm to 0.5 mm also led to an increase in yield (Table 2, entry 5). Decreasing the internal diameter leads to the formation of smaller segments. These segments have a larger interfacial area, leading to more efficient mixing.^{26, 44}

As flow rate increases, mass transfer increases, leading to a larger conversion rate. However for a given length of the PTFE tubing, the residence time will be smaller and the overall reaction may be less efficient.²⁶ For a 24 m length of PTFE tubing (0.5 mm ID), the optimum flow rate was found to be 0.2 mL/min (Table 2, entry 5), giving a 73% yield in 23.5 minutes of reaction time.

The effect temperature had on the reaction was also evaluated. To heat the reaction past the boiling point of dichloromethane, a 40 psi BPR was used. Heating was achieved by submersion of the reaction coil in a water bath. At 40 °C, a big decrease in both yield and enantioselectivity was observed (Table 2, entry 8). This suggested that at higher

temperatures, catalyst degradation started to occur in the presence of KOH. It was hypothesised that cooling the reaction down in flow to 0 °C may lead to an increase in enantioselectivity, however this was not observed. Performing the reaction at 0 °C only led to a decrease in percentage yield (Table 2, entry 9). It was concluded that the optimum temperature for this reaction in flow was room temperature.

Table 2: Results obtained from the asymmetric alkylation reaction performed in segmented flow.

No.	Flow rate (mL/min)	Reaction volume (mL)	Residence time (min)	ID (mm)	Temp. (°C)	Solvent	Yield *	ee (%)
1	0.2	2.5	12	0.8	rt	Toluene / CHCl ₃ - 7:3	1	-
2	0.1	3.6	36	0.8	rt	Toluene	8	-
3	0.3	8.9	29	0.8	rt	CH ₂ Cl ₂	53	58
4	0.2	8.9	43	0.8	rt	CH ₂ Cl ₂	52	59
5	0.2	4.7	23.5	0.5	rt	CH ₂ Cl ₂	73	56
6	0.3	4.7	15.7	0.5	rt	CH ₂ Cl ₂	69	50
7	0.1	4.7	47	0.5	rt	CH ₂ Cl ₂	65	52
8	0.2	4.7	23.5	0.5	40	CH ₂ Cl ₂	22	48
9	0.2	4.7	23.5	0.5	0	CH ₂ Cl ₂	15	56
10	0.25 ⁺	4.7	18.8	0.5	rt	CH ₂ Cl ₂	52	59
11	0.2	6.7	33.4	0.5	rt	CH ₂ Cl ₂	59	56
12	0.25 ⁺	6.7	27	0.5	rt	CH ₂ Cl ₂	69	59
13	0.32	6.7	21	0.5	rt	CH ₂ Cl ₂	77	56
14	0.4	6.7	17	0.5	rt	CH ₂ Cl ₂	47	52
15	0.5	6.7	13.4	0.5	rt	CH ₂ Cl ₂	37	52

* yield determined by quantitative ¹H NMR, using 1,3,5-trimethoxybenzene as an internal standard. ⁺ Pump A flow rate = 0.15 mL/min, Pump B flow rate = 0.10 mL/min.

Ahmed-Omer *et al.* found that increasing the flow rate of the aqueous phase compared to the organic phase generated smaller organic segments, leading to an increase in

reaction rate.²⁶ The flow rate of the aqueous phase was increased to 0.15 mL/min, whilst the organic phase remained at 0.1 mL/min (Table 2, entries 10 and 12), however, no increase in reaction rate was observed. The length of PTFE tubing was extended by a further 10 meters (Table 2, entries 11 - 15), so higher flow rates could be reached whilst maintaining similar residence times (20 - 30 minutes). The optimum conditions for this reaction employed a flow rate of 0.32 mL/min, giving a residence time of 21 minutes. The product was obtained in a 77% yield, with an ee value of 56% (Table 2, entry 13). Increasing the flow rate any more than this led to lower yields (Table 2, entries 14 - 15).

2.1.2. Preliminary attempts of optimisation in the HPCCC machine: asymmetric alkylation

After successful optimisation of the asymmetric alkylation in flow, the next step was to transfer and optimise this reaction in the HPCCC. As with flow, it was important that the chiral catalyst (**7**) was soluble in one of the phases. Dichloromethane was chosen as the solvent as the chiral catalyst (**7**) was fully soluble at 0.005 M and gave the best yields in flow. To perform the reaction in the HPCCC, 50% aqueous KOH was used as the stationary phase and dichloromethane was used as the mobile phase. The reactants and chiral catalyst (**7**) were soluble in dichloromethane and so could be injected into the machine after equilibration of the stationary phase.

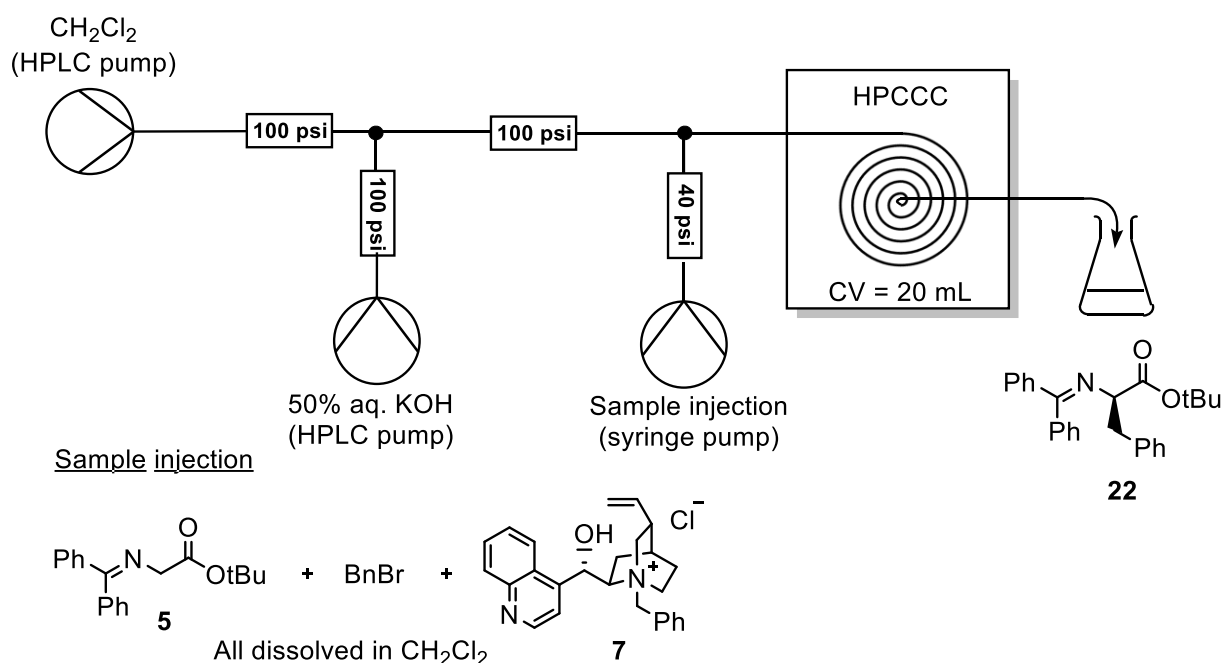


Figure 16: initial HPCCC setup for the asymmetric alkylation reaction.

However, upon pumping of the mobile phase, no stationary phase was retained in the column. This was repeated three times, and in all three attempts, the stationary phase could not be retained. For retainment of the stationary phase in an HPCCC, a biphasic solvent system with a density difference greater than 0.1 is desirable.⁴⁵ Any lower than this threshold and emulsions will form between the two layers and no stationary phase will be retained. In this biphasic solvent system, dichloromethane (density = 1.33 g/cm³) and 50% aqueous KOH (density = 1.51 g/cm³) were used.^{46, 47} There is a 0.18 g/cm³ difference between the densities of these two solvents, which suggests that stationary phase retention would be possible inside the HPCCC machine. However, mixing these two solvent mixtures in a measuring cylinder showcased how emulsions formed between the layers. The settling time of the solvent system was measured to be over 5 minutes, which was too high for use in the HPCCC (<30 seconds required).⁴

2.1.3. Troubleshooting issues with stationary phase retention

As the chiral catalyst (**7**) was only soluble in dichloromethane, chloroform and water, alternative choices for solvent systems were sparse. Ideally the catalyst (**7**) would be dissolved in the aqueous phase, however at 50% aqueous KOH this was not possible. To overcome this issue, the concentration of KOH was lowered from 50% to 25%, where the catalyst (**7**) was able to fully dissolve in the aqueous phase. The settling time between 25% aqueous KOH and dichloromethane was measured to be 270 seconds, which was too slow for use in the HPCCC. The settling time between 25% aqueous KOH and toluene was only 10 seconds. For this reason, toluene was chosen as the solvent for this reaction.

Table 3: The effects of decreasing the concentration of KOH in segmented flow.

No.	Flow rate (mL/min)	Residence time (min)	% KOH	Temp (°C)	Solvent	Yield* (%)
1	0.2	23.5	10	rt	Toluene	Trace
2	0.2	23.5	25	rt	Toluene	7
3	0.3	22.3	25	rt	Toluene	7

** yield determined by quantitative ¹H NMR, using 1,3,5-trimethoxybenzene as an internal standard*

It was hypothesised that decreasing the concentration of KOH would not affect the reaction, since the base was still in excess, however performing this reaction in flow only yielded trace amounts of product (Table 3).

Toluene would be a suitable organic solvent for optimising in the HPCCC due to the large density difference ($>0.6 \text{ g/cm}^3$) and quick settling time ($<15 \text{ s}$) between the biphasic solvents. However, the chiral catalyst (**7**) is insoluble in toluene which makes optimising in flow and in the HPCCC machine almost impossible. When using toluene as the solvent in the batch reaction, upon the addition of 50% aqueous KOH the enolate of the *tert*-butyl ester will form. The PTC will coordinate to the enolate and the enolate will be pulled deep into the organic layer.⁴⁸ When this occurs, the catalyst fully dissolves in the toluene. The reaction was reattempted in flow using toluene as the solvent. However, to get the catalyst to dissolve in toluene, a small amount of 50% aqueous KOH was added to a mixture of the *tert*-butyl ester (**5**) and the catalyst (**7**) in toluene and stirred for 5 minutes. After a homogeneous solution was observed, the 50% aqueous KOH was removed using a separating funnel, benzyl bromide was added, and the organic phase was loaded into syringe B. Syringe A was loaded with 50% aqueous KOH and the two solutions were introduced at identical flow rates using a T junction (Figure 17).

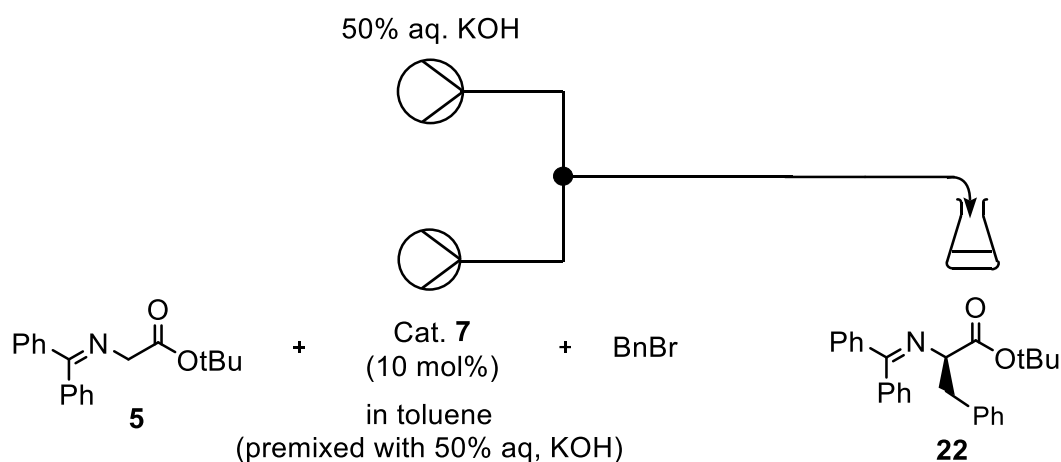


Figure 17: Revised segmented flow setup, achieving catalyst dissolution by the “premix” method.

Table 4: Results from the revised segmented flow reaction, utilising the “premix” method.

No.	Flow rate (mL/min)	Residence time (min)	Temp (°C)	Solvent	Yield * (%)	ee (%)
1	0.2	23.5	rt	Toluene	26	63
2	0.2	23.5	rt	Toluene / Chloroform 7:3	33	66
3	0.2	23.5	rt	THF	43	45

* yield determined by quantitative ¹H NMR, using 1,3,5-trimethoxybenzene as an internal standard

To make sure no background reaction was occurring in the syringe, a syringe filled with the “premixed” solution was left at room temperature for 30 minutes. This solution was analysed by ¹H NMR, which showed no product had formed.

For a residence time of 23.5 minutes, the target product was obtained in a 26% yield (Table 4, entry 1). A toluene / chloroform solvent system was evaluated, where a small increase in the yield (33%) and enantioselectivity (66% ee) was observed (Table 4, entry 2). Using this “premix method” led to a higher enantioselectivity when compared to the results obtained with dichloromethane. This was most likely because of the formation of the chiral enolate before the addition of the benzyl bromide. The reaction was performed using THF as the solvent, and although a slight increase in yield was observed, the enantioselectivity dropped to 45% (Table 4, entry 3). The reason for this drop in enantioselectivity is thought to be due to the coordinating properties of THF, where it could possibly coordinate with the catalyst and prevent it from coordinating to the enolate.

2.1.4. Utilising the “premix” method in the HPCCC machine

This “premix” methodology was transferred over to the HPCCC. 50% aqueous KOH was added to a mixture of the *tert*-butyl ester (**5**) and the catalyst (**7**) in toluene (3 mL) and stirred for 5 minutes. After a homogeneous solution was observed, the 50% aqueous KOH was removed, the benzyl bromide was added and the sample was injected immediately into the HPCCC machine.

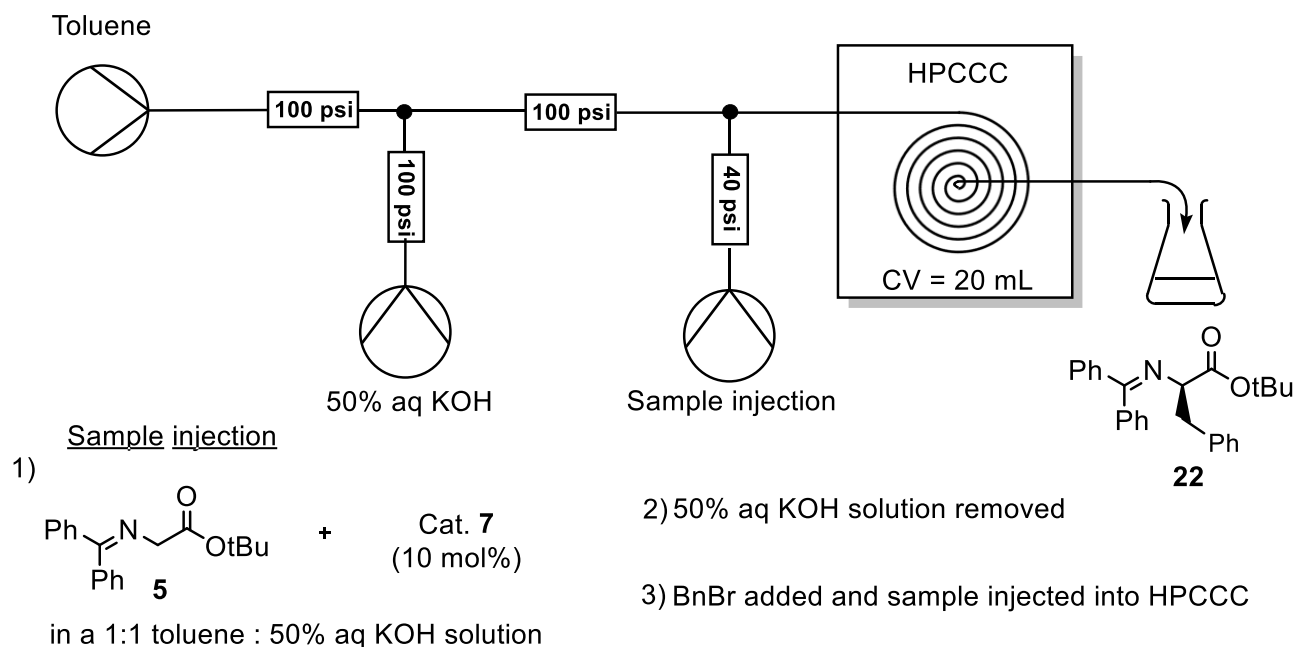


Figure 18: Revised HPCCC setup, achieving catalyst dissolution by the “premix” method.

Table 5: Results obtained from the HPCCC machine, utilising the “premix” method.

No.	Flow rate (mL/min)	Stationary phase retained (mL)	Residence time (min)	Conc of tert-butyl ester (5) injected (M)	Temp (°C)	Yield * (%)	ee (%)
1	0.3	14	47	0.07	22	38	63
2	0.5	14	30	0.07	22	38	-
3	0.7	12	17	0.07	25	38	-
4	0.9	14	16	0.07	22	38	60
5	0.2	8	40	0.14	25	50	63
6	0.7	8	12	0.14	25	54	65
7	0.7	8	12	0.2	25	45	-

* yield determined by quantitative ^1H NMR, using 1,3,5-trimethoxybenzene as an internal standard

Toluene / chloroform (7:3) solvent systems were investigated, as well as toluene / dichloromethane (7:3) solvent systems, however no stationary phase was retained for

either systems. Using pure toluene as the mobile phase allowed a large amount of stationary phase to be retained (40 - 70 %). The effect of flow rate was evaluated in the first set of experiments (Table 5, entries 1 - 4). Various flow rates were tested, however no pattern was observed. In the second set of experiments (Table 5, entries 5 - 6), increasing the concentration of the *tert*-butyl ester (**5**) led to an increase in percentage yield, and the product was obtained in a 54% yield after 12 minutes. The enantiomeric excess remained constant over various flow rates. Increasing the *tert*-butyl ester (**5**) concentration further than 0.14 M led to a decrease in yield (Table 5, entry 7).

Interestingly, entries 1, 2 and 4 (Table 5) were performed successively without replacement of the stationary phase. This showed that the stationary could be reused for these reactions without the need to replace and re-equilibrate it (a wasteful and timely process). The sample could be injected 3 times without any significant decrease in yield. Entries 5, 6 and 7 were also performed successively without replacement of the stationary phase.

2.1.5. Evaluation of a new cinchonine derived catalyst

Due to high stationary phase retention observed between toluene and the aqueous phase, the focus of further asymmetric alkylations involved the use of toluene as the organic phase. However, the chiral catalyst (**7**) was insoluble in toluene. Therefore, the use of a different chiral catalyst was investigated. It was suggested that the introduction of more lipophilic functional groups to cinchonine (**23**) would increase the solubility of the catalyst in toluene.

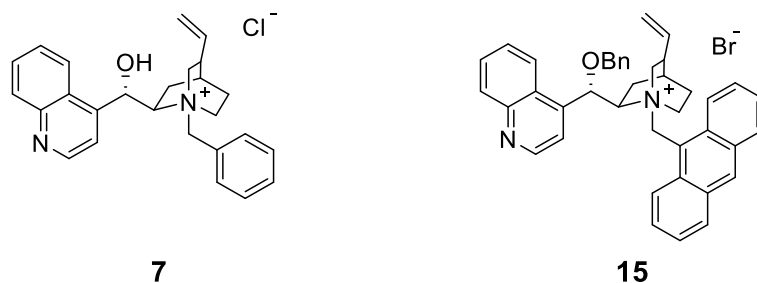
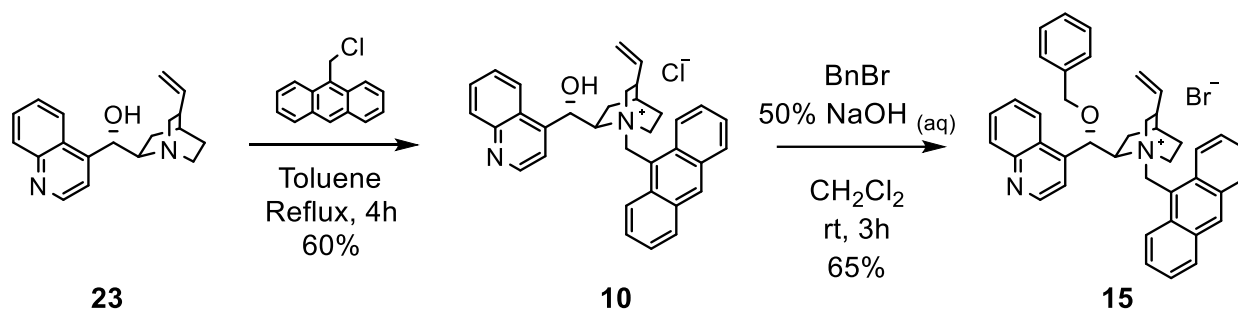


Figure 19: The previously used chiral catalyst (**7**) and the new chiral catalyst (**15**).

The cinchonine derived catalyst **15** was reported in literature. This catalyst was used to catalyse the asymmetric epoxidation of chalcone, using aqueous NaOCl as the oxidant.

The organic solvent used for this reaction was toluene. This new catalyst (**15**) contained an *N*-anthracene functional group, replacing the *N*-benzyl group in catalyst (**7**). The new catalyst also contained an *O*-benzyl group, adding to the lipophilicity of the catalyst. The new catalyst was easily synthesised from cinchonine over 2 steps in 39% yield as shown in Scheme 8.



Scheme 8: The two-step synthesis of the chiral catalyst 15.

The solubility of catalyst **15** in toluene was investigated. Upon gentle heating and sonication the catalyst was able to be fully dissolved in toluene at 0.003 M.

The asymmetric alkylation reaction using chiral catalyst **15** had not previously been reported in literature. The reaction was performed in batch so the enantioselectivity could be determined. The reaction was performed at room temperature, using 10 mol% of catalyst, obtaining the target product in a good yield (62%) with high enantioselectivity (87% *ee*).

The next step was to perform the reaction under segmented flow conditions. The chiral catalyst (**15**), *N*-(diphenylmethylene)glycine *tert*-butyl ester (**5**), and benzyl bromide were dissolved in toluene, and loaded into syringe B, whilst 50% aqueous KOH was loaded into syringe A (Figure 20).

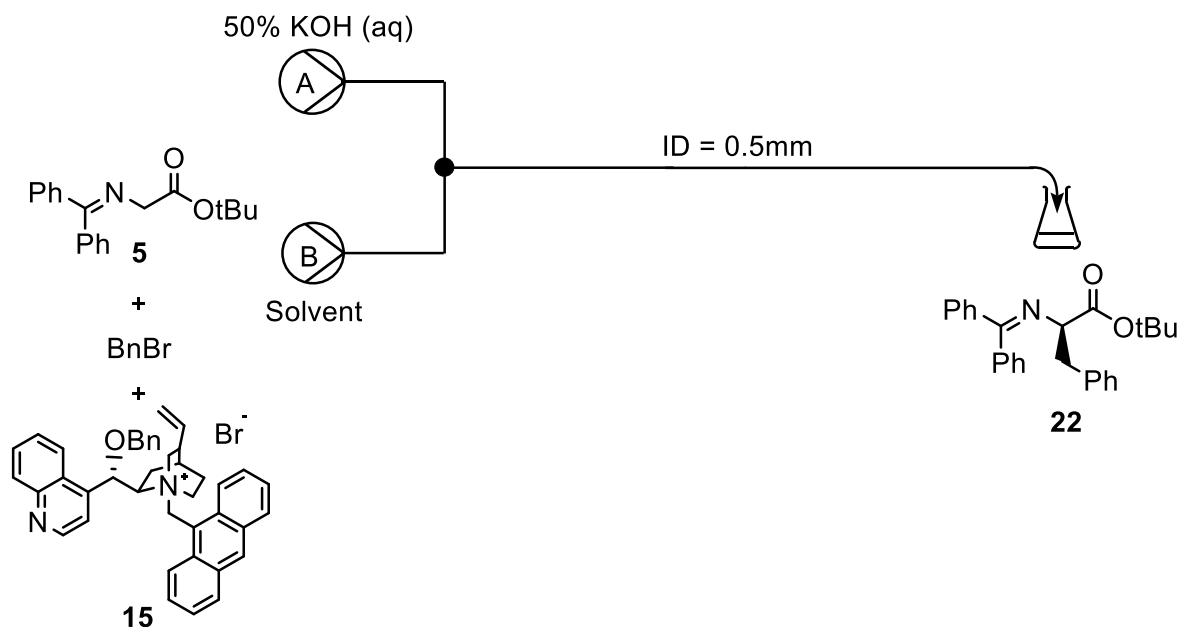


Figure 20: Segmented flow setup using chiral catalyst **15**.

Table 6: Results obtained in segmented flow using chiral catalyst **15**.

No.	Flow rate (mL/min)	ID (mm)	Residence time (min)	Catalyst (mol%)	Yield* (%)	ee (%)
1	0.2	0.5	23.5	5	42	82
2	0.16	0.5	29	5	36	82
3	0.2	0.5	23.5	10	50	89

* yield determined by quantitative ^1H NMR, using 1,3,5-trimethoxybenzene as an internal standard

The reaction was performed at both 5 mol% and 10 mol% of catalyst (**15**), with 10 mol% found to be optimum catalyst amount (Table 6, entry 3). Increasing the catalyst amount further than 10 mol% was not possible due to solubility issues with the catalyst. After a residence time of 23.5 minutes, the target product was obtained in a moderate yield (50%) and high enantioselectivity (89% ee). Performing the reaction in flow saw no drop in enantioselectivity when compared to batch.

2.1.6. Evaluation of the asymmetric alkylation in the HPCCC machine with the chiral catalyst (15)

After testing catalyst **15** in the asymmetric alkylation reaction under segmented flow conditions, the reaction was attempted in the HPCCC machine. For the first set of reactions, the amount of catalyst used was 5 mol%. Increasing the flow rate from 0.4 mL/min to 0.7 mL/min saw an increase of the yield (Table 6, entries 1-2) however this yield was not satisfactory. Increasing the catalyst loading to 10 mol% saw an increase in both percentage yield and enantiomeric excess. The temperature of the HPCCC machine was maintained between 20 - 25 °C, depending on external factors.

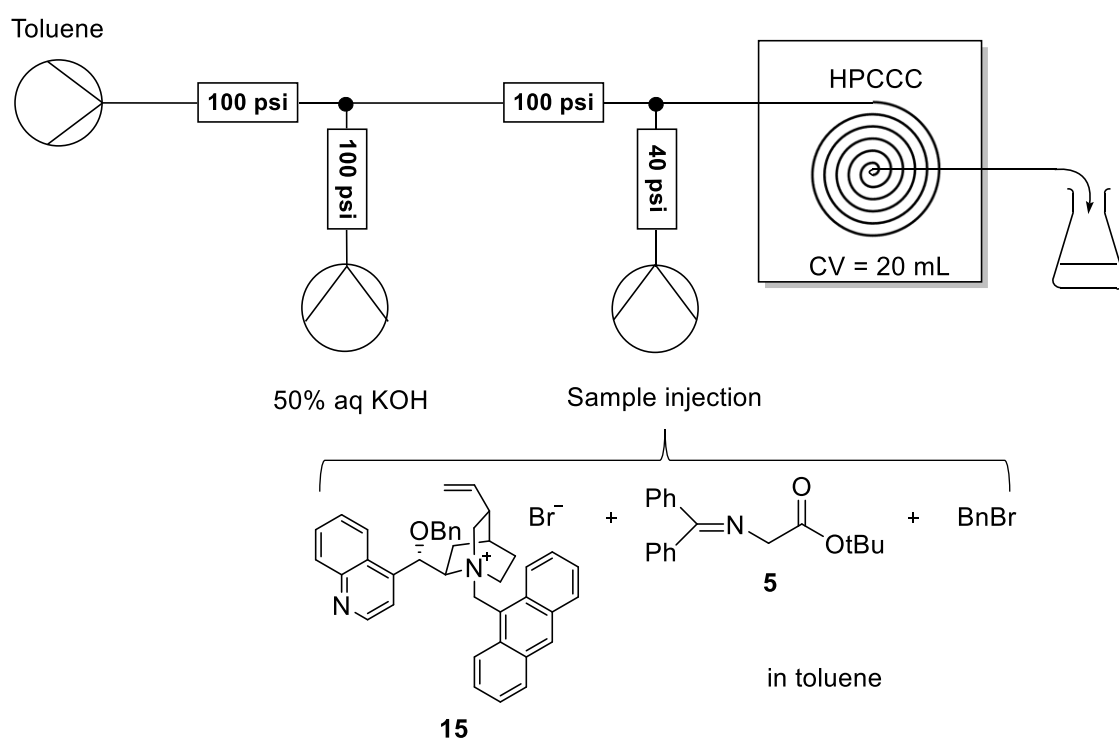


Figure 21: HPCCC setup using the chiral catalyst (**15**).

The effect of flow rate was evaluated between the range of 0.4 - 1.0 mL/min. Up until 0.7 mL/min, an increase in percentage yield was observed. However, exceeding this flow rate resulted in a decrease in yield. These results suggest that increasing the flow rate increases the efficiency of mixing in the HPCCC. This is a well-established phenomenon observed in both laminar flow and segmented flow chemistry.⁴⁹

Table 7: Results obtained in the HPCCC over a range of different flow rates using the chiral catalyst (**15**).

No.	Flow rate (mL/min)	Stationary phase retained (mL)	Residence time (min)	Catalyst (mol%)	Temp (°C)	Yield * (%)	ee (%)
1	0.4	12.9	17.7	5	25	18	80
2	0.7	15	7.1	5	25	33	80
3	0.4	16.6	10	10	20	62	88
4	0.5	14.8	10.4	10	25	61	86
5	0.6	13.8	10.3	10	25	68	87
6	0.7	12.5	10.7	10	20	73	87
7	0.8	9.6	13	10	25	57	86
8	0.9	5.4	13	10	25	31	86
9	1.0	6.1	14	10	22	53	87

* yield determined by quantitative ¹H NMR, using 1,3,5-trimethoxybenzene as an internal standard

Increasing the flow rate further than 0.7 mL/min led to a large amount of stationary phase being lost from the column during equilibration, leading to a decrease in the percentage yield. There was no change in enantioselectivity performing the reaction in batch and in the HPCCC machine. The flow rate had no effect on the enantioselectivity. The enantiomeric excess remained constant from 0.3 mL/min to 1.0 mL/min. It was concluded that 0.7 mL/min was the optimum conditions for the asymmetric alkylation reaction using benzyl bromide as the electrophile. The result for entry 6 was repeated, achieving similar results (75% NMR yield, 87% ee). This showed that the reaction was reproducible. After purification, the product for this reaction was isolated in a 65% yield. The reactants were injected twice over the space of 30 minutes, without replacement of the stationary phase. A negligible decrease in the yield was observed (1st injection = 72%, 2nd injection = 69%), and the enantioselectivity remained the same (86% ee), showcasing the reusability of the stationary phase.

The results obtained in the HPCCC gave a higher yield in a shorter amount of time when compared to batch and segmented flow. To be able to make a direct comparison between batch, segmented flow, and the HPCCC, the reaction was repeated in batch and flow, using identical reaction conditions (Figure 22).

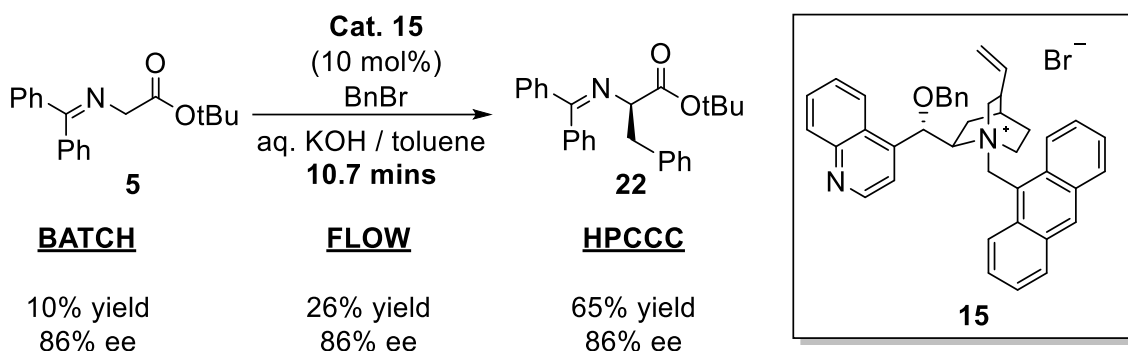


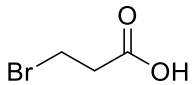
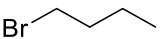
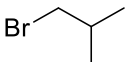
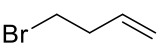
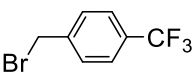
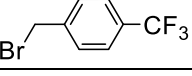
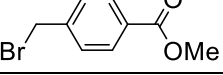
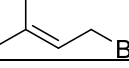
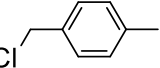
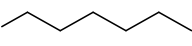
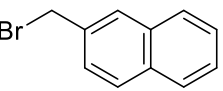
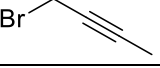
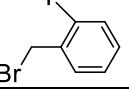
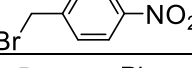
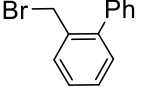
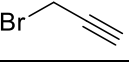


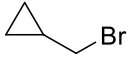
Figure 22: Direct comparison between batch, flow, HPCCC for performing the asymmetric alkylation reaction.

The batch reaction was stirred at 1500 rpm for 10.7 minutes, using the same amounts of reagents as the HPCCC reaction. After 10.7 minutes, the reaction was quenched and the target product (**22**) was isolated in a 10% yield. This yield was much lower than what was observed for the same length of time in the HPCCC machine.

The segmented flow reaction was performed in PTFE tubing (ID = 0.8 mm, volume = 7.5 mL) using the same amounts of reagents as the HPCCC reaction. The flow rate (0.7 mL/min) gave the identical reaction time to what was used in the HPCCC. The reaction was quenched and the target product (**22**) was isolated in a 26% yield. This was higher yielding than what was obtained from the batch reaction, but not as high yielding as the results obtained in the HPCCC machine. These results suggested that the mixing efficiency inside the HPCCC machine was greater than that in batch and segmented flow.

Various electrophiles were tested to extend the scope of asymmetric alkylation that could be performed in the HPCCC. The conditions used for the substrate scope were the optimised conditions found for the reaction with benzyl bromide.

Table 8: Investigating a variety of electrophiles in the asymmetric alkylation reaction.

No.	Flow rate (mL/min)	Stationary phase retained (mL)	Residence time (min)	RX	Temp (°C)	Yield (%)	ee (%)
1	0.7	10	14.3		20	0	-
2	0.7	9.8	14.6		20	0	-
3	0.7	9.2	15.4		21	0	-
4	0.7	11	12.8		22	0	-
5	0.7	7	18.6		24	35	87
6	0.7	10	14.3		18	67	87
7	0.7	10.1	14.1		21	57	87
8	0.7	8.8	16		22	61	80
9	0.7	11	12.8		20	0	-
10	0.7	11.6	12		20	0	-
11	0.7	12	11.4		21	53	81
12	0.7	12	11.4		22	25	81
13	0.7	12	11.4		20	60	87
14	0.7	12	11.4		20	60	81
15	0.7	12	11.4		20	75	81
16	0.7	13	10		21	40	81
17	0.4	11	22.5		20	0	-
18	0.4*	10	25		21	0	-
19	0.7	11	13		22	0	-

*Cs₂CO₃ (aq) used as base instead of KOH (aq).

Alkyl bromides were tested first (Table 8, entries 2 - 3), however no conversion was observed and only starting material was recovered. (Bromomethyl)cyclopropane was also investigated (Table 8, entry 19), however only starting material was recovered from this reaction. 4-Bromobutane and 3-bromopropanoic acid were also tested in this reaction, however no reaction was observed (Table 8, entries 1, 4). After finding similar substrate scopes in literature for the batch process, it was understood that these electrophiles were not reactive enough, and that more reactive electrophiles were required.^{20, 50}

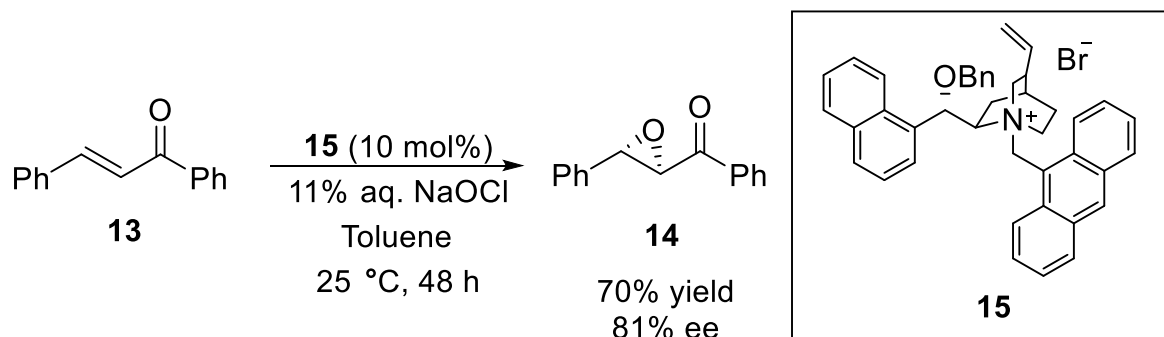
Various benzylic bromides with varying functional groups were tested (Table 8, entries 6, 7, 11, 13 - 15), the target products all obtained in good yields (>60%) with high enantioselectivities (>80% ee). 4-Methyl benzyl chloride was also tested (Table 8, entry 9), however no conversion was observed. It was concluded that benzylic chlorides reacted too slowly to be optimised in the HPCCC.

It was also discovered that allylic bromides (Table 8, entry 8) were suitable electrophiles for this reaction. Propargylic bromides (Table 8, entries 12, 16) also worked, however a slight decrease in yield was observed.

Ooi *et al.* showed that alkyl iodides could be used as electrophiles in the asymmetric alkylation reaction.²⁰ The batch reaction times for these substrates were much longer than the reaction time required when using benzyl bromide (30 hours compared to 2 hours). Using the optimised conditions obtained in previous experiments (flow rate = 0.7 mL/min), there was no conversion observed and only starting material was recovered (Table 8, entry 10). The flow rate was reduced to 0.4 mL/min to increase the reaction time (Table 8, entry 17). However, increasing the reaction time by reducing the flow rate saw no increase in conversion and only starting material was recovered. The use of saturated aqueous Cs₂CO₃ as the base was investigated (Table 8, entry 18), as it had been reported that the use of either CsOH.H₂O or Cs₂CO₃ was preferred over the use of KOH for the reaction with alkyl iodides.¹⁵ Changing the base had no observable effect on the reaction and again only starting material was recovered. It was concluded that the reaction with alkyl iodides was too slow to optimise in the HPCCC.

2.1.7. Investigation of the asymmetric epoxidation of chalcone

Another reaction of interest was the asymmetric epoxidation of chalcone in toluene, using 11% aqueous NaOCl as the oxidant (Scheme 9).²² This reaction also employed the chiral catalyst **15**. This meant there would be no solubility issues when performing the asymmetric epoxidation in flow or the HPLCC machine.



Scheme 9: The asymmetric epoxidation of chalcone using chiral catalyst **15**.

The biphasic asymmetric epoxidation reaction was first performed under segmented flow conditions. Chalcone and the chiral catalyst **15** were dissolved in toluene and loaded into syringe A, whilst 11% aqueous NaOCl was loaded into syringe B. Syringe A and syringe B were pumped at identical flow rates.

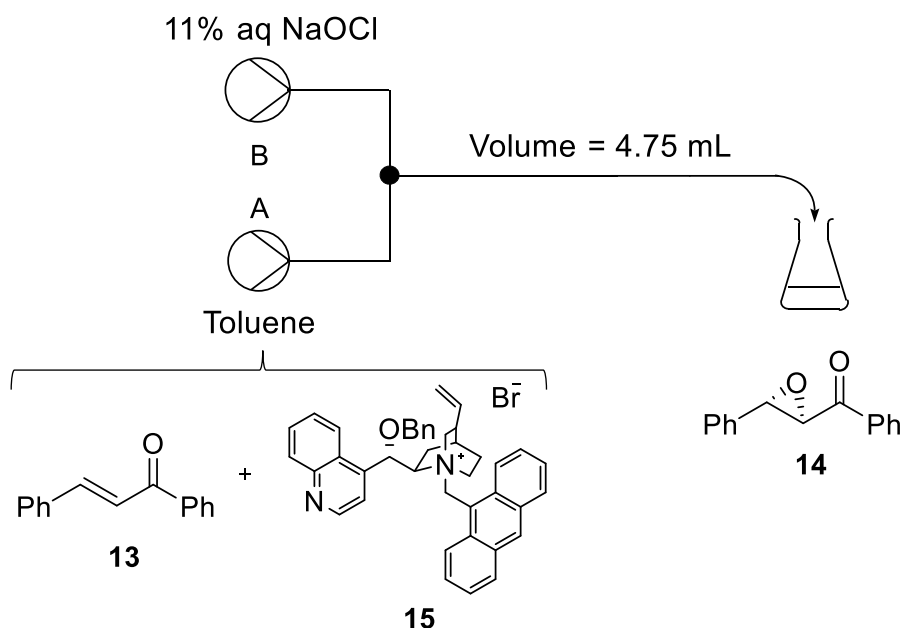


Figure 23: Segmented flow setup for the asymmetric epoxidation of chalcone using chiral catalyst **15**.

The initial reaction was performed at room temperature with a combined flow rate of 0.2 mL/min, giving a residence time of 23.5 minutes. ¹H NMR showed predominantly starting material, with only trace amounts of the product formed (Table 9, entry 1). The flow rate was decreased to allow a longer residence time, however still only trace amounts of the product were formed (Table 9, entry 2). An increase in yield was observed when the reaction was heated to 50 °C and 90 °C, however increasing the temperature also led to a decrease in enantioselectivity (Table 9, entries 4 - 5).

Table 9: Results obtained from the asymmetric epoxidation of chalcone using chiral catalyst (15) in segmented flow.

No.	Flow rate (mL/min)	Residence time (min)	ID (mm)	Temp (°C)	Yield * (%)	ee (%)
1	0.2	23.5	0.5	rt	Trace	-
2	0.15	32	0.5	rt	Trace	-
3	0.2	24	0.8	50	11	+
4	0.2	24	0.8	90	22	62

** yield determined by quantitative ¹H NMR, using 1,3,5-trimethoxybenzene as an internal standard. + ee not determined.*

Since the biphasic asymmetric epoxidation reaction did not yield greater than 22% product, the reaction was evaluated in the HPCCC machine. Toluene was employed as the mobile phase, whilst 11% aqueous NaOCl was used as the stationary phase. The stationary phase retention for this solvent system was high (75%). Various flow rates were evaluated, however only trace amounts of product were observed in the ¹H NMR spectra (Table 10).

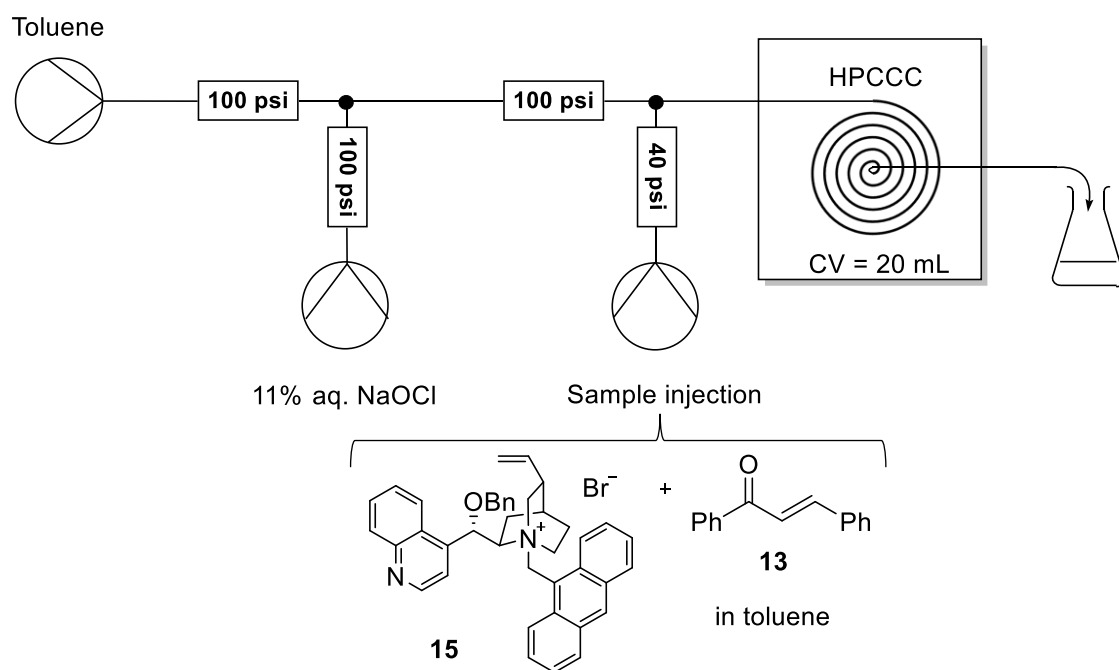


Figure 24: HPCCC setup for the asymmetric epoxidation of chalcone using chiral catalyst (**15**).

Table 10: Results obtained for the asymmetric epoxidation reaction performed in the HPCCC machine.

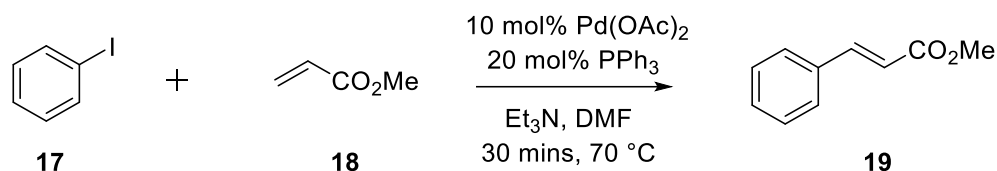
No.	Flow rate (mL/min)	Stationary phase retained (mL)	Residence time (min)	Concentration of chalcone injected (M)	Temp (°C)	Yield (%)
1	0.3	15	50	0.05	25	Trace
2	0.7	15	21	0.05	25	Trace
3	0.7	13	19	0.1	25	Trace

Doubling the concentration of chalcone injected had no effect on the percentage yield (Table 10, entry 3). It was concluded that this reaction was perhaps too slow to be optimised in segmented flow and the HPCCC. In batch, this reaction required a long reaction time (48 hours) to run to full conversion, which may be an explanation for the trace amount of product formed.

2.2. The Heck reaction

2.2.1. Finding a suitable Heck reaction to intensify in the HPCCC machine

The initial reaction of interest was the cross-coupling reaction between iodobenzene (**17**) and methyl acrylate (**18**) (Scheme 10). This reaction had already been intensified under segmented flow conditions using an inert segmenting phase.³⁸



Scheme 10: The Heck reaction to be investigated inside the HPCCC machine.

To decide which palladium catalyst was the most suited catalyst for use in the HPCCC machine, the reaction was first performed in batch. Pd(OAc)₂ and Pd(PPh₃)₄ were tested, and at 70 °C for 21 - 24 hours similar yields were obtained (Table 11, entries 2, 4). Even though using Pd(PPh₃)₄ resulted in a higher yield, it also led to the formation of a larger amount of palladium black when compared with Pd(OAc)₂. It is important that no solid is formed during the reaction, as this can lead to a blockage in the HPCCC. For this reason, the use of Pd(OAc)₂ was investigated further.

*Table 11: Batch results for the cross-coupling reaction between iodobenzene (**17**) and methyl acrylate (**18**).*

No.	Catalyst (10 mol%)	Ligand (20 mol%)	Solvent	Base	Time (h)	Temp (°C)	Yield (%)
1	Pd(OAc) ₂	PPh ₃	DMF	NEt ₃	2	80	Trace
2	Pd(OAc) ₂	PPh ₃	DMF	NEt ₃	20.5	80	62
3	Pd(OAc) ₂	N/A	Triethanolamine	N/A	16	100	33
4	Pd(PPh ₃) ₄	N/A	DMF	NEt ₃	24	80	66
5	Pd(OAc) ₂	PPh ₃	DMF	NEt ₃	26	30	6
6	Pd(OAc) ₂	PPh ₃	DMF	NEt ₃	71	30	13

As the optimum operating temperature of the HPCCC machine is 30 °C, the reaction was performed at 30 °C in batch to see if the reaction would occur at a lower temperature.

The rate of reaction was significantly slower at 30 °C, with only a 6% yield after 26 hours, and 13% after 72 hours (Table 11, entries 5 - 6).

Even though the batch reaction at 30 °C was very slow, the reaction was attempted in the HPCCC. Decane was used as the stationary phase and DMF was used as the mobile phase. As the density of decane is lower than the density of DMF, the reaction would be performed in reverse phase in the column, and the mobile phase would be pumped in the opposite direction. A solution of iodobenzene (**17**), methyl acrylate (**18**) and NEt₃ dissolved in DMF was loaded into syringe A. Pd(OAc)₂ and PPh₃ dissolved in DMF was loaded into syringe B (Figure 25). The sample was injected into the mobile phase using a syringe pump and a T-connector at equal flow rates. Both the mobile and stationary phases were analysed for product, however only trace amounts of product was formed. The temperature in the HPCCC machine was raised to 70 °C so the Heck reaction could be attempted at a higher temperature. However, at this higher temperature the stationary phase (decane) was not retained in the column, meaning no reaction could be attempted. At 50 °C, 45% of stationary phase was retained. The reaction was performed (flow rate = 0.7 mL/min, reaction time = 16 mins) however only starting material was recovered.

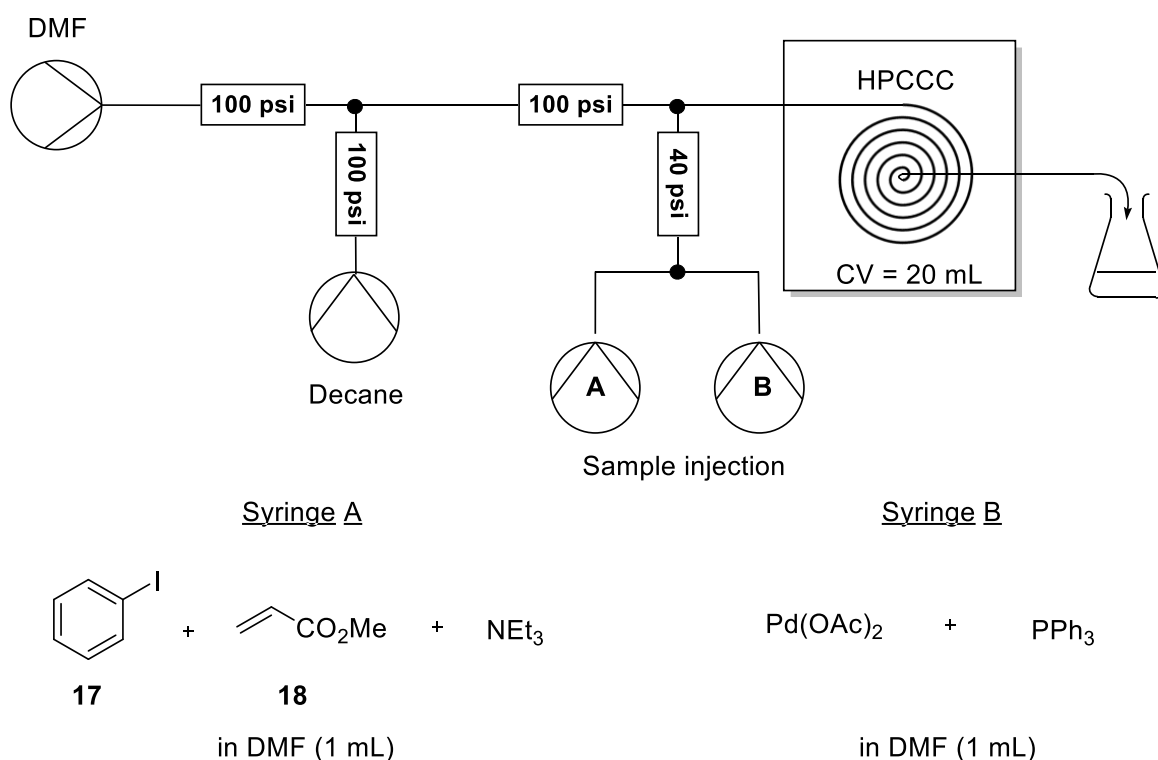


Figure 25: HPCCC setup for the Heck reaction between iodobenzene (**17**) and methyl acrylate (**18**).

Investigation into the Heck reaction had yielded little success, largely due to the temperature constraint when operating the HPCCC. Therefore, an alternative catalyst-ligand combination was evaluated. Netherton *et al.* had shown that using a sterically hindered, electron rich phosphine and bulky tertiary amine could lead to a significantly more active catalyst. Therefore, the reaction could be performed under much milder conditions and temperatures. The reaction employed a Pd₂(dba)₃ / P(*t*-Bu)₃ catalyst / ligand combination, whilst using Cy₂NMe as the base.⁵¹ Due to the air-sensitivity of trialkylphosphines, an air stable phosphonium salt ([(*t*-Bu)₃PH]BF₄) was employed, as it had been showed to give comparable results in the Heck reaction.⁵² In the literature, the optimum solvent was dioxane, however THF, toluene and DMF were also reported to be suitable. For intensification in the HPCCC machine, it is essential that the solvent system is biphasic. Both THF and dioxane are miscible with all solvents, whilst toluene is only immiscible with water. To overcome this, the reaction was evaluated in DMF, and the product was obtained in 75% yield after 70 hours (Table 12, entry 3).

Table 12: Batch results for the cross-coupling reaction between iodobenzene (**17**) and methyl acrylate (**18**), using Pd₂(dba)₃ as the catalyst.

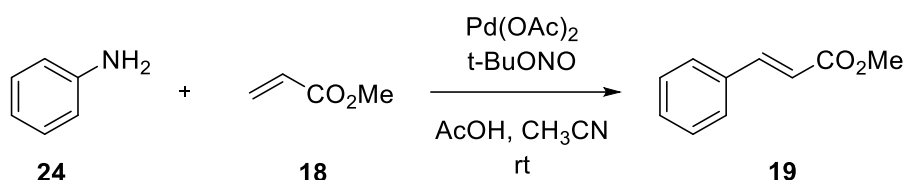
No.	Catalyst (15 mol%)	Ligand (30 mol%)	Solvent	Base	Time (h)	Temp (°C)	Yield (%)
1	Pd ₂ (dba) ₃	[(<i>t</i> -Bu) ₃ PH]BF ₄	Toluene	Cy ₂ NMe	18	30	10
2	Pd ₂ (dba) ₃	[(<i>t</i> -Bu) ₃ PH]BF ₄	DMF	Cy ₂ NMe	18	30	16
3	Pd ₂ (dba) ₃	[(<i>t</i> -Bu) ₃ PH]BF ₄	DMF	Cy ₂ NMe	70	30	75

Although the revised catalyst-ligand combination gave good yields in batch, it also provided obstacles when transferring the reaction into the HPCCC. Firstly, a 70 hour reaction time is beyond the limits of the HPCCC, due to the very low flow rates that would need to be introduced. This would hinder mixing and the intensification process. Secondly, by employing the trialkylphosphonium salt, the *in situ* formation P(*t*-Bu)₃ is accompanied by the precipitation of ammonium tetrafluoroborate salt. Since this salt is insoluble in DMF, this would be problematic when injecting the catalyst into the HPCCC. Filtering off this solid would be difficult due to the rapid air (O₂) oxidation of the

catalyst / ligand combination.⁵² Due to the issues described, an alternative Heck reaction that was better suited to the HPCCC system was investigated.

2.2.2. Investigating the diazonium Heck reaction

The tandem diazonium Heck reaction between aniline (**24**) and methyl acrylate (**18**) was a Heck reaction that only required very mild conditions to progress to completion (Scheme 11).



*Scheme 11: The tandem diazonium Heck reaction between aniline (**24**) and methyl acrylate (**18**).*

The reaction had already been intensified using segmented flow conditions, the target product being obtained in a 54% yield after 27 minutes.³⁸ The reaction had also been performed using commercially available *p*-nitrobenzenediazonium tetrafluoroborate (**20**), an isolated intermediate that could efficiently be used in the Heck reaction with methyl acrylate (**18**). After intensification under segmented flow conditions, the target product was obtained in a 64% yield after 27 minutes.³⁸ The diazonium Heck reaction seemed like an ideal candidate for intensification in the HPCCC machine, due to the lower reaction time (<24 hours) and room temperature reaction conditions.

To transfer the Heck reaction to the HPCCC, the reaction solvent (DMF) was employed as the mobile phase, whilst the inert mixing solvent (*n*-hexane) was employed as the stationary phase. As the density of *n*-hexane is lower than the density of DMF, the reaction would be performed in reverse phase in the column, and the mobile phase would be pumped in the opposite direction. The sample was injected into the HPCCC using a syringe pump and a T-connector. The diazonium salt and acetic acid dissolved in DMF was loaded into syringe A, whilst the palladium catalyst and the alkene dissolved in DMF was loaded into syringe B (Figure 26). It was hoped that due to the intense mixing between the two immiscible phases present in the HPCCC, that using *n*-hexane as the

inert stationary phase would increase the rate of reaction in a similar way that segmentation does in microreactors.

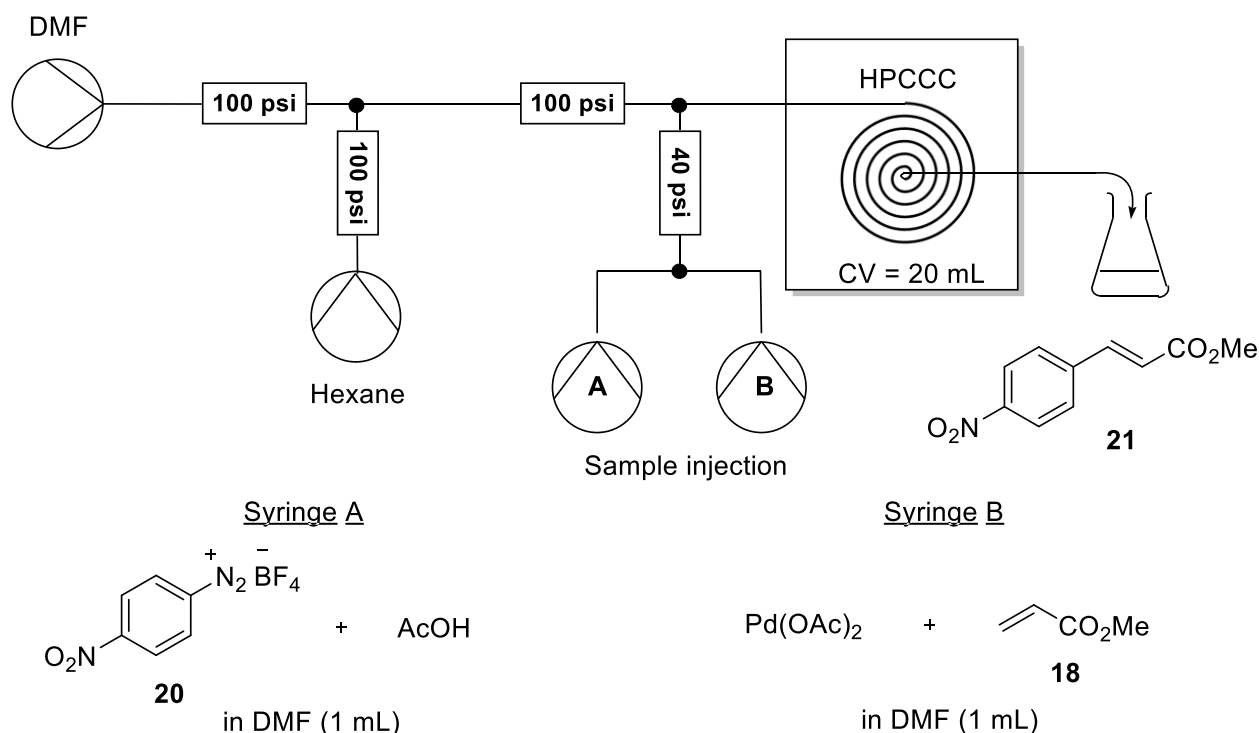


Figure 26: HPCCC setup for the Heck reaction between the diazonium salt (**20**) and methyl acrylate (**18**).

Table 13: Results from the Heck reaction between the diazonium salt (**20**) and methyl acrylate (**18**), performed inside the HPCCC machine.

No.	Flow rate (mL/min)	Stationary phase retained (mL)	Residence time (min)	Temp (°C)	Yield * (%)
1	0.7	15	7	27	28
2	0.4	15	12.5	25	76

* yield determined by quantitative ¹H NMR, using 1,3,5-trimethoxybenzene as an internal standard

After equilibration of the HPCCC, 5 mL of *n*-hexane was recovered, equating to a stationary phase retention of 75%. At a flow rate of 0.7 mL/min, the desired product was obtained in a 28% yield. Since the residence time for this reaction was very low (7 minutes), the flow rate was decreased to 0.4 mL/min, allowing for a residence time of

12.5 minutes. An increase in residence time significantly improved the yield, where the desired product was obtained in a 76% NMR yield (Table 13, entry 2). After purification, an isolated yield of 69% was obtained. Comparing this result to the results obtained using segmented flow showed an increase in percentage yield (64% to 69%) and a decrease in reaction time (27 minutes to 12.5 minutes), suggesting again that the efficiency of mixing inside the HPCCC is greater than in segmented flow.

2.3. Quantification of the mixing efficiency inside the HPCCC

It was previously mentioned that the mixing efficiency of microreactors can be quantified using the Villermaux-Dushman reaction.⁴⁰ The results obtained from the biphasic reactions performed in the HPCCC machine strongly suggested an increase in mixing efficiency when compared with batch and flow. The Villermaux-Dushman reaction was to be evaluated inside the HPCCC machine. The segregation index obtained would then be compared with values obtained in batch and flow, so the mixing efficiency could be quantitatively compared between all three techniques.

The reaction was first carried out in a flow setup, using PTFE tubes with an internal diameter (ID) = 0.8 mm (Figure 27). All solutions were made up individually, using a concentration set described by L. Falk and J. Commenge.⁴⁰ The buffer solution (B) was made up by the addition of 20 mL aqueous NaOH (0.045 M) to 20 mL aqueous H₃BO₃ (0.045 M) together, followed by the addition of 20 mL aqueous KI (0.016 M) and 20 mL aqueous KIO₃ (0.003 M).

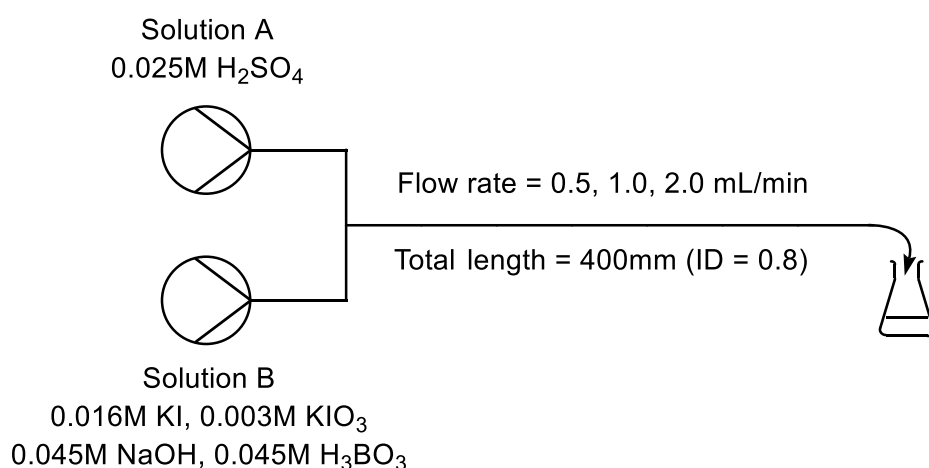


Figure 27: Flow chemistry setup for the Villermaux-Dushman reaction.

Different flow rates were tested to see if this would affect the rate of mixing. The concentration of $[I_3^-]$ was calculated using the Beer Lambert law. At 0.5 mL/min, the $[I_3^-]$ concentration was 5.73×10^{-5} mol/L, leading to an X_s of 0.035. At 1.0 mL/min, the $[I_3^-]$ concentration decreased to 5.25×10^{-5} mol/L, leading to an X_s of 0.032. At 2.0 mL/min, the $[I_3^-]$ concentration decreased again to 4.36×10^{-5} , leading to an X_s of 0.026. These results showed that increasing the flow rate increased the efficiency of mixing in the microreactor.

Translating the Villermaux-Dushman reaction to the HPCCC machine proved a lot more difficult than originally thought. For reactions to be intensified in the HPCCC, a biphasic solvent system must be used. This is important for achieving stationary phase retention. The repeated mixing and settling between the mobile phase and the stationary phase is what attributes to the highly efficient mixing in the HPCCC machine. The Villermaux-Dushman reaction is a monophasic reaction, meaning no stationary phase can be retained. This makes the monophasic Villermaux-Dushman reaction unsuitable for quantification of the mixing efficiency inside the HPCCC machine.

To this date, there have been no reports about measuring the mixing efficiency of a biphasic solvent system. A potential alternative was to investigate a novel modified biphasic Villermaux-Dushman reaction, replacing H_2SO_4 with *p*-TsOH, a strong organic acid that can be dissolved in organic solvents. A biphasic solvent system using diethylether and water was proposed, due to the low setting time between the two layers (<20 s) and the solubility of *p*-TsOH in diethylether. Preliminary tests were performed, however no conclusive results were obtained. More research is required before this novel modified biphasic Villermaux-Dushman reaction can be used as an accurate quantification method for the efficiency of mixing.

3. Conclusion

In this research, chiral phase transfer catalysis reactions were successfully performed in segmented flow for the first time. The phase transfer catalysed asymmetric alkylation of *N*-(diphenylmethylene)glycine *tert*-butyl ester (**5**) with benzyl bromide, using chiral catalyst **7** as the PTC, was successfully intensified in segmented flow. The target product was obtained in a 71% yield in 21 minutes. In batch, the target product was obtained in a 62% yield in 5 hours. Performing the reaction in segmented flow increased the yield of the reaction whilst decreasing the reaction time. However, a slight drop in enantioselectivity was noticed in segmented flow (66% ee to 56% ee).

Biphasic reactions were successfully performed in an HPCCC machine for the first time. The phase transfer catalysed asymmetric alkylation of *N*-(diphenylmethylene)glycine *tert*-butyl ester (**5**) with benzyl bromide, using chiral catalyst **15** as the PTC was successfully intensified in the HPCCC. The target product was obtained in a 65% isolated after 10.7 minutes of reaction time, with no drop in enantioselectivity when compared to batch (87% ee). The reactants were injected twice over the space of 30 minutes, without replacement of the stationary phase. No deterioration in the yield was observed (1st injection = 67%, 2nd injection = 63%), showcasing the reusability of the stationary phase.

The reaction was performed in batch and segmented flow using identical reaction conditions. In 10.7 minutes of reaction time, the target product was obtained in a 10% yield in batch, and a 26% yield in segmented flow. This direct comparison showed the advantages of using the HPCCC for biphasic reactions, suggesting that the mixing efficiency inside the machine is greater than that of batch and segmented flow.

A substrate scope was performed in the HPCCC machine for the asymmetric alkylation reaction. Various electrophiles with differing functional groups were employed. Benzylic and allylic bromides worked very well for this reaction (53 - 75% yield, 80 - 87% ee), whilst propargylic bromides saw a notable decrease in yield (25 - 40% yield, 81% ee). Alkyl iodides, alkyl bromides and benzyl chlorides were found to react too slowly to be intensified in the HPCCC.

The Heck reaction between *p*-nitrobenzenediazonium tetrafluoroborate (**20**) and methyl acrylate (**18**) was also successfully intensified with the HPCCC machine, using *n*-hexane

as an inert “mixing” phase to increase the efficiency of mixing in the system. The reaction had previously been intensified in segmented flow, obtaining the target product in a 64% yield after 27 minutes. In the HPCCC machine, the target product was obtained in a 69% yield after 12.5 minutes. The increase in yield and decrease in reaction time gave further evidence of the increased mixing efficiency inside the HPCCC machine. These results also showed that monophasic reactions such as the Heck reaction, can be intensified in the HPCCC by the introduction of an inert “mixing” phase. Heck reactions at elevated temperatures were investigated in the HPCCC machine, however stationary phase retention was not possible at temperatures greater than 70 °C.

In conclusion, HPCCC is an effective, efficient and novel method to intensify both monophasic and biphasic reactions. The very intense mixing lends the HPCCC as a useful tool that can significantly accelerate reactions whilst maintaining yields and enantioselectivity. In addition, the HPCCC machine has been shown through numerous examples to outperform both batch and segmented flow techniques for a variety of biphasic reactions. Reactions can be easily scaled up to semi-preparative, preparative and pilot scale by the use of larger columns, without the need to create new methods. Although the HPCCC is a newly investigated enabling technology in organic synthesis, there are certain criteria that must be met in order for a reaction to be performed:

- All reactants and catalysts must be soluble in at least one of the phases in the biphasic system.
- A density difference of more than 0.1 g/cm³ between the two phases.
- The settling time between the two phases must be less than 30 seconds.
- The reaction time in batch must not be longer than 24 hours.
- The temperature of the reaction in batch ideally will be between 15 - 40 °C.

4. Experimental

4.1. General

All HPLC experiments were performed at Bioextractions Ltd. (Tredegar, UK) on a Dynamic Extractions Mini HPLC machine, which was fitted with an analytical scale column with a volume of 20 mL and an ID of 0.8 mm.

All ^1H and ^{13}C NMR spectra were obtained on either a Bruker Avance 300 (300 MHz ^1H , 76 MHz ^{13}C) or a Bruker Avance 400 (400 MHz ^1H , 100 MHz ^{13}C) spectrometer at 25 °C in the solvent stated. Chemical shifts are reported in parts per million (ppm) and all coupling constants, J, are quoted in Hz. Multiplicities are reported with the following symbols: s = singlet, d = doublet, t = triplet, q = quartet, m = multiplet and multiples thereof.

Mass spectrometric measurements were performed by R. Jenkins, R. Hick, T. Williams and S. Waller at Cardiff University on a Water LCR Premier XEtof. The molecular ion peaks values quoted for molecular ion plus hydrogen $[\text{M}+\text{H}]^+$ or molecular ion plus bromine $[\text{M}+\text{Br}]^+$

Infrared spectra were recorded on a Shimadzu IRAffinity-1 Fourier Transform ATIR spectrometer as thin films using a pike miracle ATR accessory. Characteristic peaks are quoted ($\nu_{\text{max}} / \text{cm}^{-1}$).

Room temperature (rt) refers to 20 - 25 °C. Temperatures of 0 °C were obtained using ice/water baths. All reactions involving heating were carried out using DrySyn blocks and a contact thermometer. In vacuo refers to the use of a rotary evaporator under reduced pressure. Dry solvents such THF, diethyl ether and toluene were obtained after passing these previously degassed solvents through activated alumina columns (Mbraun, SPS-800). Dry dichloromethane was obtained using phosphorous pentoxide, and then distilling when needed. All other solvents and commercial reagents were used as supplied without further purification unless stated otherwise. Thin-layer chromatography (TLC) was performed on pre-coated aluminium sheets of Merck silica gel 60 F254 (0.20 mm) and visualised by UV radiation (254 nm). Manual column chromatography was performed using silica gel 60 (Merck, 230-400 mesh) under increased pressure (Flash

Chromatography), while automated column chromatography was performed on a Biotage® Isolera Four. The solvents were used as laboratory grade.

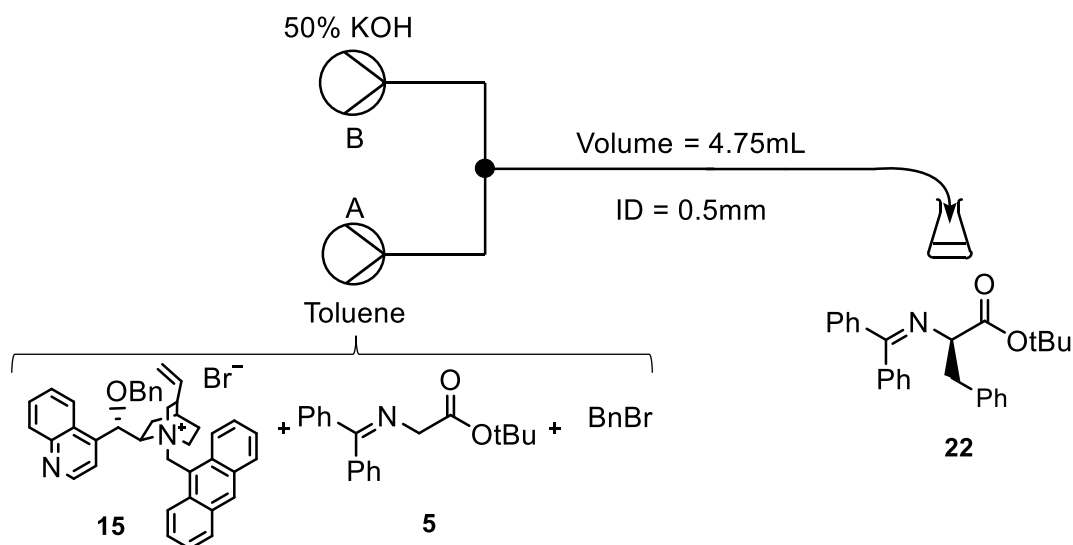
The HPLC measurements were carried out on a Shimadzu apparatus. The different modules were SIL-10ADVP (autoinjector), LC-10ATVP (liquid chromatograph), FCV-10ALVP (pump), DGU-14A (degasser), CTO-10ASVP (column oven), SCL-10AVP (system controller) and SPD-M10A (diode array detector). The solvents used were *n*-hexane and 2-propanol and were of an HPLC grade. The chiral column used for the separation of the enantiomers were (Regis (RR) Whelk-01 column (0.46 cm Ø x 25 cm).

4.2. Asymmetric alkylation

4.2.1. General batch procedure for the asymmetric alkylation of *N*-(diphenylmethylene)glycine *tert*-butyl ester

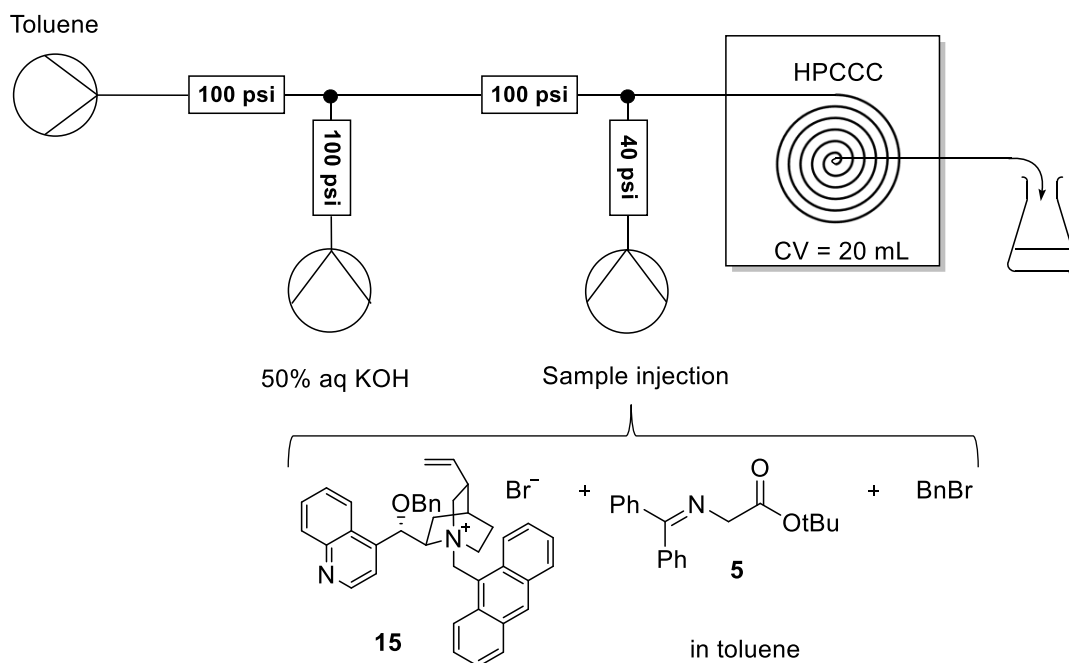
In a round bottomed flask, benzyl bromide (0.12 mL, 1 mmol) was added to a mixture of *N*-(diphenylmethylene)glycine *tert*-butyl ester (59 mg, 0.2 mmol) and *N*-benzylcinchonidinium chloride (8.4 mg, 0.02 mmol) in toluene/chloroform (7:3, 0.75 mL). 50% aqueous KOH (0.25 mL) was then added, and the reaction mixture was stirred at room temperature until the starting material had been consumed (7 h). The suspension was diluted with ethyl acetate (20 mL), washed with water (2 x 5 ml), dried over MgSO₄, filtered, and concentrated in vacuo. The residue was purified by flash column chromatography (*n*-hexane/ethyl acetate) to afford the target product as a colourless oil. The enantioselectivity was determined by chiral HPLC (Regis (RR) Whelk-01 column, 5:95 IPA / *n*-hexane, 1 mL/min, 23 °C, 254 nm).

4.2.2. Flow setup and general flow procedure for the asymmetric alkylation of *N*-(diphenylmethylene)glycine *tert*-butyl ester



A solution of *N*-(diphenylmethylene)glycine *tert*-butyl ester (116 mg, 0.4 mmol), benzyl bromide (0.24 mL, 2 mmol) and chiral catalyst **15** (26.2 mg, 0.04 mmol) in toluene (8.5 mL) was loaded into syringe A. 50% aqueous KOH (8.5 mL) was loaded into syringe B. Syringe A and B were then connected to the microflow system (PTFE) through a designated inlet using a T-connector. Tubing length 24 m, residence time = 23.5 min, internal diameter = 0.5 mm. The solutions were then delivered into the microchannel at 0.1 mL/min (combined 0.2 mL/min), in a continuous segmented flow manner using KD Scientific syringe pumps. The reaction product was quenched in water and diluted with EtOAc. The organic layer was washed with water (2 x 5 ml), dried over MgSO₄, filtered, and concentrated in vacuo. The residue was purified by flash column chromatography (*n*-hexane/ethyl acetate) to afford the target product.

4.2.3. HPCCC setup and general procedure for the asymmetric alkylation of *N*-(diphenylmethylene)glycine *tert*-butyl ester



Equilibration of the HPCCC

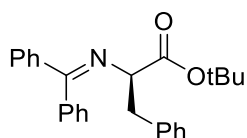
This reaction was performed under normal phase HPCCC conditions (50% aq. KOH employed as stationary phase, tail-to-head mode). Firstly, mobile phase (toluene) is pumped through the column to displace any aqueous solvent used in the washing of the column. This allows easy detection of stationary phase elution, and also stops the stationary phase being diluted by the water. To fill the HPCCC column with stationary phase, a solution of KOH dissolved in deionised water (50% aq. solution) was pumped through the column until the aqueous stationary phase was observed at the outlet. Upon filling of the machine, the stationary phase pump was switched off and the HPCCC was spun at 2100 rpm. The mobile phase (toluene) was then pumped at 0.7 mL/min to allow equilibration of the stationary phase. Once stationary phase stopped eluting from the column, equilibration had been achieved.

Sample injection

A solution of *N*-(diphenylmethylene)glycine *tert*-butyl ester (29 mg, 0.1 mmol), R-Br (0.5 mmol) and chiral catalyst **15** (6.5 mg, 0.01 mmol) in toluene (3 mL) was loaded into a 3 mL syringe. The sample was injected into the mobile phase using a syringe pump at the required flow rate. The reaction product was quenched in water and diluted with ethyl acetate. The organic layer was washed with water (2 x 5 mL), dried over MgSO₄, filtered, and concentrated in vacuo. The residue was purified by flash column chromatography (*n*-hexane/ethyl acetate) to afford the target product.

4.2.4. Characterisation of alkylation products

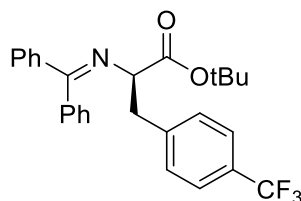
(*R*) *tert*-butyl 2-[(diphenylmethylene)amino]-3-phenylpropanoate (22)



Performed according to the “HPCCC General Procedure”. Compound afforded as a colourless oil (25 mg, 65%).

$[\alpha]_D^{20} = +139.2^\circ$ ($c = 0.5$, CHCl₃). ¹H NMR (500 MHz, CDCl₃): $\delta = 7.60 - 7.55$ (m, 2H, Ar-H), 7.39 - 7.24 (m, 6H, Ar-H), 7.21 - 7.13 (m, 3H, Ar-H), 7.07 - 7.03 (m, 2H, Ar-H), 6.60 (br d, $J = 6.0$ Hz, 2H, Ar-H), 4.10 (dd, $J = 9.3, 4.3$ Hz, 1H, NC-H), 3.23 (dd, $J = 13.4, 4.3$ Hz, 1H, CH₂), 3.16 (dd, $J = 13.4, 9.3$ Hz, 1H, CH₂), 1.44 (s, 9H, CH₃). ¹³C NMR (100 MHz, CDCl₃): $\delta = 170.9, 170.3$ (C=N, C=O), 139.6, 138.4, 136.4, 130.1, 129.9, 128.7, 128.2, 128.1, 128.1, 127.9, 127.7, 126.1, 81.1 (C-O), 68.0 (C-N), 39.6 (CH₂), 28.1 (CH₃). The enantioselectivity (86% ee) was determined by chiral HPLC (Regis (*RR*) Whelk-01 column, 5:95 IPA / *n*-Hexane, 1 mL/min, 25 °C, 254 nm, retention times: S (minor) 5.3 min, *R* (major) 10.0 min. Absolute configuration was assigned according to literature. Spectroscopic data are in agreement with literature.^{53, 54}

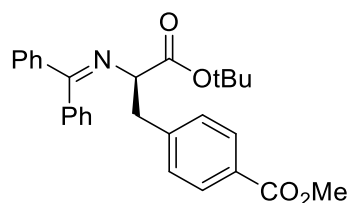
(*R*) tert-butyl 2-[(diphenylmethylene)amino]-3-(4-(trifluoromethyl)phenyl)propanoate (25)



Performed according to the “HPCCC General Procedure”. Compound afforded as a white solid (30 mg, 67%), m.p.: 109 - 112 °C. Literature m.p.: 106.6 - 112.7 °C.

$[\alpha]_D^{20} = +146.9^\circ$ ($c = 0.6$, CHCl_3). $^1\text{H NMR}$ (500 MHz, CDCl_3): $\delta = 7.54$ (d, $J = 7.5$ Hz, 2H, Ar-H), 7.41 (d, $J = 8.0$ Hz, 2H, Ar-H), 7.37 - 7.20 (m, 6H, Ar-H), 7.13 (d, $J = 8.0$ Hz, 2H, Ar-H), 6.59 (d, $J = 5.8$ Hz, 2H, Ar-H), 4.09 (dd, $J = 9.1, 4.1$ Hz, 1H, NC-H), 3.27 - 3.13 (m, 2H, CH_2), 1.41 (s, 9H, CH_3). $^{13}\text{C NMR}$ (100 MHz, CDCl_3): $\delta = 170.7, 170.4$ (C=N, C=O), 142.7, 142.7, 139.3, 136.1, 130.3, 130.1, 128.7, 128.4, 128.2, 128.0, 127.5, 125.0 (q, $^3J_{\text{C-F}} = 3.7$ Hz), 81.5 (C-O), 67.5 (C-N), 39.3 (CH_2), 28.0 (CH_3). The enantioselectivity (87% ee) was determined by chiral HPLC (Regis (*RR*) Whelk-01 column, 5:95 IPA / *n*-hexane, 1 mL/min, 22 °C, 200 nm, retention times: *S* (minor) 4.7 min, *R* (major) 10.6 min. Absolute configuration was assigned according to literature. ⁵⁵

methyl (*R*)-4-(3-(*tert*-butoxy)-2-[(diphenylmethylene)amino]-3-oxopropyl)benzoate (26)

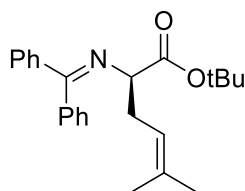


Performed according to the “HPCCC General Procedure”. Compound afforded as a white solid (25 mg, 57%), m.p.: 102 - 106 °C.

$[\alpha]_D^{20} = +107.3^\circ$ ($c = 0.3$, CHCl_3). $^1\text{H NMR}$ (500 MHz, CDCl_3): $\delta = 7.87$ (d, $J = 8.4$ Hz, 2H, Ar-H), 7.58 - 7.54 (m, 2H, Ar-H), 7.41 - 7.26 (m, 6H, Ar-H), 7.14 (d, $J = 8.2$ Hz, 2H, Ar-H), 6.64 (d, $J = 5.8$ Hz, Ar-H), 4.14 (dd, $J = 9.1, 4.5$ Hz, 1H, NC-H), 3.89 (s, 3H, O- CH_3),

3.31 - 3.19 (m, 2H, CH₂), 1.44 (s, 9H, CH₃). ¹³C NMR (100 MHz, CDCl₃): δ = 170.7, 170.5 (C=N, C=O), 167.2 (C=O), 144.1, 139.4, 136.2, 132.4, 130.3, 130.1, 129.9, 129.7, 129.4, 129.4, 128.7, 128.4, 128.3, 128.2, 128.1, 128.0, 127.6, 81.4 (C-O), 67.4 (C-N), 52.0 (OCH₃) 39.3 (CH₂), 28.0 (CH₃). HRMS (ESP): [M+H]⁺ calc 444.2177 found 444.2175 (0.5 ppm) [C₂₈H₃₀NO₄]⁺. V_{max}/cm⁻¹: 3055, 2976, 2932, 1721, 1611, 1574, 1435, 1416, 1368, 1277, 1148, 1103. The enantioselectivity (87% ee) was determined by chiral HPLC (Regis (RR) Whelk-01 column, 5:95 IPA / *n*-hexane, 1 mL/min, 25 °C, 254 nm, retention times: S (minor) 12.6 min, R (major) 22.4 min. Absolute configuration was assigned by analogy with previous substrates.

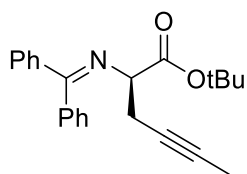
***tert*-butyl (*R*)-2-((diphenylmethylene)amino)-5-methylhex-4-enoate (27)**



Performed according to the “HPLCC General Procedure”. Compound afforded as a colourless oil (22 mg, 61%).

[α]_D²⁰ = +68.9° (c = 0.3, CHCl₃). ¹H NMR (500 MHz, CDCl₃): δ = 7.65 - 7.61 (m, 2H, Ar-H), 7.41 - 7.26 (m, 6H, Ar-H), 7.17 - 7.13 (m, 2H, Ar-H), 5.02 (tt, *J* = 7.6, 1.4 Hz, 1H, C=CH) 3.95 (dd, *J* = 7.8, 5.5 Hz, 1H, NC-H), 3.89 (s, 3H, O-CH₃) 2.62 - 2.48 (m, 2H, CH₂), 1.65 (s, 3H, C=C-CH₃), 1.56 (s, 3H, C=C-CH₃) 1.44 (s, 9H, CH₃). ¹³C NMR (100 MHz, CDCl₃): δ = 171.3, 169.6 (C=N, C=O), 139.8, 136.8, 133.9, 130.1, 128.8, 128.4, 128.3, 128.0, 128.0, 120.2, 80.8 (C-O), 66.4 (C-N), 32.4 (CH₂), 28.1 (CH₃), 25.8 (C=C-CH₃), 18.0 (C=C-CH₃). HRMS (ESP): [M+H]⁺ calc 364.2280 found 364.2277 (0.8 ppm) [C₂₄H₃₀NO₂]⁺. V_{max}/cm⁻¹: 3059, 2976, 2928, 1732, 1622, 1447, 1368, 1285, 1254, 1150, 696. The enantioselectivity (80% ee) was determined by chiral HPLC (Regis (RR) Whelk-01 column, 5:95 IPA / *n*-hexane, 1 mL/min, 25 °C, 294 nm, retention times: S (minor) 4.6 min, R (major) 6.0 min. Absolute configuration was assigned according to literature. Spectroscopic data are in agreement with literature.⁵⁶

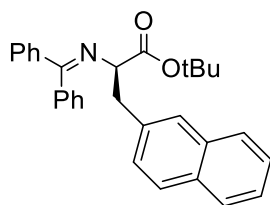
***tert*-butyl (*R*)-2-((diphenylmethylene)amino)hex-4-ynoate (28)**



Performed according to the "HPCCC General Procedure". Compound afforded as a pale yellow oil (9 mg, 25%).

$[\alpha]_D^{20} = +24.7^\circ$ ($c = 0.6$, CHCl_3). $^1\text{H NMR}$ (500 MHz, CDCl_3): $\delta = 7.68 - 7.63$ (m, 2H, Ar-H), 7.49 - 7.30 (m, 6H, Ar-H), 7.26 - 7.21 (m, 2H, Ar-H), 4.12 (dd, $J = 8.2, 5.3$ Hz, 1H, NC-H), 2.83 - 2.60 (m, 2H, CH_2), 1.73 (t, $J = 2.5$ Hz, 3H, $\text{C}\equiv\text{C}-\text{CH}_3$), 1.45 (s, 9H, CH_3). $^{13}\text{C NMR}$ (100 MHz, CDCl_3): $\delta = 171.0, 170.0$ (C=N, C=O), 139.8, 136.5, 130.3, 130.1, 129.0, 128.6, 128.3, 128.2, 128.0, 81.3 (C-O), 77.3 (C \equiv C), 75.9 (C \equiv C) 65.5 (C-N), 28.0 (CH_3), 23.7 (CH_2), 3.6 (CH_3). HRMS (ESP): $[\text{M}+\text{H}]^+$ calc 348.1965 found 348.1964 (0.3 ppm) $[\text{C}_{23}\text{H}_{26}\text{NO}_2]^+$. $V_{\text{max}}/\text{cm}^{-1}$: 3057, 2980, 2922, 1728, 1622, 1447, 1368, 1265, 1152, 698. The enantioselectivity (81% ee) was determined by chiral HPLC (Regis (*RR*) Whelk-01 column, 5:95 IPA / *n*-hexane, 1 mL/min, 22 °C, 254 nm, retention times: S (minor) 5.1 min, R (major) 6.7 min. Absolute configuration was assigned by analogy with previous substrates.

***tert*-butyl (*R*)-2-((diphenylmethylene)amino)-3-(naphthalen-2-yl)propanoate (29)**

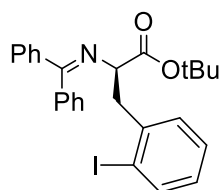


Performed according to the "HPCCC General Procedure". Compound afforded as a pale yellow oil (23 mg, 53%).

$[\alpha]_D^{20} = +124^\circ$ ($c = 0.05$, CHCl_3). $^1\text{H NMR}$ (500 MHz, CDCl_3): $\delta = 7.79 - 7.74$ (m, 1H, Ar-H), 7.70 - 7.64 (m, 2H, Ar-H), 7.58 - 7.53 (m, 2H, Ar-H), 7.51 (s, 1H, Ar-H), 7.44 - 7.38 (m, 2H, Ar-H), 7.37-7.33 (m, 1H, Ar-H), 7.33-7.26 (m, 3H, Ar-H), 7.22 - 7.14 (m, 3H, Ar-H), 6.54 (br d, $J = 5.5$ Hz, 2H, Ar-H), 4.25 (dd, $J = 9.3, 4.3$ Hz, 1H, NC-H), 3.44 - 3.28

(m, 2H, CH₂), 1.45 (s, 9H, CH₃). ¹³C NMR (100 MHz, CDCl₃): δ = 170.9, 170.4 (C=N, C=O), 139.6, 136.3, 135.9, 133.4, 132.1, 130.1, 128.7, 128.4, 128.2, 128.0, 127.9, 127.7, 127.6, 127.5, 125.8, 125.2, 81.2 (C-O), 67.9 (C-N), 39.8 (CH₂), 28.1 (CH₃). The enantioselectivity (81% ee) was determined by chiral HPLC (Regis (RR) Whelk-01 column, 5:95 IPA / *n*-hexane, 1 mL/min, 25 °C, 254 nm, retention times: S (minor) 7.6 min, *R* (major) 18.1 min. Absolute configuration was assigned according to literature. Spectroscopic data are in agreement with literature.^{54, 56}

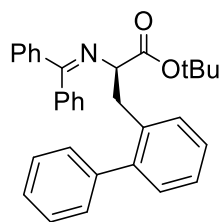
***tert*-butyl (*R*)-2-((diphenylmethylene)amino)-3-(2-iodophenyl)propanoate (30)**



Performed according to the “HPCCC General Procedure”. Compound afforded as a pale yellow oil (31 mg, 60%).

[α]_D²⁰ = +186° (c = 0.03, CHCl₃). ¹H NMR (500 MHz, CDCl₃): δ = 7.72 (dd, *J* = 7.7, 1.1 Hz, 1H, Ar-H), 7.61 - 7.56 (m, 2H, Ar-H), 7.40 - 7.23 (m, 6H, Ar-H), 7.21 (m, 2H, Ar-H), 6.90 - 6.82 (m, 1H, Ar-H), 6.55 (br d, *J* = 3.4 Hz, 2H, Ar-H), 4.33 (dd, *J* = 9.9, 3.8 Hz, 1H, NC-H), 3.40 (dd, *J* = 13.5, 3.8 Hz, 1H, CH₂), 3.28 (dd, *J* = 13.5, 9.9 Hz, 1H, CH₂), 1.47 (s, 9H, CH₃). ¹³C NMR (100 MHz, CDCl₃): δ = 170.8, 170.6 (C=N, C=O), 140.8, 139.4, 139.2, 136.2, 132.1, 130.1, 128.8, 128.3, 128.2, 128.1, 127.9, 127.7, 101.4 (Ph-I), 81.3 (C-O), 65.2 (C-N), 43.9 (CH₂), 28.1 (CH₃). The enantioselectivity (87% ee) was determined by chiral HPLC (Regis (RR) Whelk-01 column, 5:95 IPA / *n*-hexane, 1 mL/min, 25 °C, 254 nm, retention times: S (minor) 5.9 min, *R* (major) 15.9 min. Absolute configuration was assigned according to literature. Spectroscopic data are in agreement with literature.⁵⁷

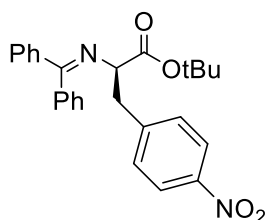
***tert*-butyl (*R*)-3-([1,1'-biphenyl]-2-yl)-2-((diphenylmethylene)amino)propanoate (31)**



Performed according to the "HPCCC General Procedure". Compound afforded as a colourless oil (34 mg, 74%).

$[\alpha]_D^{20} = +206.7^\circ$ ($c = 0.06$, CHCl_3). $^1\text{H NMR}$ (500 MHz, CDCl_3): $\delta = 7.50 - 7.45$ (m, 2H, Ar-H), 7.34 - 7.06 (m, 12H, Ar-H), 7.01 - 6.97 (m, 1H, Ar-H), 6.80 - 6.73 (m, 2H, Ar-H), 6.45 (br d, $J = 4.3$ Hz, 2H, Ar-H), 3.85 (dd, $J = 9.8, 3.8$ Hz, 1H, NC-H), 3.24 (dd, $J = 13.5, 3.5$ Hz, 1H, CH_2), 3.05 (dd, $J = 13.5, 9.8$ Hz, 1H, CH_2), 1.24 (s, 9H, CH_3). $^{13}\text{C NMR}$ (100 MHz, CDCl_3): $\delta = 170.9, 170.1$ (C=N, C=O), 142.8, 141.4, 139.6, 136.4, 135.8, 132.4, 131.2, 130.3, 130.1, 130.1, 130.0, 129.2, 129.1, 128.8, 128.3, 128.3, 128.1, 128.1, 127.9, 127.8, 127.0, 126.6, 126.1, 80.8 (C-O), 66.9 (C-N), 36.8 (CH_2), 28.0 (CH_3). HRMS (ESP): $[\text{M}+\text{H}]^+$ calc 462.2435 found 462.2433 (0.4 ppm) $[\text{C}_{32}\text{H}_{32}\text{NO}_2]^+$. $V_{\text{max}}/\text{cm}^{-1}$: 3057, 3022, 2976, 2932, 1728, 1661, 1622, 1597, 1479, 1447, 1368, 1148. The enantioselectivity (81% ee) was determined by chiral HPLC (Regis (*RR*) Whelk-01 column, 5:95 IPA / *n*-hexane, 1 mL/min, 25 °C, 254 nm, retention times: *S* (minor) 6.8 min, *R* (major) 22.7 min. Absolute configuration was assigned by analogy with previous substrates.

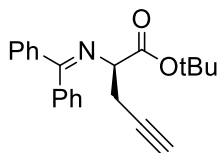
***tert*-butyl (*R*)-2-((diphenylmethylene)amino)-3-(4-nitrophenyl)propanoate (32)**



Performed according to the "HPCCC General Procedure". Compound afforded as a pale yellow oil (26 mg, 60%).

$[\alpha]_D^{20} = +107.4^\circ$ ($c = 0.7$, CHCl_3). $^1\text{H NMR}$ (500 MHz, CDCl_3): $\delta = 8.01 - 7.97$ (m, 2H, Ar-H), 7.51 - 7.47 (m, 2H, Ar-H), 7.34 - 7.28 (m, 2H, Ar-H), 7.27 - 7.21 (m, 4H, Ar-H), 7.20 - 7.16 (m, 2H, Ar-H), 6.64 (br d, $J = 6.8$ Hz, 2H, Ar-H), 4.10 (dd, $J = 8.4, 5.0$ Hz, 1H, NC-H), 3.27 - 3.17 (m, 2H, CH_2), 1.37 (s, 9H, CH_3). $^{13}\text{C NMR}$ (100 MHz, CDCl_3): $\delta = 171.0, 170.1$ (C=N, C=O), 146.6, 146.5, 139.1, 136.0, 130.7, 130.5, 128.7, 128.6, 128.3, 128.1, 127.5, 123.3, 81.7 (C-O), 67.0 (C-N), 39.4 (CH_2), 28.1 (CH_3). HRMS (ESP): $[\text{M}+\text{H}]^+$ calc 431.1971 found 431.1971 (0.0 ppm) $[\text{C}_{26}\text{H}_{27}\text{N}_2\text{O}_4]^+$. $V_{\text{max}}/\text{cm}^{-1}$: 3057, 2978, 2931, 1730, 1622, 1599, 1518, 1490, 1447, 1285, 1148, 847, 696. The enantioselectivity (81% ee) was determined by chiral HPLC (Regis (*RR*) Whelk-01 column, 5:95 IPA / *n*-hexane, 1 mL/min, 25 °C, 277 nm, retention times: *S* (minor) 9.6 min, *R* (major) 18.0 min. Absolute configuration was assigned according to literature. Spectroscopic data are in agreement with literature.⁵⁸

***tert*-butyl (*R*)-2-((diphenylmethylene)amino)pent-4-ynoate (33)**

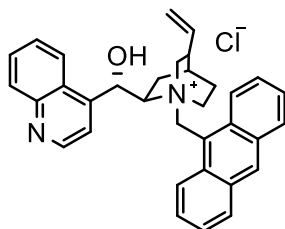


Performed according to the "HPCCC General Procedure". Compound afforded as a pale yellow oil (13 mg, 40%).

$[\alpha]_D^{20} = +77.5^\circ$ ($c = 0.03$, CHCl_3). $^1\text{H NMR}$ (500 MHz, CDCl_3): $\delta = 7.68 - 7.63$ (m, 2H, Ar-H), 7.51 - 7.37 (m, 4H, Ar-H), 7.36 - 7.31 (m, 2H, Ar-H), 7.28 - 7.24 (m, 2H, Ar-H), 4.17 (dd, $J = 8.1, 5.2$ Hz, 1H, NC-H), 2.84 - 2.72 (m, 2H, CH_2), 1.45 (s, 9H, CH_3). $^{13}\text{C NMR}$ (100 MHz, CDCl_3): $\delta = 171.4, 169.6$ (C=N, C=O), 139.6, 136.3, 130.4, 129.0, 128.6, 128.4, 128.3, 128.0, 81.6, 81.3, ($\equiv\text{CH}$, C-O), 70.1 ($\equiv\text{C}$ -), 64.8 (C-N), 28.0 (CH_3), 23.4 (CH_2). The enantioselectivity (81% ee) was determined by chiral HPLC (Regis (*RR*) Whelk-01 column, 5:95 IPA / *n*-hexane, 1 mL/min, 25 °C, 254 nm, retention times: *S* (minor) 4.8 min, *R* (major) 6.0 min. Absolute configuration was assigned according to literature. Spectroscopic data are in agreement with literature.²⁰

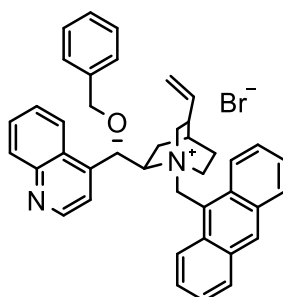
4.2.5 Synthesis of the chiral catalyst (10)

(2R, 5R, 1'S)-1-(9-anthracenyl)methyl-5-ethylene-2-[1-hydroxy-1-(quinolin-4-yl)]methyl-1-azoniabicyclo[2.2.2]octane chloride (10)



A mixture of cinchonine (500 mg, 1.70 mmol) and 9-chloromethylantracene (390mg, 1.72mmol) was heated at reflux in toluene (20ml) under argon overnight (16 hours). The solution was then cooled to room temperature and the resulting precipitate filtered. The residue was recrystallised from chloroform/petroleum ether to give the title product (531mg, 60%) as a yellow solid, m.p.: 165 - 168 °C. ¹H NMR (500 MHz, CDCl₃): δ = 9.22 (d, *J* = 8.7 Hz, 1H), 8.90 (d, *J* = 8.2 Hz, 1H), 8.87 - 8.80 (m, 1H), 8.44 (d, *J* = 9.0 Hz, 1H), 8.07 - 8.00 (m, 1H), 7.89 (s, 1H), 7.57 (t, *J* = 8.6 Hz, 2H), 7.48 (d, *J* = 8.3 Hz, 1H), 7.31 - 7.17 (m, 3H), 7.15 - 7.03 (m, 2H), 7.00 - 6.86 (m, 3H), 6.49 (d, *J* = 13.7 Hz, 1H), 5.64 - 5.54 (m, 1H), 5.03 (d, *J* = 10.5 Hz, 1H), 4.87 (d, *J* = 17.2 Hz, 1H), 4.77 - 4.60 (m, 1H), 4.48 - 4.38 (m, 1H), 4.25 (t, *J* = 11.6 Hz, 1H), 2.55 - 2.45 (m, 1H), 2.36 - 2.28 (m, 1H), 1.95 (t, *J* = 12.8 Hz, 1H), 1.78 - 1.60 (m, 3H), 1.55 - 1.49 (m, 1H), 1.40 - 1.31 (m, 1H), 0.70 - 0.58 (m, 1H). ¹³C NMR (125 MHz, CDCl₃): δ = 149.4, 147.0, 145.5, 135.5, 133.1, 132.7, 130.9, 130.3, 130.0, 129.0, 128.5, 128.4, 128.2, 127.6, 127.3, 126.8, 124.9, 124.9, 124.6, 124.4, 124.1, 120.0, 118.1, 117.5, 67.6, 66.8, 57.5, 54.2, 54.0, 38.1, 26.3, 24.1, 22.6. Spectroscopic data are in agreement with literature.²²

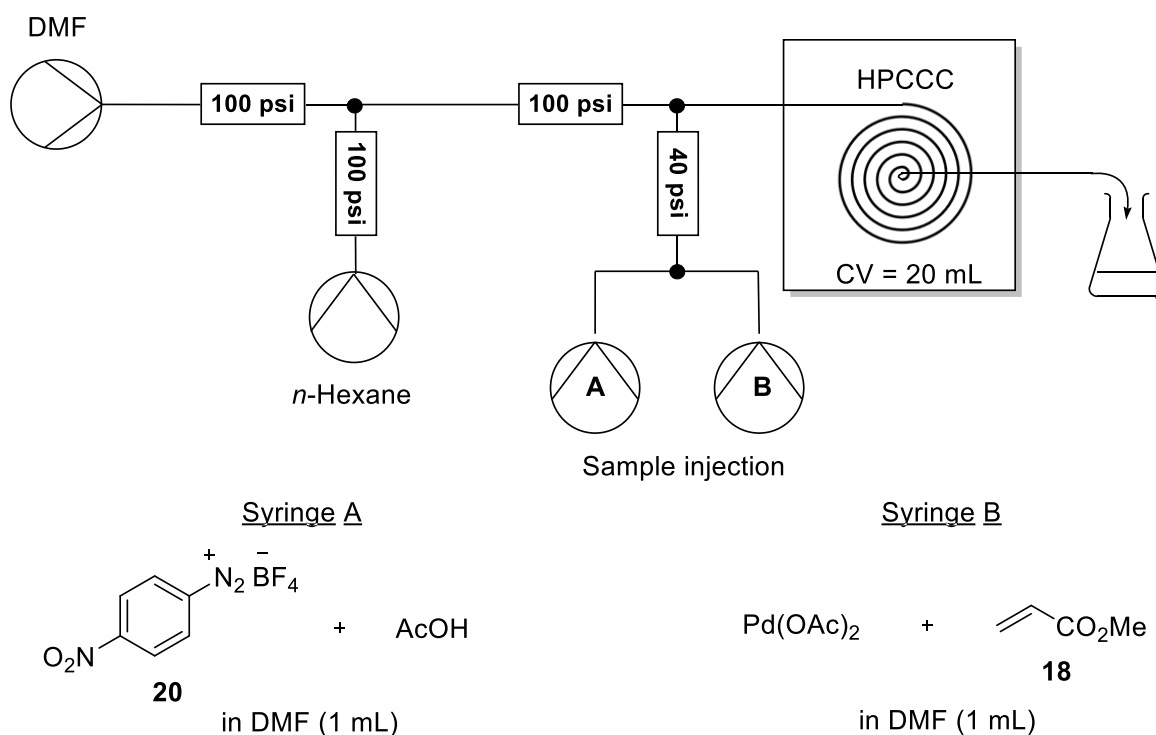
(2R, 5R, 1'S)-1-(1-anthracenyl)methyl-5-ethylene-2-[1-benzyloxy-1-(quinol-4-yl)]methyl-1-azoniabicyclo[2.2.2]octane bromide (15)



50% aqueous sodium hydroxide (0.25 mL, 0.325 mmol) was added to a solution of the *N*-anthracene salt (**10**) (0.5 g, 0.95 mmol) and benzyl bromide (0.325 mL, 2.75 mmol) in dichloromethane (8 mL) and the mixture was stirred vigorously for 5 hours (1500 rpm). Water was then added and the aqueous layer extracted with dichloromethane (10 mL). The combined organics were dried over magnesium sulfate, filtered, and concentrated under reduced pressure. The residue was purified by chromatography on silica gel to give the title product (0.40g, 65%) as a yellow solid, m.p.: 125 - 127 °C. ¹H NMR (500 MHz, CDCl₃): δ = 9.90 - 9.60 (m, 1H), 9.39 - 8.92 (m, 2H), 8.59 (s, 1H), 8.23 - 8.13 (m, 1H), 8.10 - 7.93 (m, 3H), 7.90 - 7.69 (m, 4H) 7.63 - 7.47 (m, 6H), 7.39 - 7.30 (m, 2H), 6.85 - 6.58 (m, 2H), 5.97 - 5.39 (m, 4H), 5.31 - 5.18 (m, 1H), 5.03 - 4.81 (m, 3H), 4.40 - 4.27 (m, 1H), 3.03 - 2.87 (m, 1H), 2.68 - 2.33 (m, 2H), 2.12 - 1.98 (m, 3H), 1.65 - 1.52 (m, 1H), 1.27 - 1.21 (m, 1H). ¹³C NMR (125 MHz, CDCl₃): δ = 149.2, 148.7, 139.7, 136.4, 135.8, 134.0, 133.4, 132.4, 131.5, 130.9, 130.0, 129.2, 128.8, 128.7, 128.6, 128.6, 127.5, 127.5, 127.3, 127.1, 126.9, 126.1, 125.4, 124.9, 123.3, 118.9, 117.9, 117.6, 75.7, 71.3, 66.0, 57.2, 55.2, 54.9, 37.7, 26.4, 23.9, 23.1. HRMS (ESP): [M+Br]⁺ calc 575.3073 found 575.3062 (1.9 ppm) [C₄₁H₃₉N₂O]⁺. Spectroscopic data are in agreement with literature.²²

4.3. Heck reaction

4.3.1. HPCCC setup and general procedure for the diazonium Heck reaction

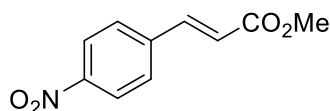


This reaction was performed under reverse phase HPCCC conditions (*n*-hexane employed as stationary phase, head-to-tail mode). Firstly, mobile phase (DMF) is pumped through the column to displace any aqueous solvent used in the washing of the column. This allows easy detection of stationary phase elution, and also stops the stationary phase being diluted by the water. To fill the HPCCC column with stationary phase, *n*-hexane was pumped through the column until the *n*-hexane was observed at the outlet. Upon filling of the machine, the stationary phase pump was switched off and the HPCCC was spun at 2100 rpm. The mobile phase (DMF) was then pumped at 0.7 mL/min to allow equilibration of the stationary phase. Once stationary phase stopped eluting from the column, equilibration had been achieved.

Sample injection

A solution of *p*-nitrobenzenediazonium tetrafluoroborate (25mg, 0.107mmol) and AcOH (0.083 mL) dissolved in DMF (1 mL) was loaded into syringe A. A solution of Pd(OAc)₂ (2.4 mg, 0.0107 mmol) and methyl acrylate (0.01 mL, 0.107 mmol) dissolved in DMF (1 mL) was loaded into syringe B. The sample was injected into the mobile phase using a syringe pump at the required flow rate. The reaction product was quenched in water and diluted with ethyl acetate. The product was extracted with ethyl acetate (3 times), and the organic layer was washed with water (4 times), dried over MgSO₄, filtered, and concentrated in vacuo. The residue was purified by flash column chromatography to afford the target product (15 mg, 69% isolated yield) as an oil.

4.3.2. Characterisation of Heck reaction products methyl (E)-3-(4-nitrophenyl)acrylate (21)

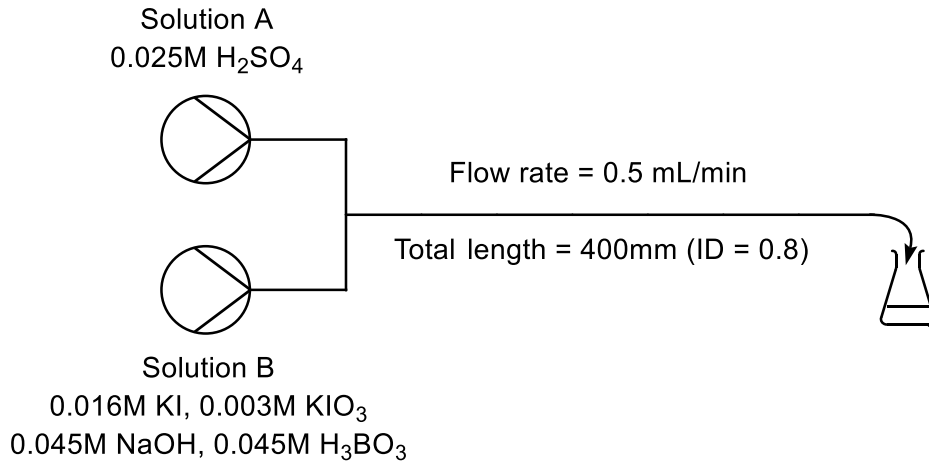


Performed according to the “HPCCC General Procedure” for Heck reactions. Compound afforded as a pale yellow oil (15 mg, 69%).

¹H NMR (500 MHz, CDCl₃): δ = 8.25 (d, *J* = 8.8 Hz, 2H, Ar-H), 7.72 (d, *J* = 16.1 Hz, 1H, C=C-H), 7.69 - 7.65 (m, 2H, Ar-H), 6.56 (d, *J* = 16.0 Hz, 1H, C=C-H), 3.84 (s, 3H, CH₃).
¹³C NMR (100 MHz, CDCl₃): δ = 166.5 (C=O), 148.6, 141.9, 140.5, 128.7, 124.2, 122.1 (Ph, C=C), 52.1 (CH₃). Spectroscopic data are in agreement with literature.⁵⁹

4.4. Calculation of Segregation index

Calculation of X_s - flow rate = 0.5 mL/min



$$X_s = \frac{Y}{Y_{ST}} \quad (\text{eq. 4})$$

$$\text{Where: } Y = \frac{4([I_2] + [I_3^-])}{[H^+]_0} \quad (\text{eq. 5})$$

$$Y_{ST} = \frac{6[IO_3^-]_0}{6[IO_3^-]_0 + [H_2BO_3^-]_0} \quad (\text{eq. 6})$$

The concentration of I_3^- was calculated using the Beer Lambert law ($\epsilon_{353 \text{ nm}}$ of $I_3^- = 26,047$ L/mol/cm).⁴⁰

$$[I_3^-] = \frac{A}{(\epsilon_{353 \text{ nm}}) (l)}$$

$$[I_3^-] = \frac{1.4926}{(26047) (1)} = 5.25 \times 10^{-5} \text{ mol/L}$$

To work out the concentration of I_2 , K_B first needs to be calculated using equation 2:

$$\text{Log}_{10}(K_B) = \frac{555}{T} + 7.355 - 2.575 \log_{10}(T) \quad (\text{eq. 2})$$

$$\text{Log}_{10}(K_B) = \frac{555}{292} + 7.355 - 2.575 \log_{10}(292)$$

$$\text{Log}_{10}(K_B) = 2.907$$

$$K_B = 808$$

The calculated equilibrium constant can be substituted into the mass balance equation for I_2 (eq. 7).⁶⁰ This quadratic equation is then solved to give the concentration of I_2 :

$$\frac{5}{3}[I_2]^2 + ([I^-]_0 - \frac{8}{3}[I_3^-])[I_2] - \frac{[I_3^-]}{K_B} \quad (\text{eq. 7})$$

$$\frac{5}{3}[I_2]^2 + (0.016 - \frac{8}{3} \times 5.73 \times 10^{-5})[I_2] - \frac{5.73 \times 10^{-5}}{808}$$

$$\frac{5}{3}[I_2]^2 + 0.0158 [I_2] - 7.094 \times 10^{-8} = 0$$

$$[I_2] = 4.48 \times 10^{-6} \text{ mol/L}$$

The segmentation index can now be calculated using the equations for Y and Y_{ST} :

$$Y = \frac{4([I_2] + [I_3^-])}{[H^+]_0} \quad (\text{eq. 5})$$

$$Y = \frac{4(4.48 \times 10^{-6} + 5.73 \times 10^{-5})}{0.025} = 9.88 \times 10^{-3}$$

$$Y_{ST} = \frac{6[IO_3^-]_0}{6[IO_3^-]_0 + [H_2BO_3^-]_0} \quad (\text{eq. 6})$$

$$Y_{ST} = \frac{6(0.003)}{6(0.003) + 0.045} = 0.286$$

$$X_s = \frac{Y}{Y_{ST}} \quad (\text{eq. 4})$$

$$\frac{9.88 \times 10^{-3}}{0.286} = 0.0345$$

The procedure was repeated to work out the segregation index at higher flow rates (1.0 mL/min and 2.0 mL/min).

5. References

1. Berthod, A. *Countercurrent Chromatography, The Support Free Liquid Stationary Phase*, Elsevier, Amsterdam, 2002, Vol. 38.
2. D. J. Keay, L. Janaway, High Performance Countercurrent Chromatography (HPLCCC) finally allows the advantages of liquid/liquid chromatography to be used in mainstream purification in medicinal chemistry, *Chromatography today*, 2008, 32-34.
3. a) W. D. Conway, *Countercurrent Chromatography Apparatus Theory & Applications*, VCH Publishers, New York, 1990. b) P. Wood, PhD thesis, Brunel University, 2002.
4. J. B. Friesen, G. F. Pauli, *Journal of Liquid Chromatography & Related Technologies*, **2005**, 28, 2777-2806.
5. A. Berthod, *Journal of Chromatography*, **1991**, 550, 677-693.
6. Y. Ito, W. D. Conway, *Journal of Chromatography*, **1984**, 301, 405-414.
7. a) Q. Du, H. Jiang, Y. Ito, *Journal of Liquid Chromatography & Related Technologies*, **2001**, 24, 2363-2369. b) L. Chen, D. E. Games, J. Jones, H. Kidwell, *Journal of Liquid Chromatography & Related Technologies*, **2003**, 26, 1623-1636. c) H. Oka, Y. Ikai, J. Hayakawa, K. Harada, M. Suzuki, A. Shimizu, T. Hayashi, K. Takeba, H. Nakazawa, Y. Ito, *Journal of Chromatography A*, **1996**, 723, 61-68.
8. K. Skalicka-Woźniak, *Phytochem. Rev.* **2014**, 13, 547-572.
9. E. Koziół, F. S. S. Deniz, I. E. Orhan, L. Marcourt, B. Budzyńska, J. Wolfender, A. D. Crawford, K. Skalick- Woźniak, *Phytomedicine* **2019**, 54, 259-264.
10. A. Urbain, A. Marston, K. Hostettmann, *Pharm. Biology.* **2005**, 43, 647-650.
11. C. Deamicis, Q. Yang, C. Bright, N. A. Edwards, G. H. Harris, S. Kaur, P. L. Wood, P. Hewitson, S. Ignatova, *Org. Process Res. Dev.* **2017**, 21, 1638-1643.
12. a) M. Mąkosza, *Tetrahedron Lett.* **1966**, 7, 5489-5492. b) M. Mąkosza, *Tetrahedron Lett.* **1969**, 10, 673-676.
13. S. Shirakawa, K. Maruoka, *Angew. Chem. Int. Ed.* **2013**, 52, 4312-4348.
14. C. M. Starks, *J. Am. Chem. Soc.* **1971**, 93, 195-199.
15. T. Ooi, K. Maruoka, *Angew. Chem. Int. Ed.* **2007**, 46, 4222-4266.

16. M. J. O'Donnell, W. D. Bennett, S. Wu, *J. Am. Chem. Soc.* **1989**, *111*, 2353-2355.
17. M. Małkośza, *Pure Appl. Chem.* **1975**, *43*, 439-462.
18. B. Lygo, P. G. Wainwright, *Tetrahedron Lett.* **1997**, *38*, 8595-8598.
19. E. J. Corey, F. Xu, M. C. Noe, *J. Am. Chem. Soc.* **1997**, *119*, 12414-12415.
20. T. Ooi, M. Kameda, K. Maruoka, *J. Am. Chem. Soc.* **2003**, *125*, 5139-5151.
21. R. Herchl, M. Waser, *Tetrahedron* **2014**, *70*, 1935-1960.
22. B. Lygo, P. G. Wainwright, *Tetrahedron* **1999**, *55*, 6289-6300.
23. T. Ooi, D. Ohara, M. Tamura, K. Maruoka, *J. Am. Chem. Soc.* **2004**, *126*, 6844-6845.
24. S. G. Newman, K. F. Jensen, *Green Chem.* **2013**, *15*, 1456-1472.
25. N. Weeranoppanant, *React. Chem. Eng.* **2019**, *4*, 235-243.
26. B. Ahmed-Omer, D. Barrow, T. Wirth, *Adv. Synth. Catal.* **2006**, *348*, 1043-1048.
27. M. J. Hutchings, B. Ahmed-Omer, T. Wirth in *Microreactors in Organic Chemistry and Catalysis*, Ed.: T. Wirth, Wiley-VCH, Weinheim, **2008**, pp 122-139.
28. J. Jovanovic, E. V. Rebrov, T. A. Nijhuis, V. Hessel, J. C. Schouten, *Ind. Eng. Chem. Res.* **2010**, *49*, 2681-2687.
29. M. Ueno, H. Hisamoto, T. Kitamori, S. Kobayashi, *Chem. Commun.* **2003**, 936-937.
30. D. De Zani, M. Colombo, *J. Flow Chem.* **2012**, *1*, 5-7.
31. a) E. Šinkovec, M. Krajnc, *Org. Process Res. Dev.* **2011**, *15*, 817-823. b) B. Ahmed-Omer, D. Barrow, T. Wirth, *Chem. Eng. J.* **2008**, S135, S280-S283. c) B. Ahmed, J. C. Brandt, T. Wirth, *Org. Biomol. Chem.* **2007**, *5*, 733-740
32. R. F. Heck, J. P. Nolley, *Org. Chem.* **1972**, *37*, 2320-2322.
33. C. Y. Hong, N. Kado, L. E. Overman, *J. Am. Chem. Soc.* **1993**, *115*, 11028-11029.
34. J. J. Master, J. T. Link, L. B. Snyder, W. B. Young, S. J. Danishefsky, *Angew. Chem. Int. Ed. Engl.* **1995**, *34*, 1723-1726.
35. P. Hu, H. M. Chi, K. C. DeBacker, X. Gong, J. H. Keim, I. T. Hsu, S. A. Snyder, *Nature*. **2019**, *569*, 703-707.
36. H. A. Dieck, R. F. Heck, *J. Am. Chem. Soc.*, **1974**, *96*, 1133-1136.
37. B. M. Bhanage, F. G. Zhao, M. Shirai, M. Arai, *Tetrahedron Lett.* **1998**, *39*, 9509-9512.
38. B. Ahmed-Omer, D. A. Barrow, T. Wirth, *Tetrahedron Lett.* **2009**, *50*, 3352-3355.

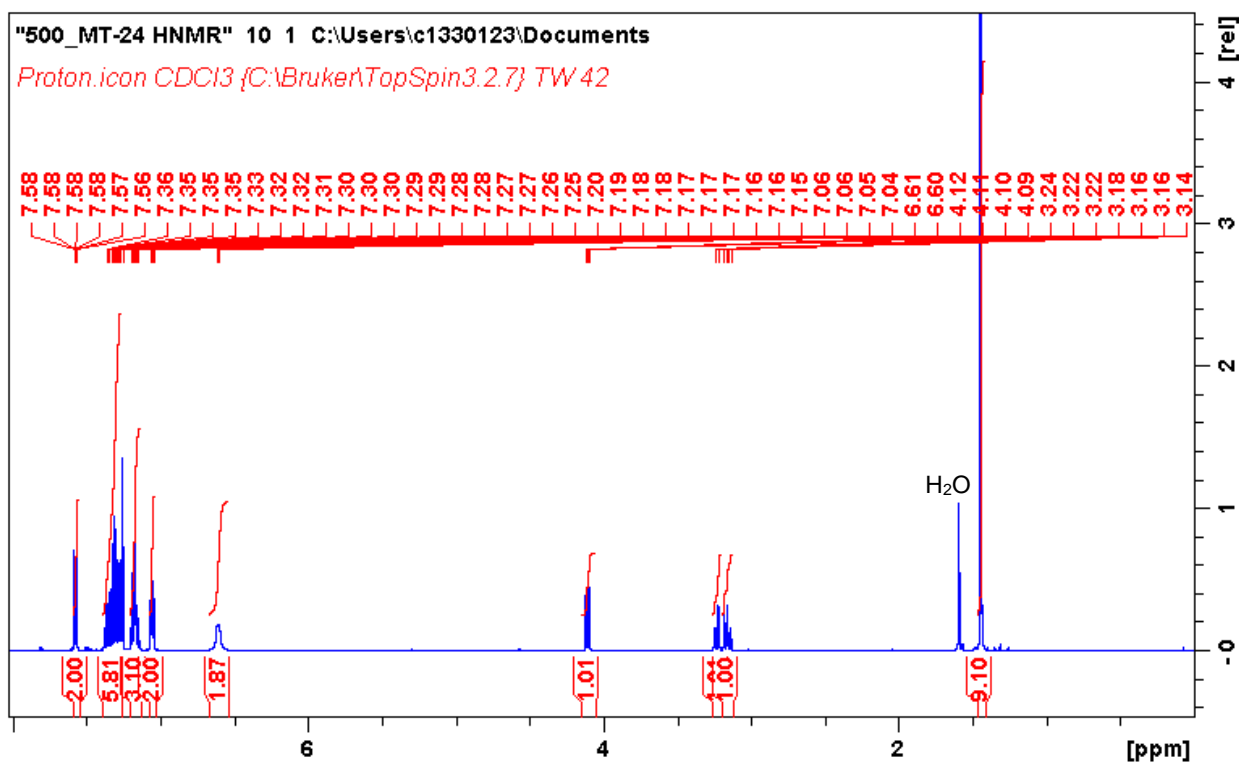
39. a) M. Engler, N. Kockmann, T. Kiefer, P. Woias, *Chem. Eng. J.* **2004**, *101*, 315-322. b) S.H. Wong, M.C.L. Ward, C.W. Wharton, *Sens. Actuators B* **2004**, *100*, 359-379. c) S. Ehlers, K. Elgeti, T. Menzel, G. Wiessmeier, *Chem. Eng. Process.* **2000**, *39*, 291-298.
40. J. M. Commenge, L. Falk, *Chem. Eng. Proc.* **2011**, *50*, 979-990.
41. N. Baccar, R. Kieffer, C. Charcosset, *Chem. Eng. J.* **2009**, *148*, 517-524
42. a) J. S Zhang, K. Wang, Y. C. Lu, G. S. Luo, *Chem. Eng. Process.* **2010**, *49*, 740-747. b) K. Wang, H. Zhang, Y. Shen, A. Adamo, K. F. Jensen, *React. Chem. Eng.* **2018**, *3*, 707-713. c) X. Shi, Y. Xiang, L. X. Wen, J. F. Chen, *Ind. Eng. Chem. Res.* 2012, *51*, 13944-13952
43. M. Yoo, B. Jeong, J. Lee, H. Park, S. Jew, *Org. Lett.* **2005**, *7*, 1129-1131.
44. A. Ghaini, M. Kashid, D. Agar, *Chem. Eng. Process.* **2010**, *49*, 358-366.
45. N. B. Mandava, Y. Ito, in *Countercurrent Chromatography: Theory and Practise*, Ed.: Y. Ito, Marcel Dekker, New York, **1988**, *44*, 79-442.
46. M. J. O'Neil, *The Merck Index - An Encyclopedia of Chemicals, Drugs, and Biologicals*, Royal Society of Chemistry, Cambridge, UK, 15th edn., **2013**, 1124
47. G. Akerloff, P. Bender, *J. Am. Chem. Soc.* **1941**, *63*, 1088.
48. M. J. O'Donnell, *Catalytic Asymmetric Syntheses*, Wiley-VCH, New York, 2nd edn., **2000**.
49. J. R. Burns, C. Ramshaw, *Chem. Eng. Commun.* **2002**, *189*, 1611-1628.
50. T. Ooi, M. Kameda, K. Maruoka, *J. Am. Chem. Soc.* **1999**, *121*, 6519-6520.
51. A. F. Littke, G. C. Fu, *J. Am. Chem. Soc.* **2001**, *123*, 6989-7000.
52. M. R. Netherton, G. C. Fu, *Org. Lett.* **2001**, *3*, 4295-4298.
53. M. Waser, K. Gratzer, R. Herchl, N. Müller, *Org. Biomol. Chem.* **2012**, *10*, 251-254.
54. T. Okino, Y. Takemoto, *Org. Lett.* **2001**, *3*, 1515-1517.
55. H. Young, Q. Guthrie, C. Proulx, *J. Org. Chem.* **2020**, *85*, 1748-1755.
56. X. Huo, J. Fu, X. He, J. Chen, F. Xie, W. Zhang, *Chem. Commun.* **2018**, *54*, 599-602.
57. P. Nun, V. Pèrez, M. Calmès, J. Martinez, F. Lamaty, *Chem. Eur. J.* **2012**, *18*, 3773-3779.
58. a) A. Siva, E. Murugan, *Synthesis* **2005**, *17*, 2927-2933. b) D. Feng, J. Wan, F. Teng, X. Ma, *Catal. Commun.* **2017**, *100*, 127-133.

59. Z. Zhang, Z. Wang, *J. Org. Chem.* **2006**, 71, 7485-7487.
60. M. N. Kashid, A. Renken, L. K. Minsker, in *Microstructured Devices for Chemical Processing*, Wiley-VCH, Weinheim, **2014**, pp 129-178

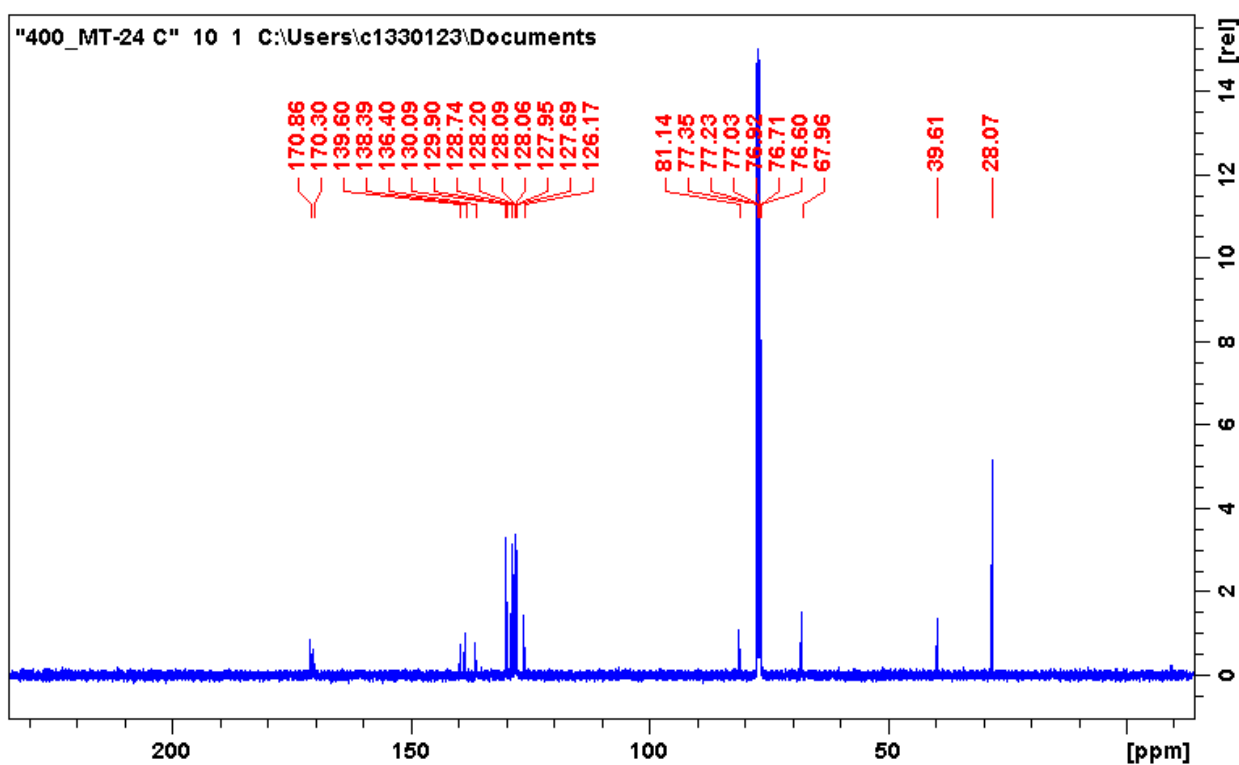
6. Appendix

(R) tert-butyl 2-[(diphenylmethylene)amino]-3-phenylpropanoate (22)

¹H NMR

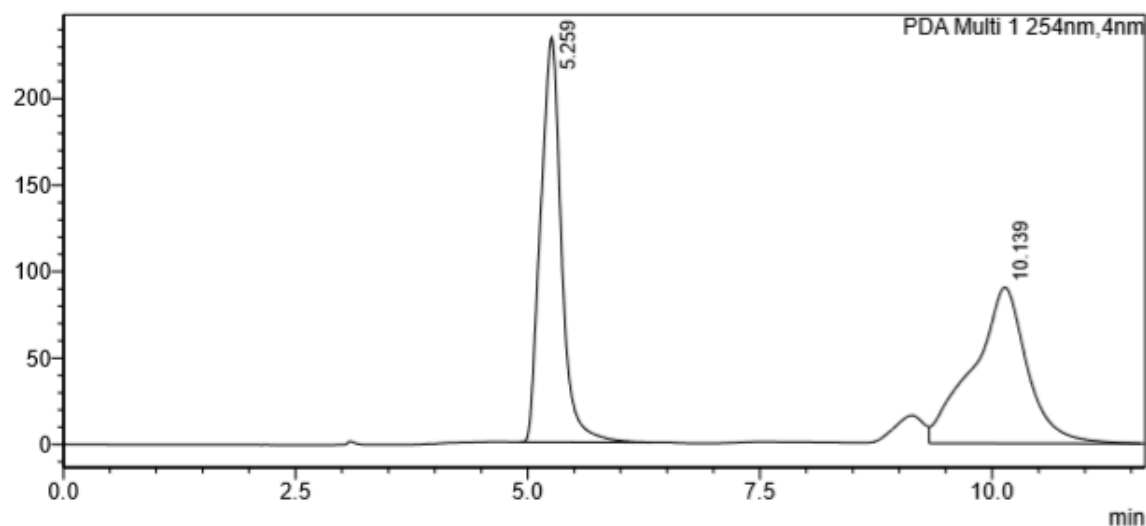


¹³C NMR



<Chromatogram>

mAU

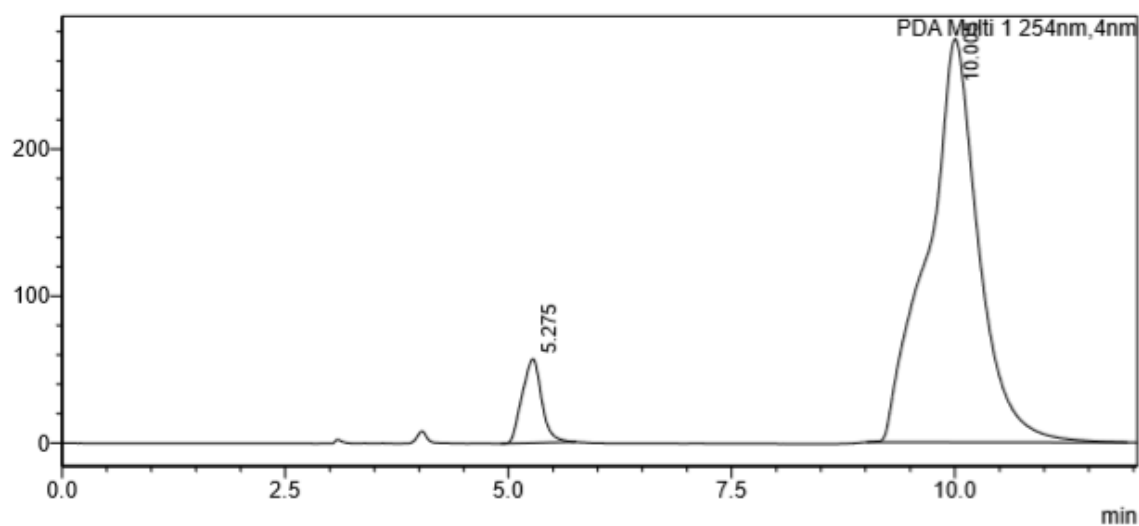


Peak Table
PDA Ch1 254nm

Ret. Time	Area%
5.259	49.731
10.139	50.269
	100.000

<Chromatogram>

mAU



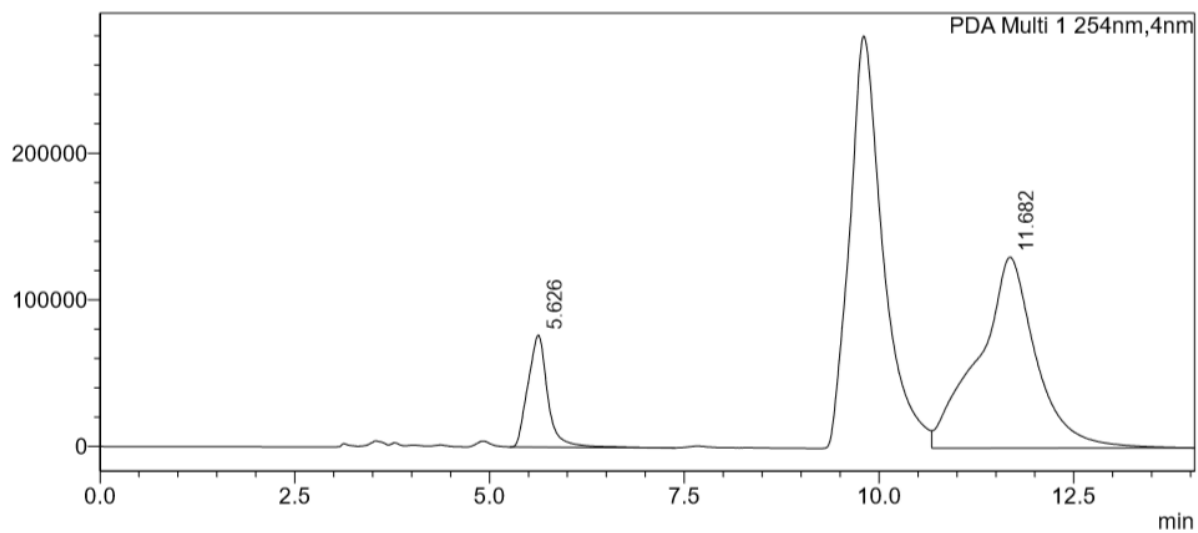
Peak Table
PDA Ch1 254nm

Ret. Time	Area%
5.275	7.378
10.005	92.622
	100.000

Figure 28: HPLC chromatograms for (**22**). Racemic mixture (top), chiral catalyzed mixture using catalyst **15** (bottom)

<Chromatogram>

uAU



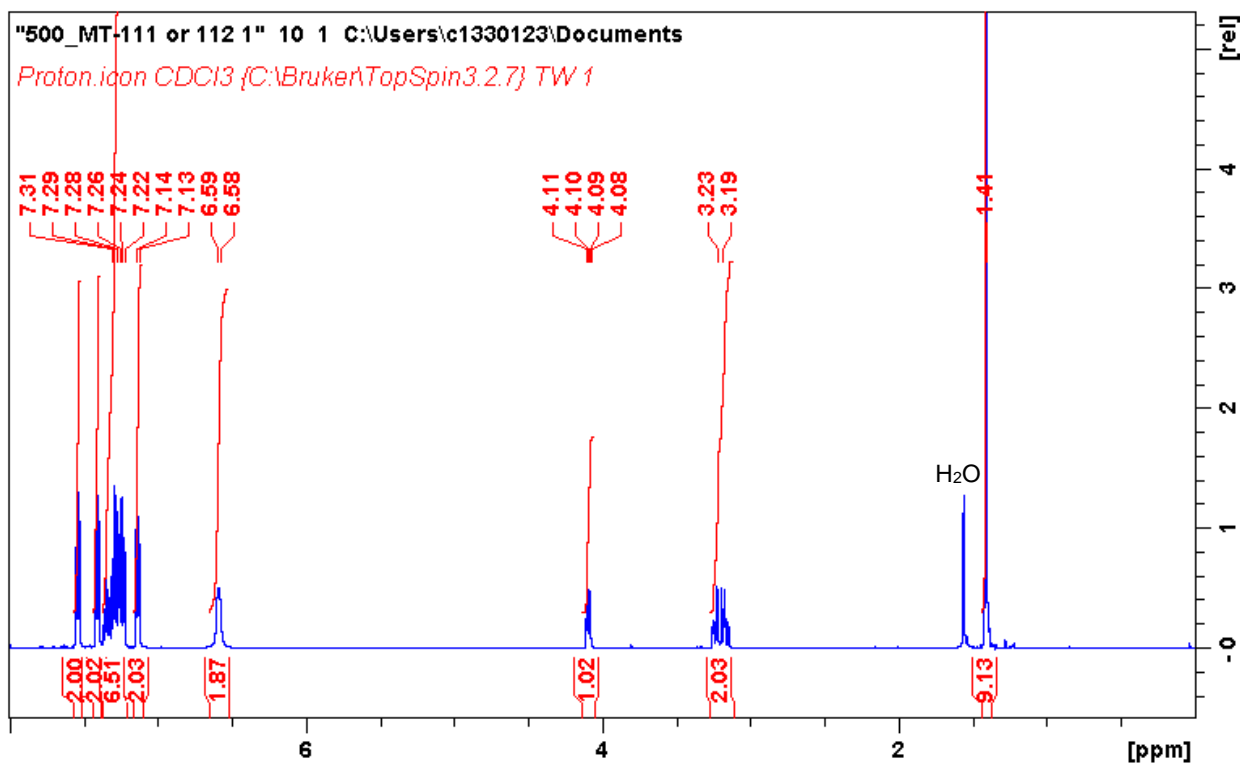
Peak Table
PDA Ch1 254nm

Ret. Time	Area%
5.626	16.820
11.682	83.180
	100.000

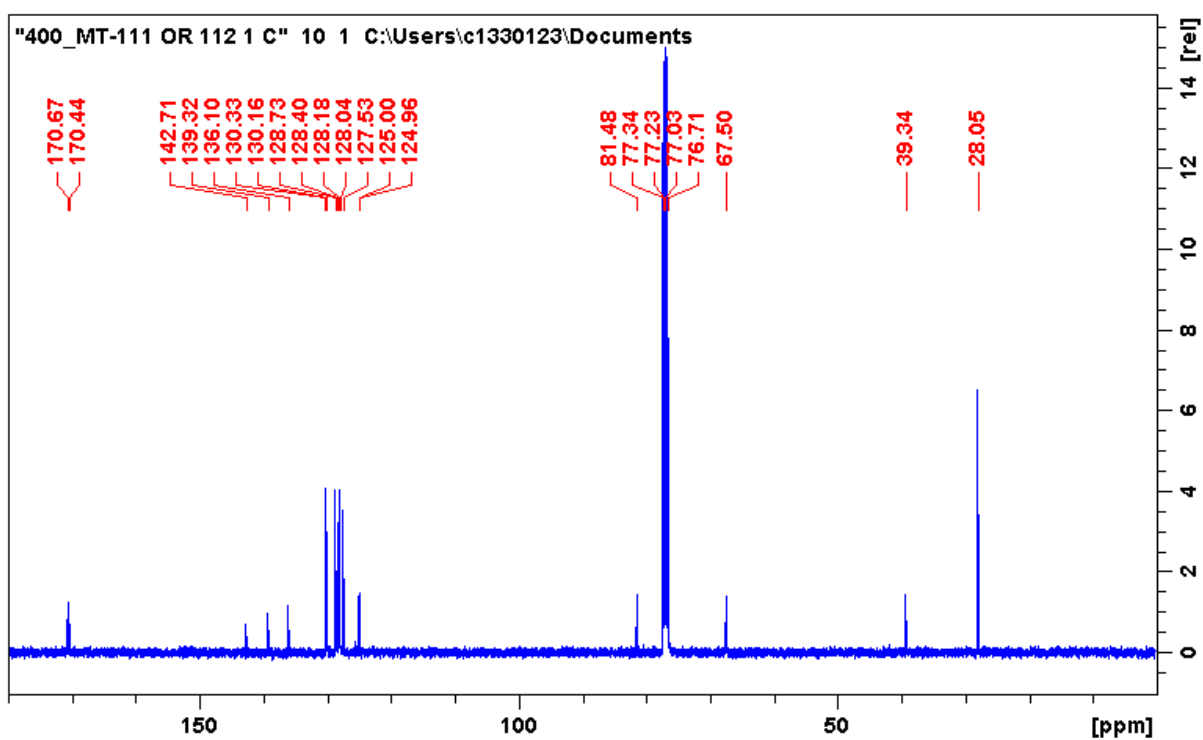
Figure 29: HPLC chromatogram for (22), using chiral catalyst 7.

(R) tert-butyl 2-[(diphenylmethylene)amino]-3-(4-(trifluoromethyl)phenyl)propanoate (25)

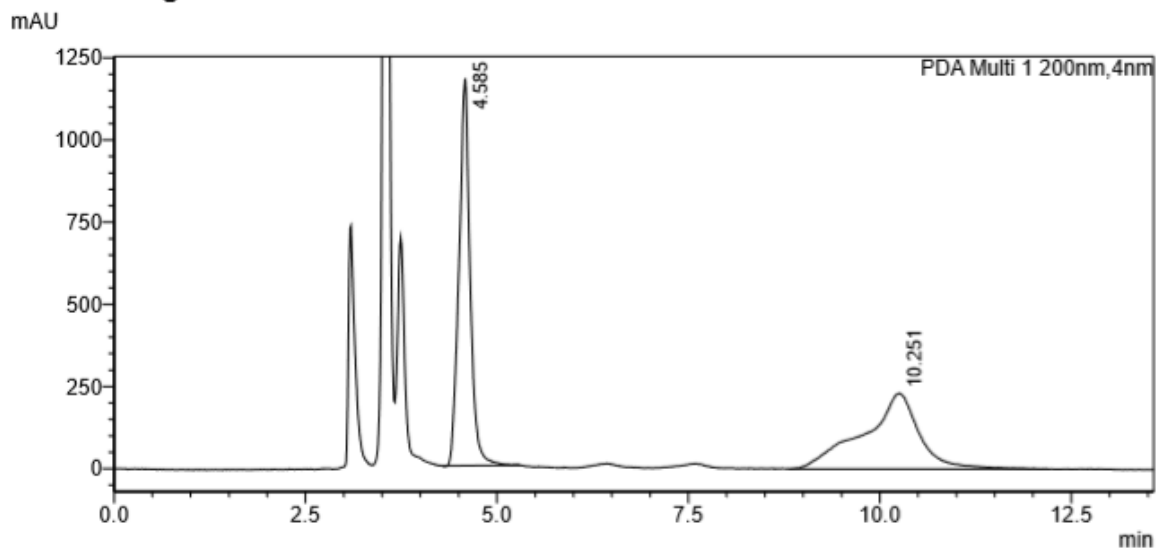
¹H NMR



¹³C NMR

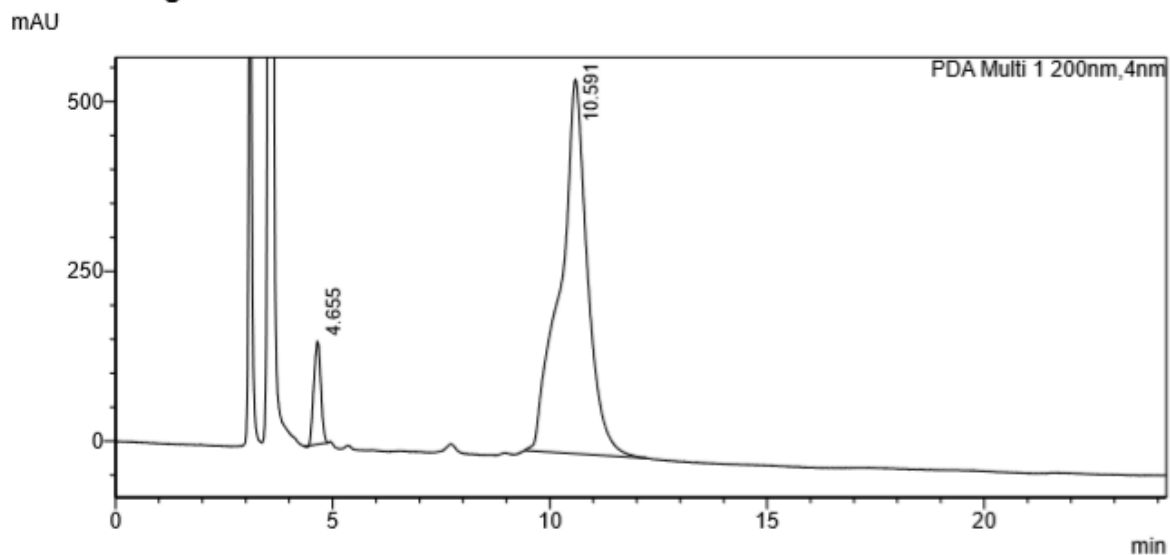


<Chromatogram>



Ret. Time	Area%
4.385	50.689
10.251	49.311
	100.000

<Chromatogram>

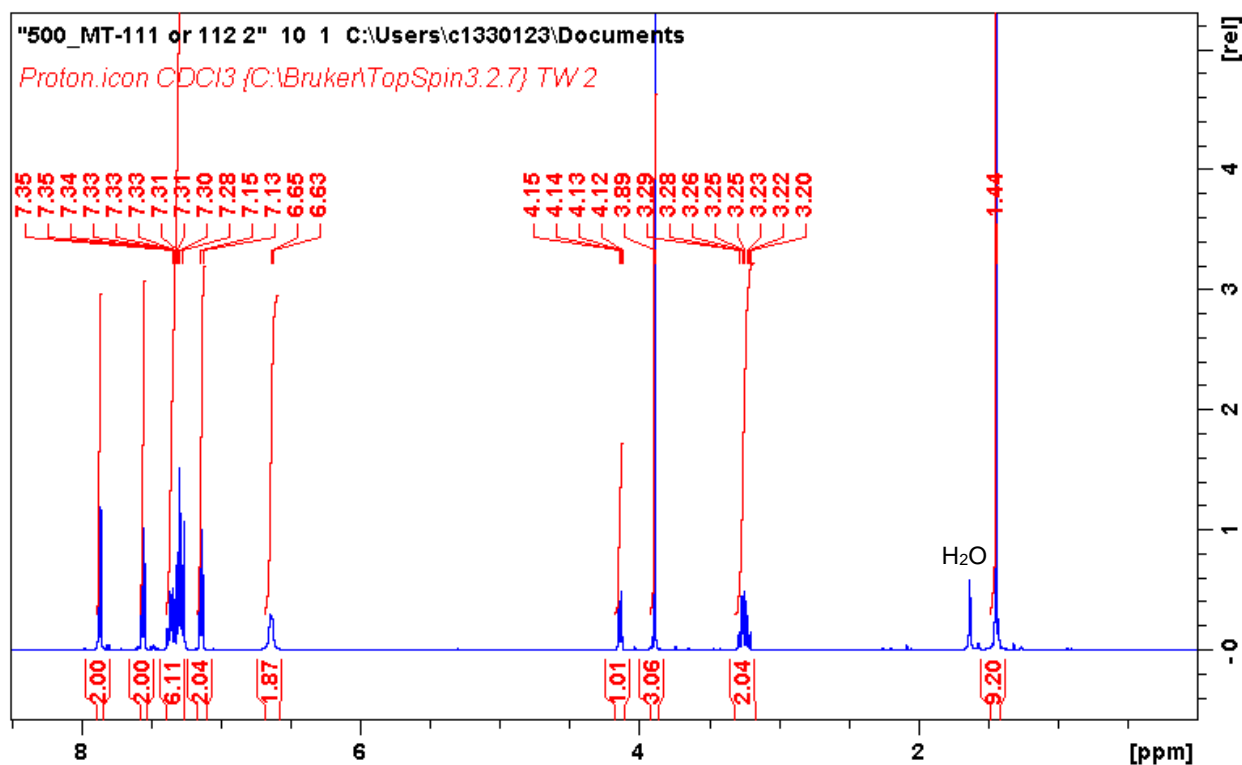


Ret. Time	Area%
4.655	6.651
10.591	93.349
	100.000

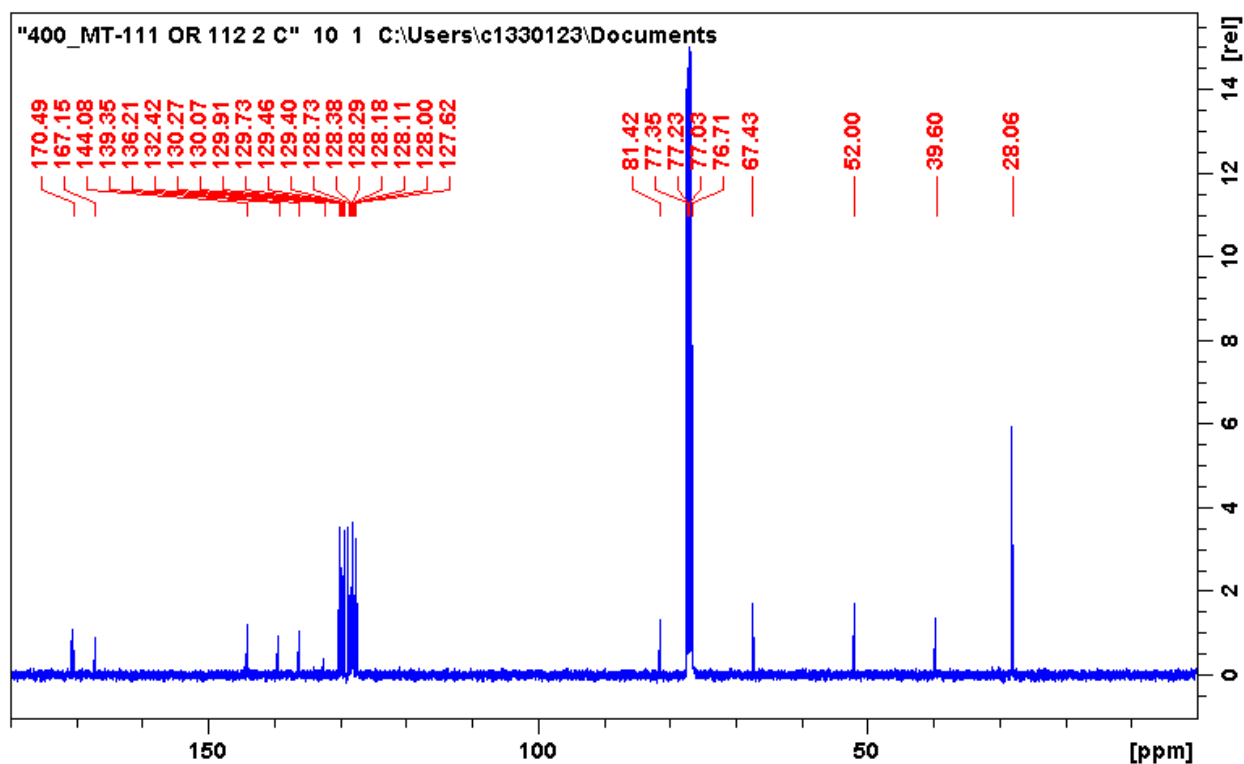
Figure 30: HPLC chromatograms for (25). Racemic mixture (top), chiral catalysed mixture using catalyst 15 (bottom)

methyl (*R*)-4-(3-(*tert*-butoxy)-2-((diphenylmethylene)amino)-3-oxopropyl)benzoate (26)

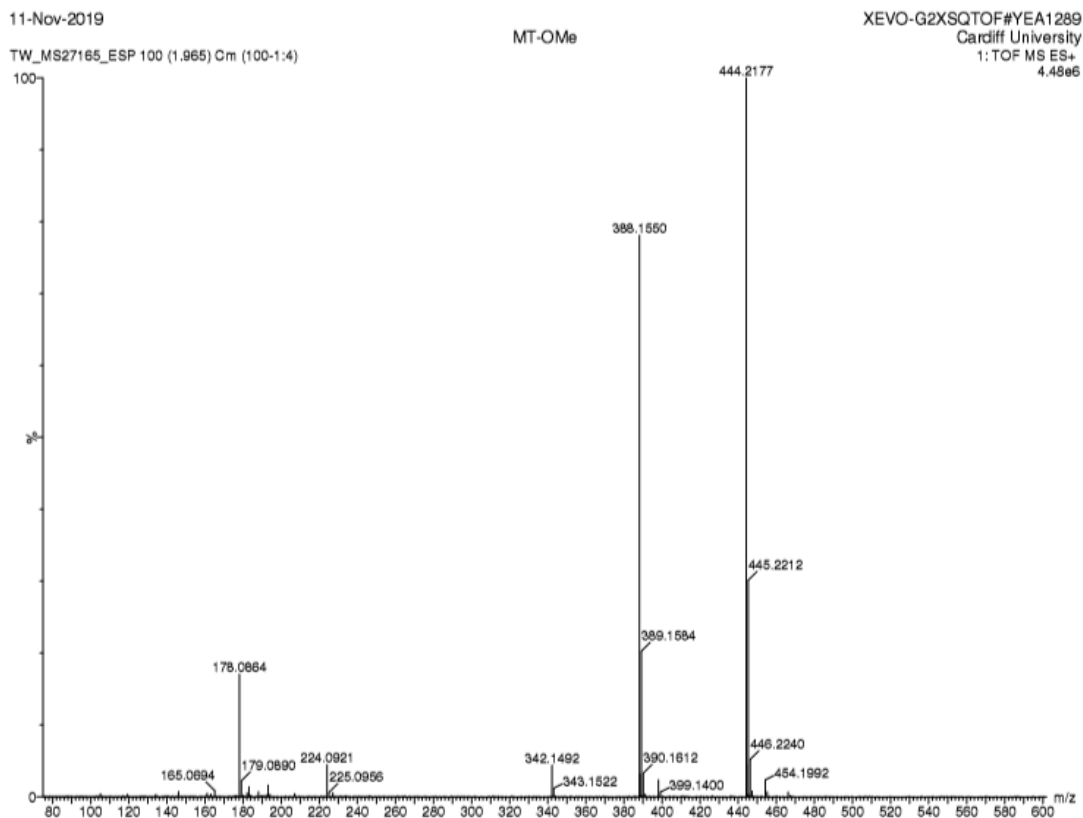
¹H NMR



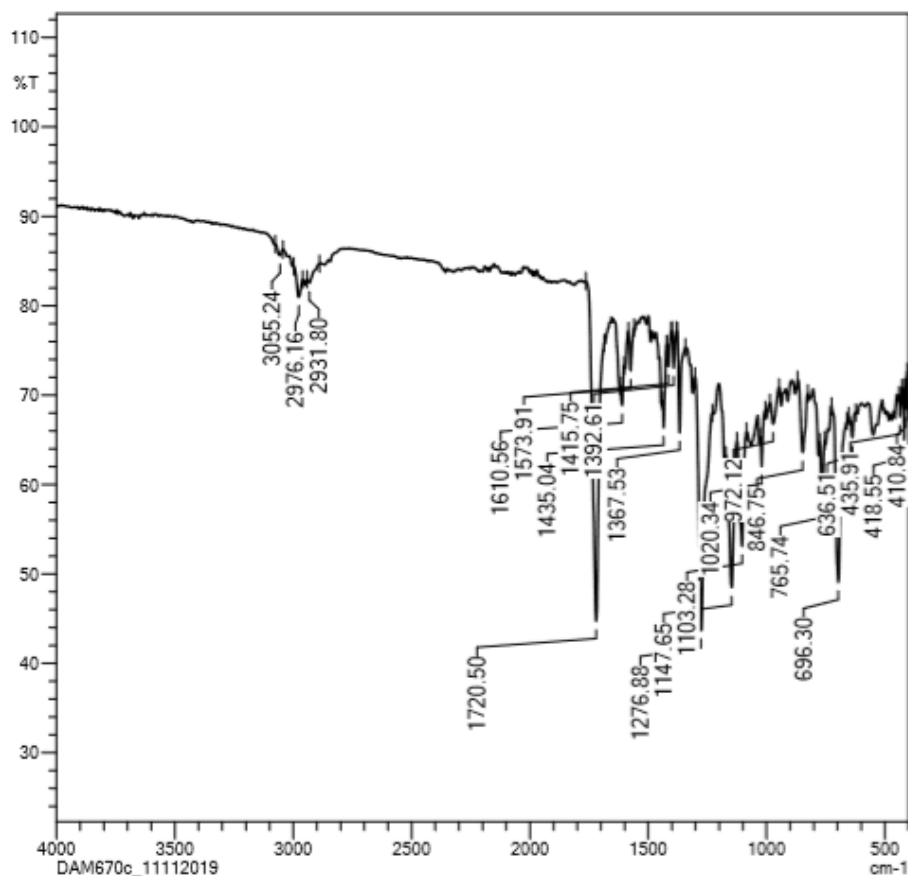
¹³C NMR



HRMS

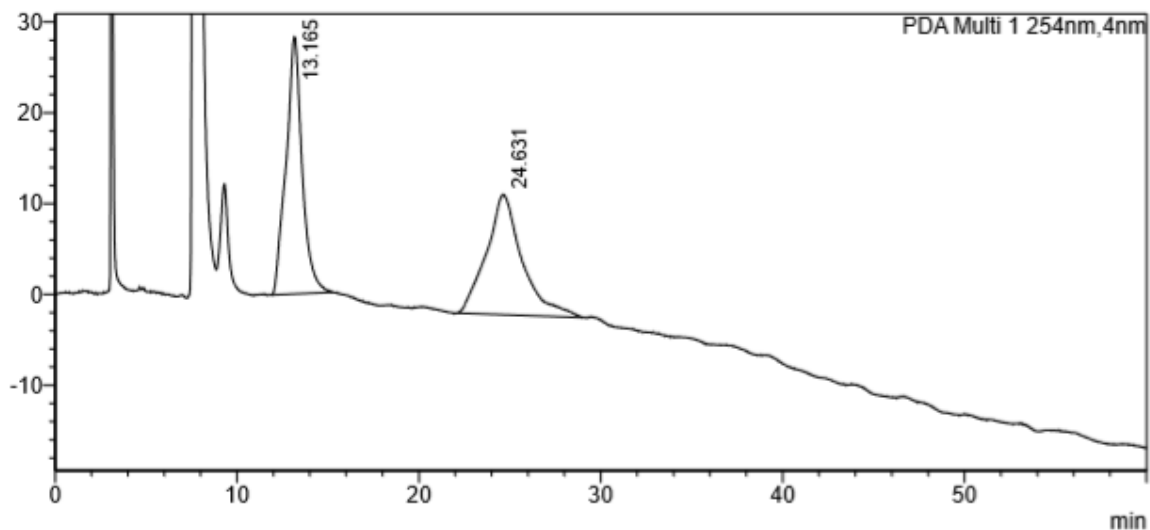


IR



<Chromatogram>

mAU

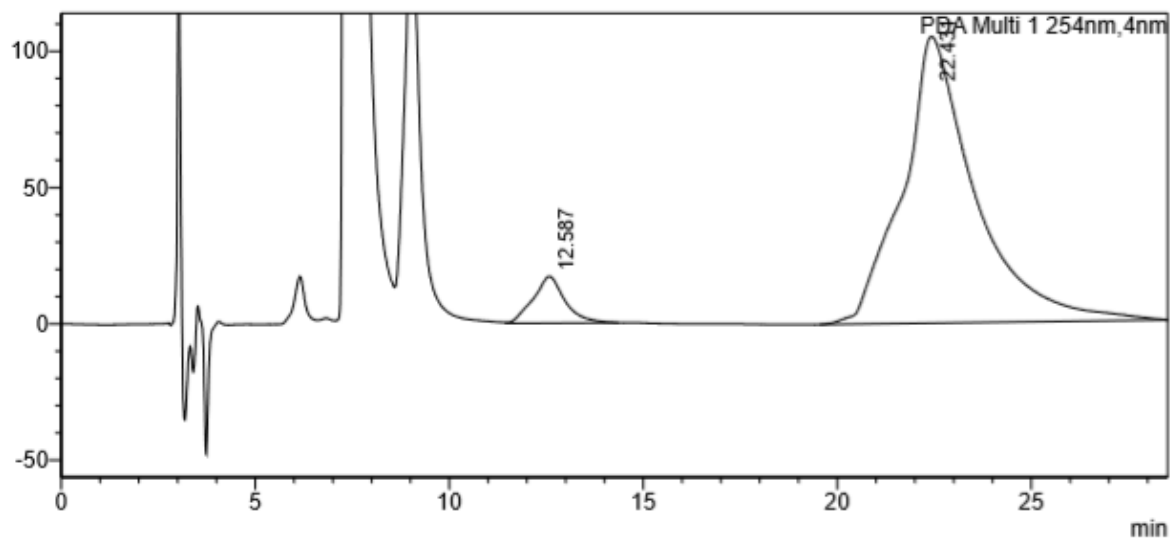


Peak Table
PDA Ch1 254nm

Ret. Time	Area%
13.165	49.056
24.631	50.944
	100.000

<Chromatogram>

mAU



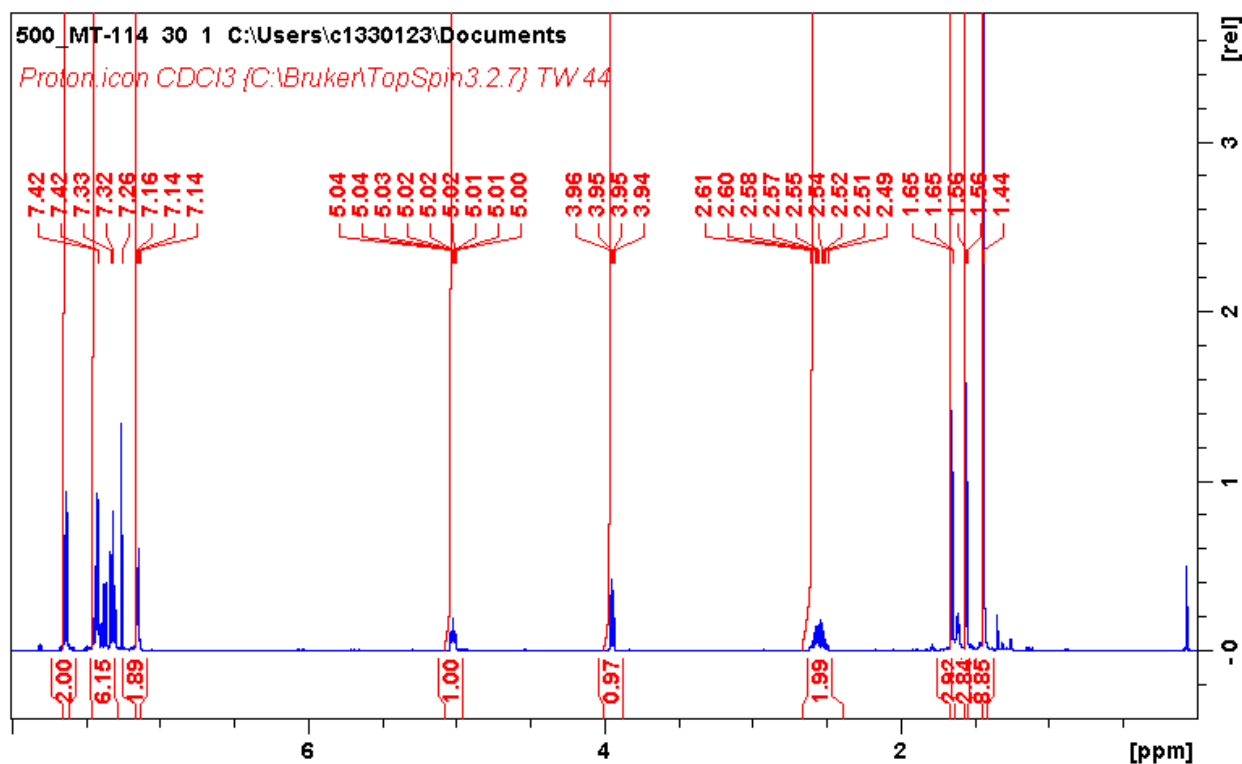
Peak Table
PDA Ch1 254nm

Ret. Time	Area%
12.587	6.685
22.431	93.315
	100.000

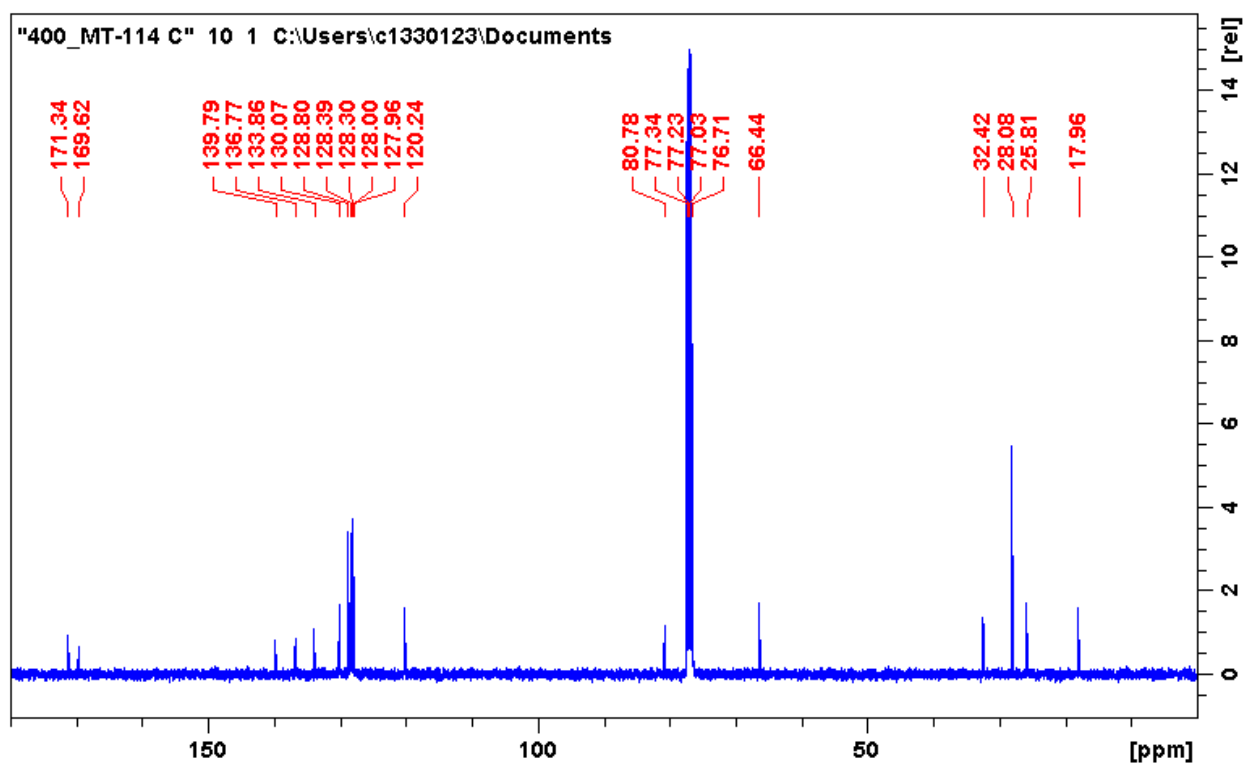
Figure 31: HPLC chromatograms for (26). Racemic mixture (top), chiral catalyzed mixture using catalyst 15 (bottom)

tert-butyl (R)-2-((diphenylmethylene)amino)-5-methylhex-4-enoate (27)

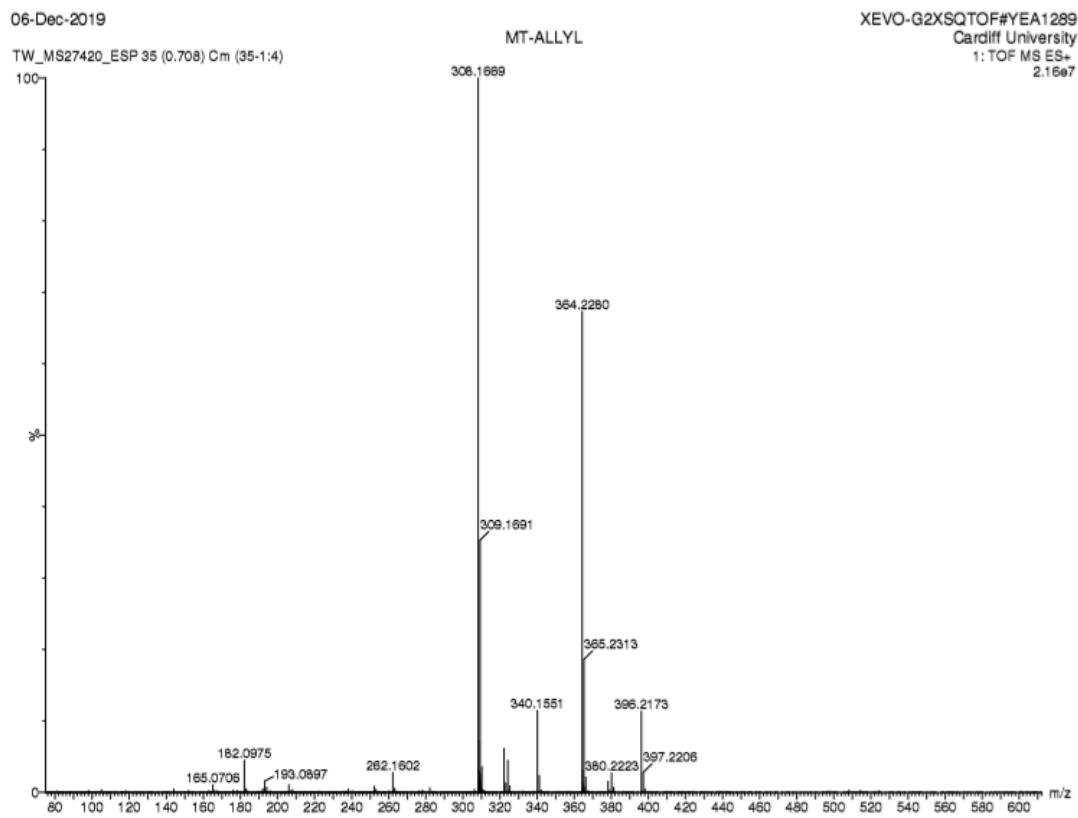
¹H NMR



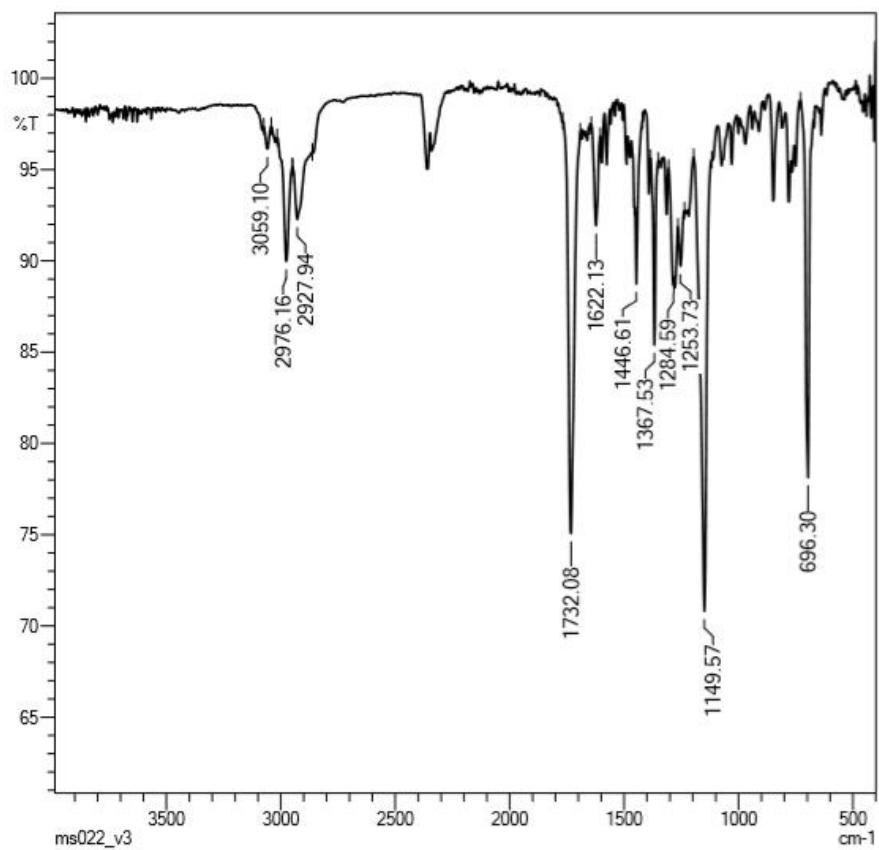
¹³C NMR



HRMS

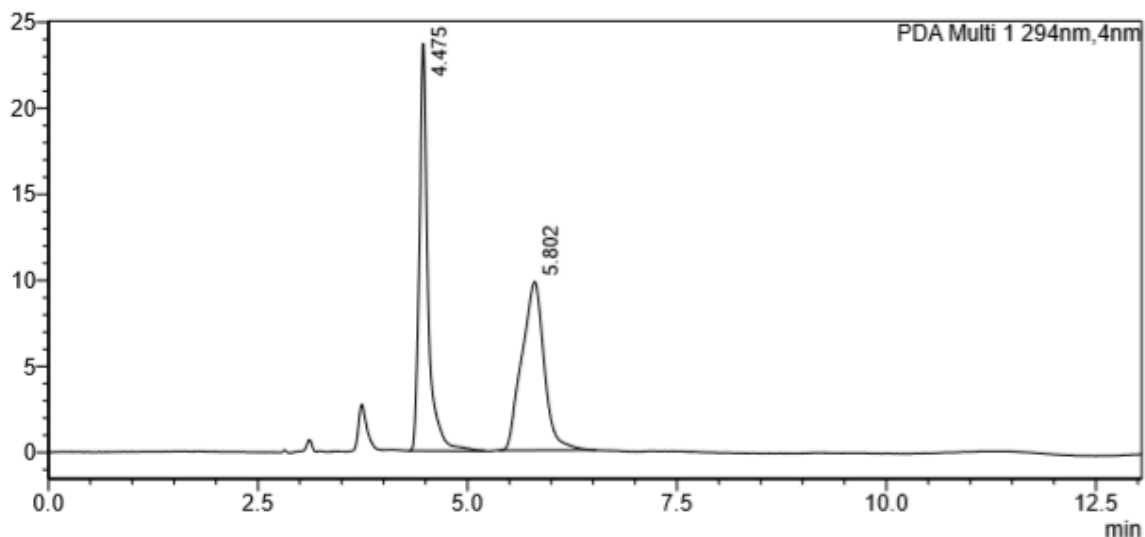


IR



<Chromatogram>

mAU

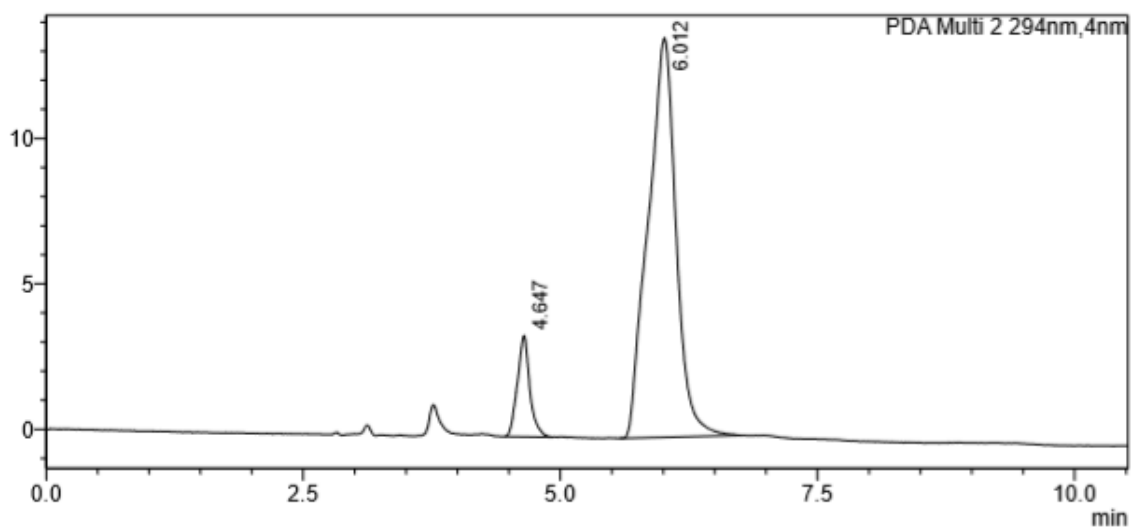


Peak Table

Ret. Time	Area%
4.475	48.563
5.802	51.437
	100.000

<Chromatogram>

mAU



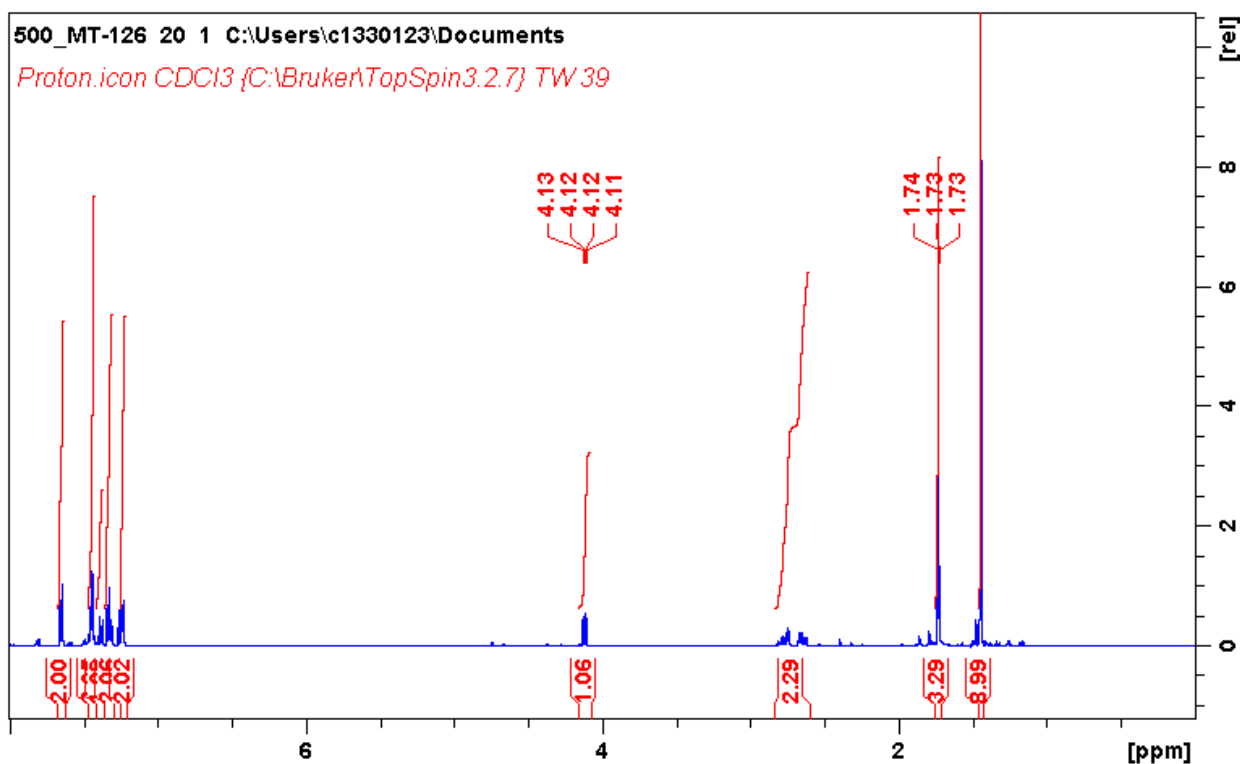
Peak Table

Ret. Time	Area%
4.647	10.115
6.012	89.885
	100.000

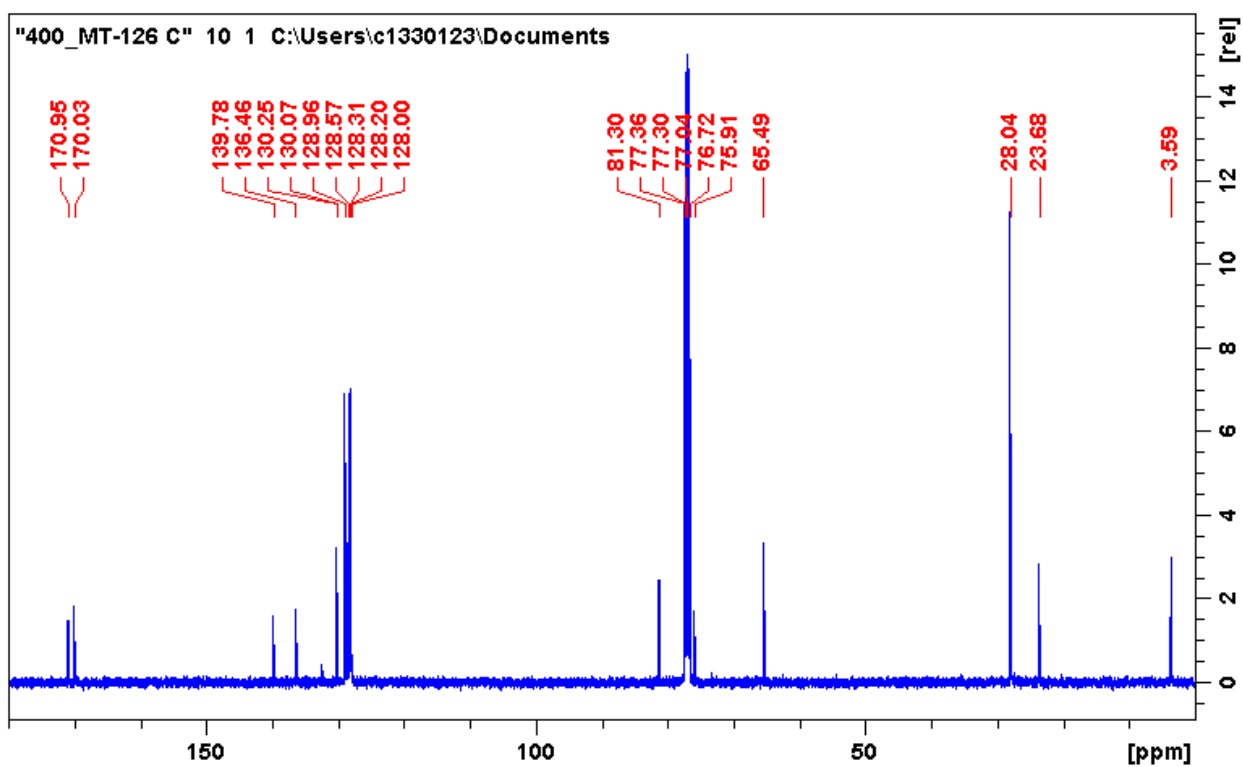
Figure 32: HPLC chromatograms for (27). Racemic mixture (top), chiral catalysed mixture using catalyst 15 (bottom)

tert-butyl (R)-2-((diphenylmethylene)amino)hex-4-ynoate (28)

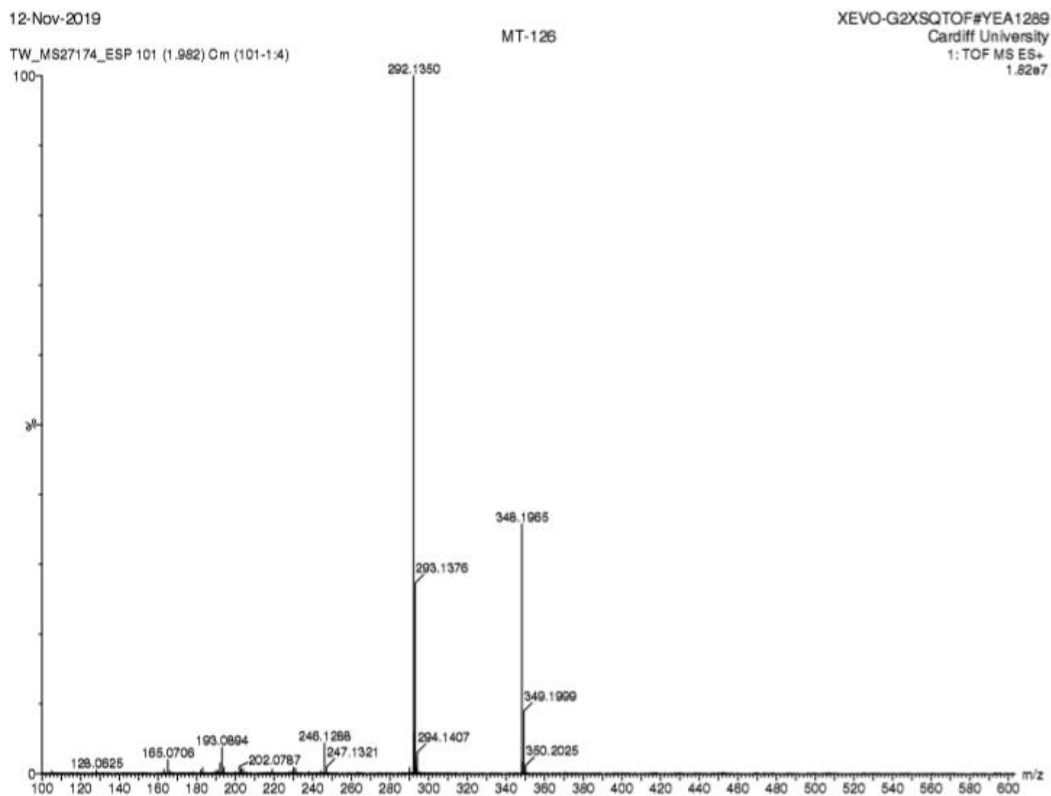
¹H NMR



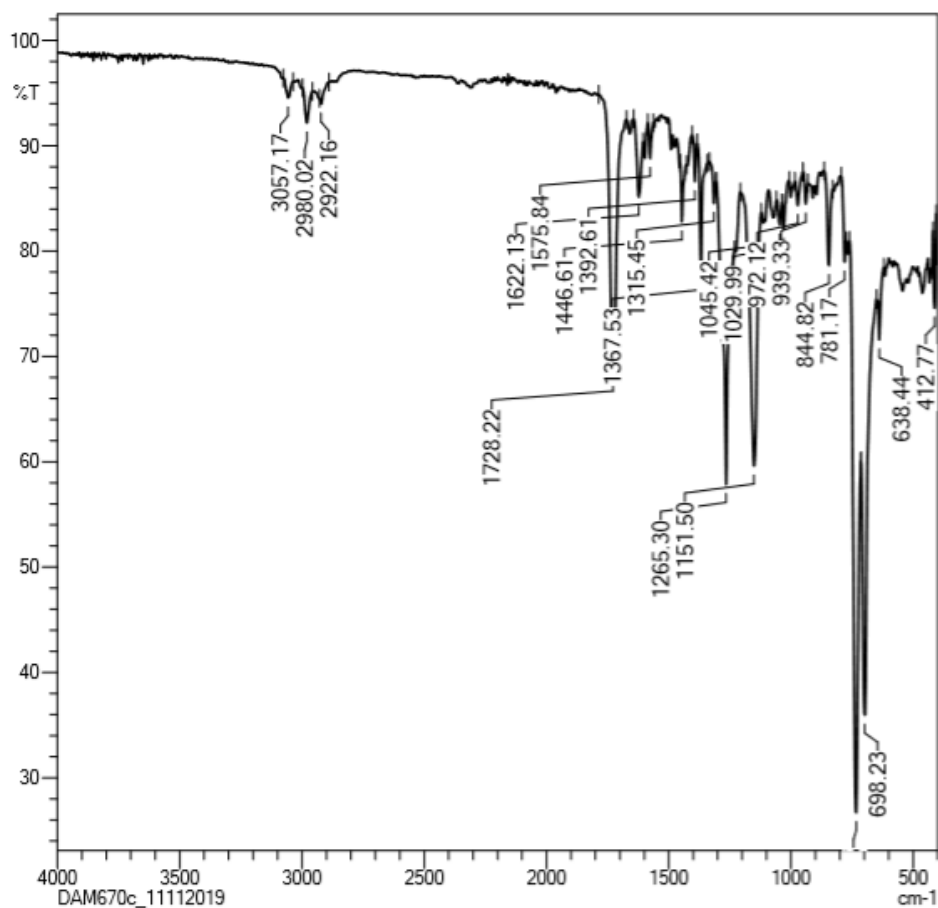
¹³C NMR



HRMS

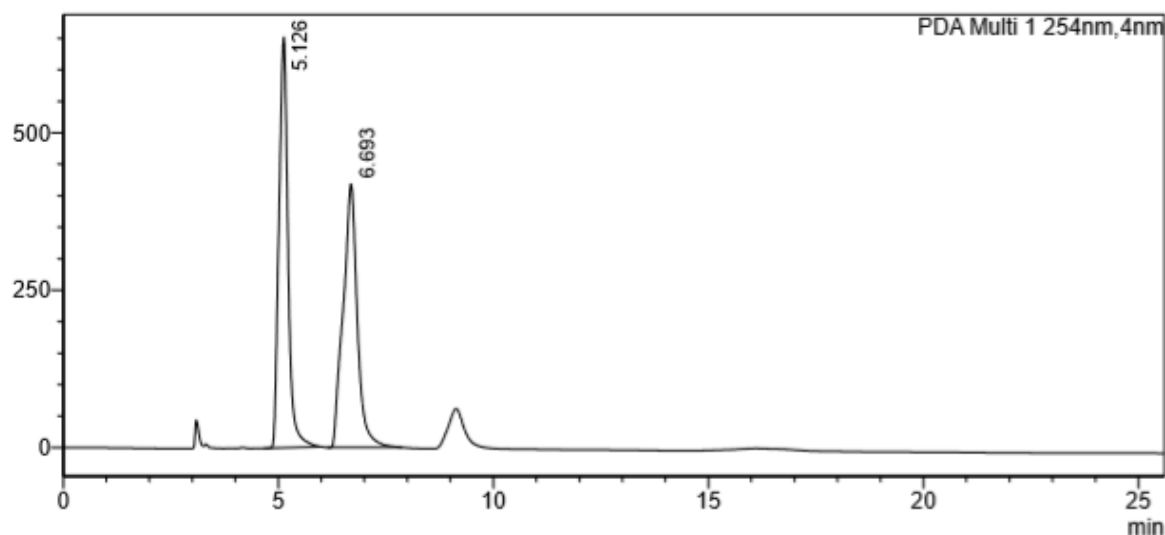


IR



<Chromatogram>

mAU

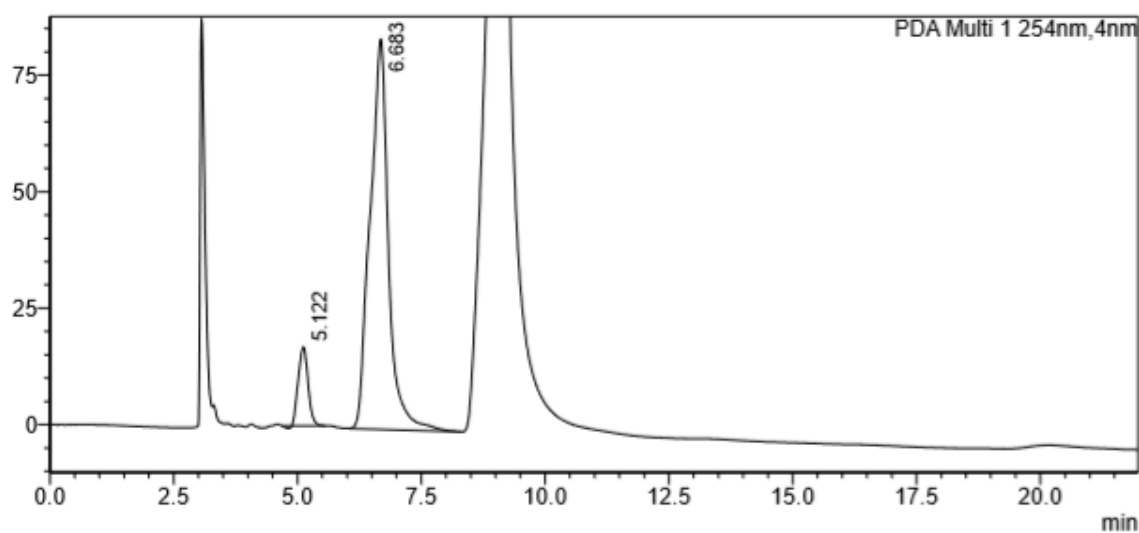


Peak Table

Ret. Time	Area%
5.126	49.934
6.693	50.066
	100.000

<Chromatogram>

mAU



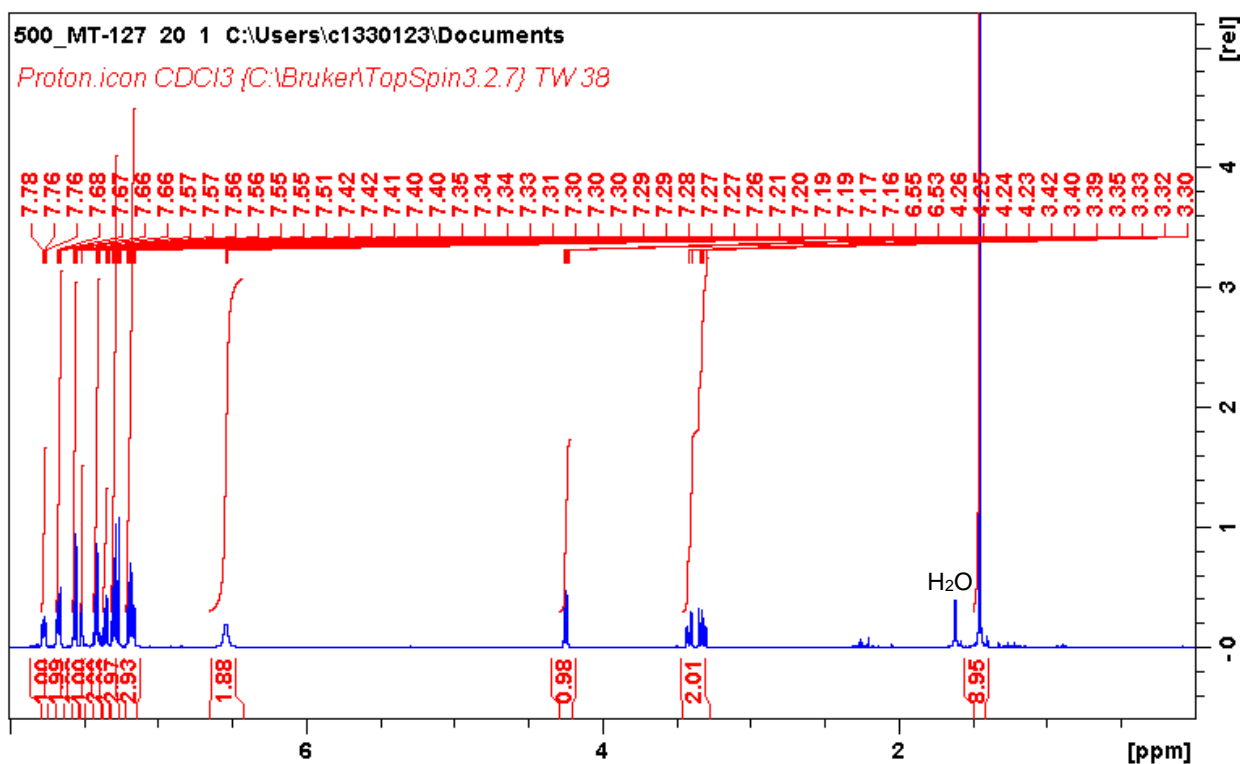
Peak Table

Ret. Time	Area%
5.122	9.676
6.683	90.324
	100.000

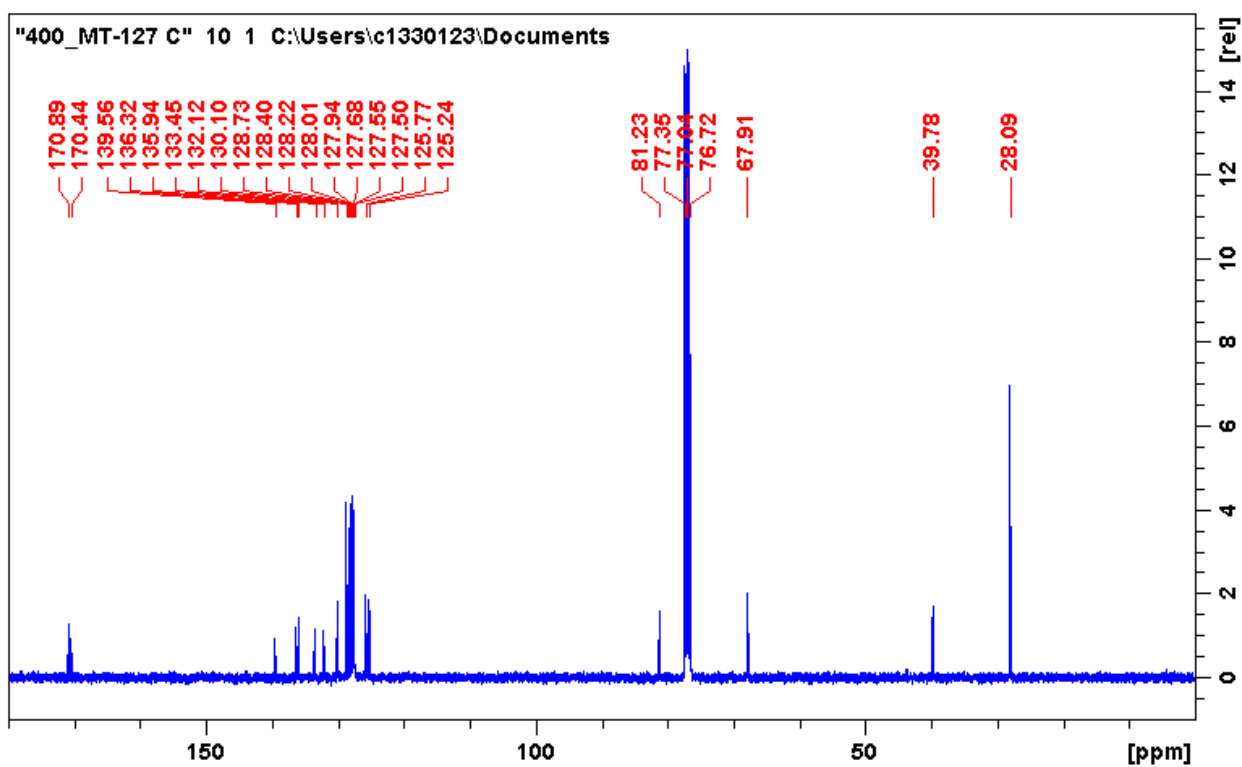
Figure 33: HPLC chromatograms for (28). Racemic mixture (top), chiral catalyzed mixture using catalyst 15 (bottom)

tert-butyl (R)-2-((diphenylmethylene)amino)-3-(naphthalen-2-yl)propanoate (29)

¹H NMR

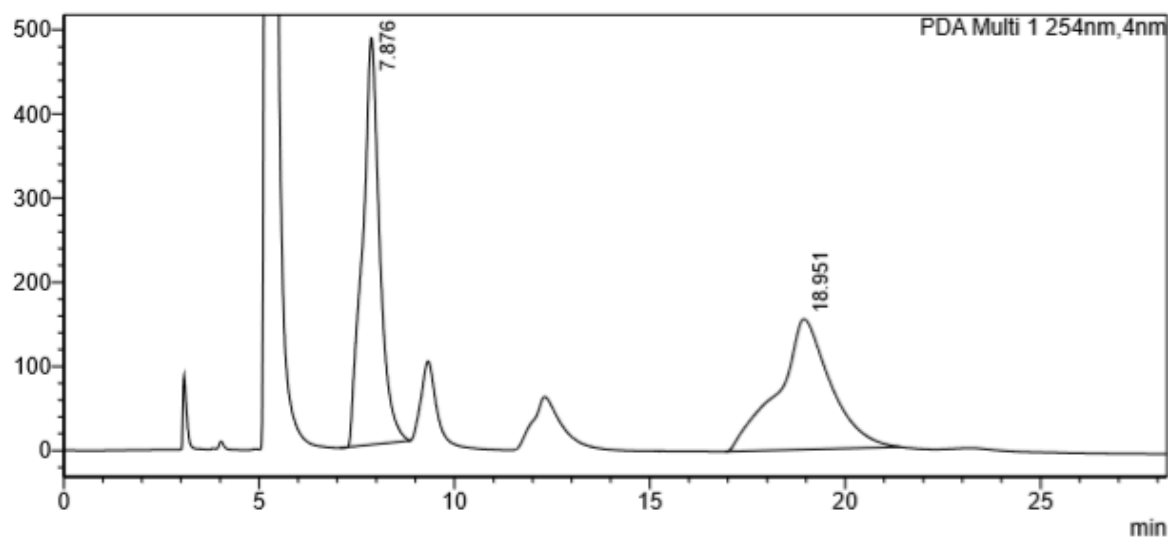


¹³C NMR



<Chromatogram>

mAU

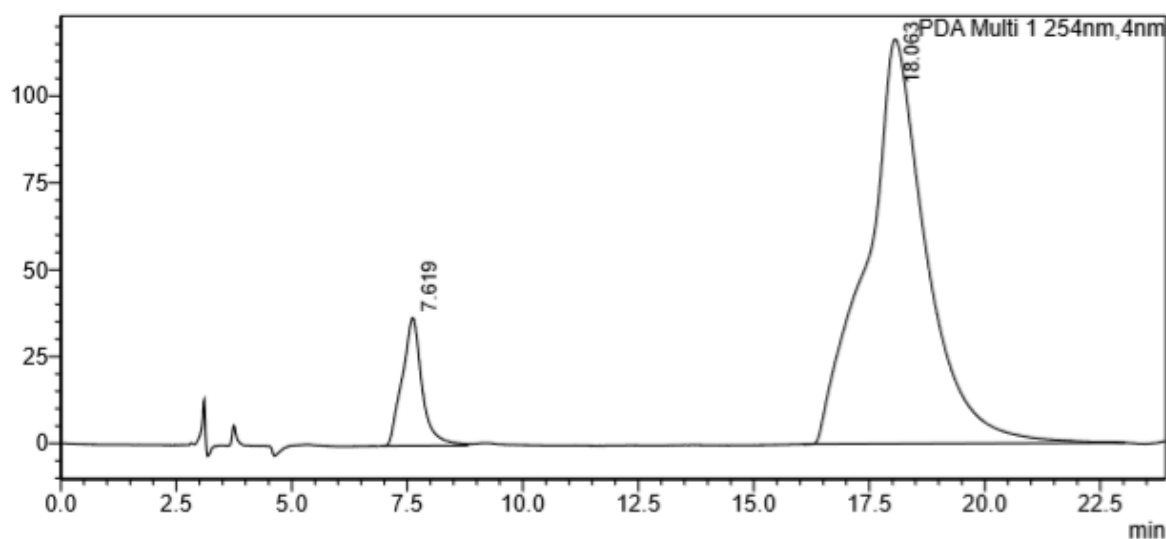


Peak Table
PDA Ch1 254nm

Ret. Time	Area%
7.876	50.281
18.951	49.719
	100.000

<Chromatogram>

mAU



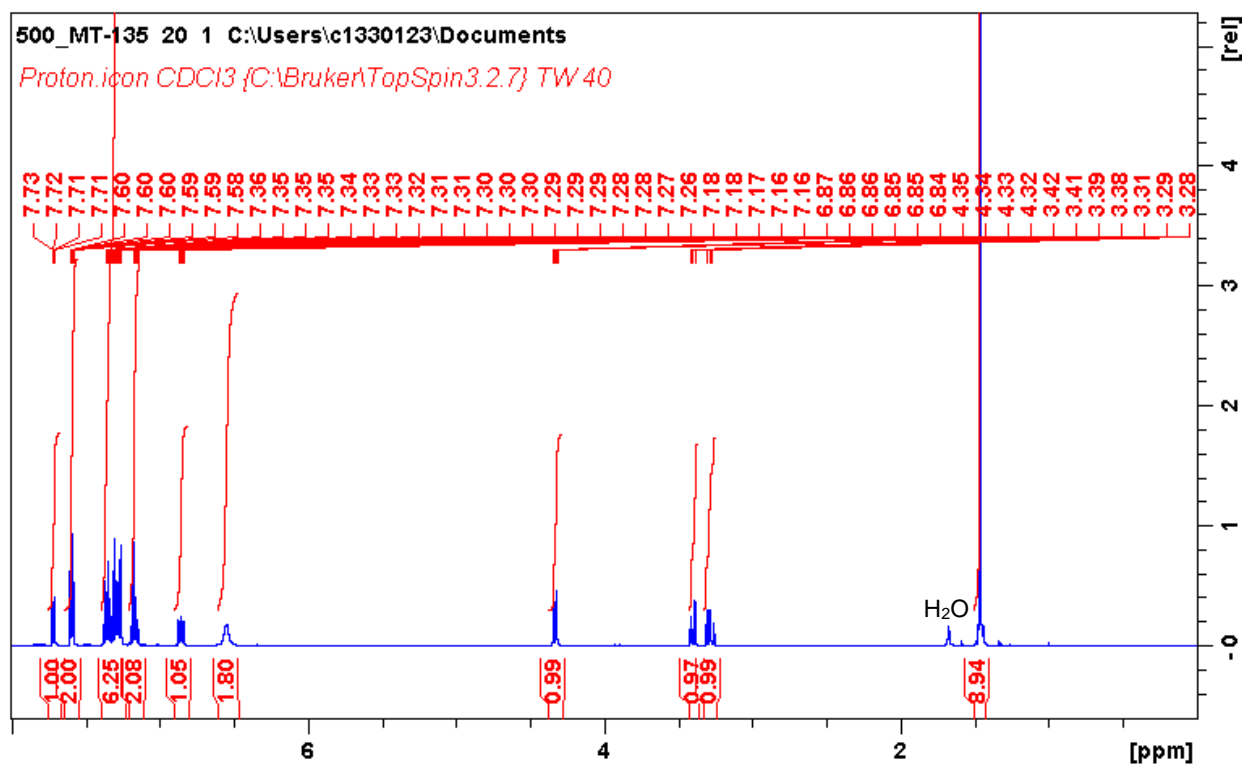
Peak Table
PDA Ch1 254nm

Ret. Time	Area%
7.619	9.570
18.063	90.430
	100.000

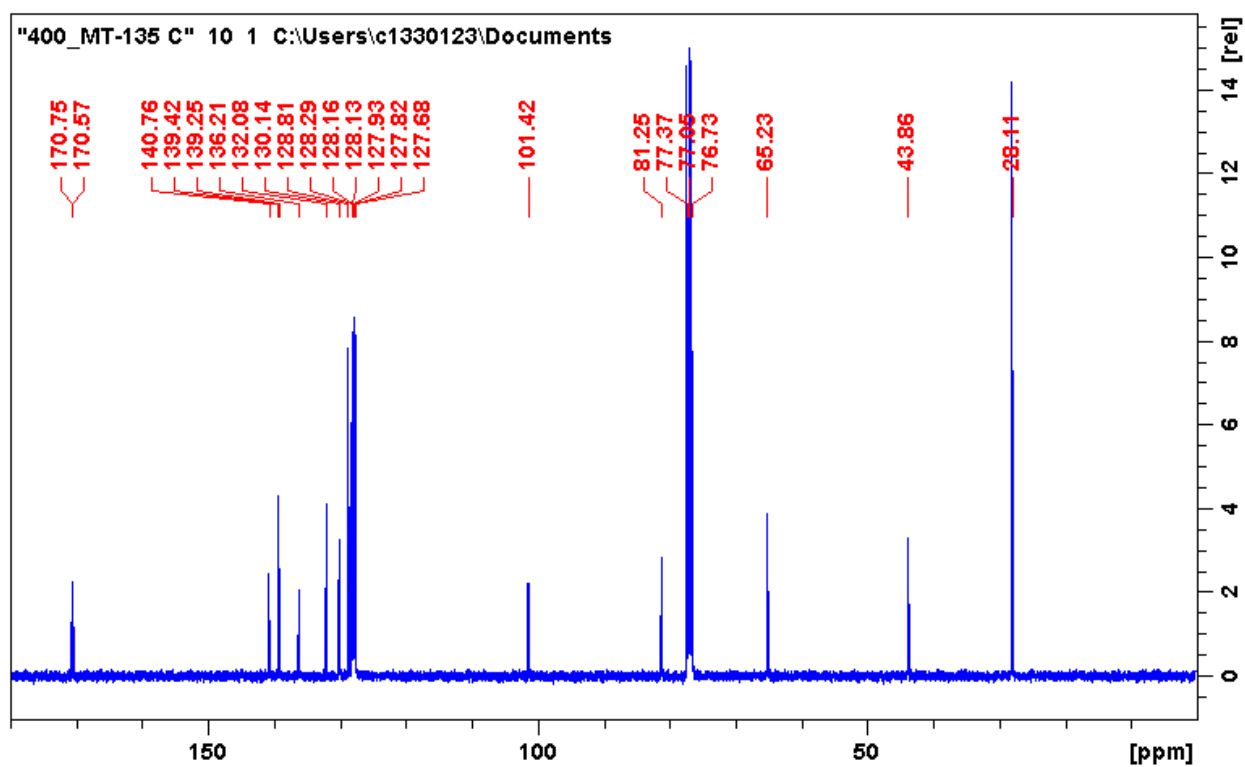
Figure 34: HPLC chromatograms for (29). Racemic mixture (top), chiral catalyzed mixture using catalyst 15 (bottom)

tert-butyl (R)-2-((diphenylmethylene)amino)-3-(2-iodophenyl)propanoate (30)

¹H NMR

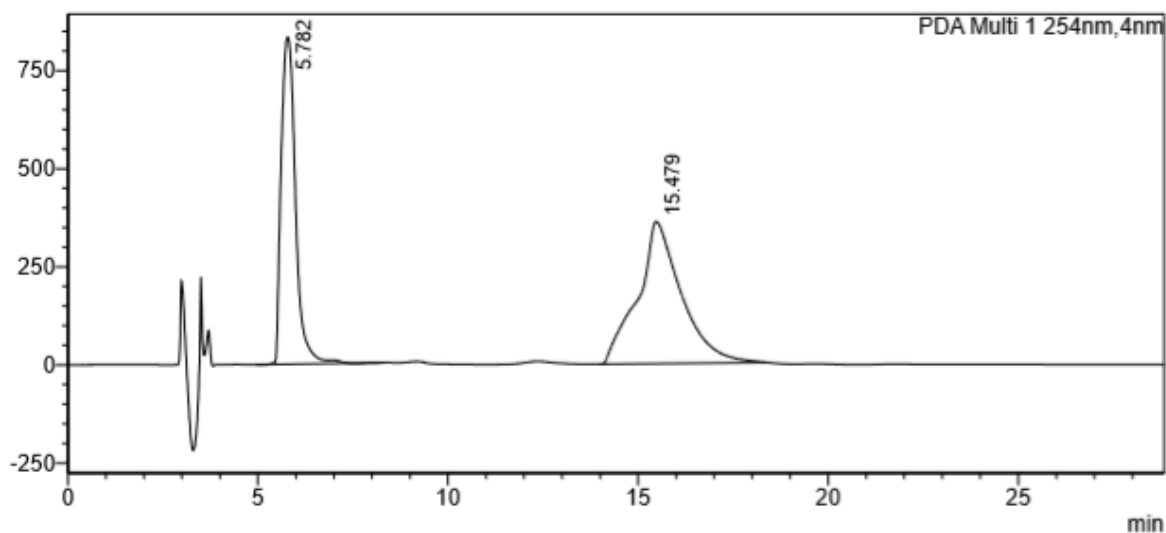


¹³C NMR



<Chromatogram>

mAU

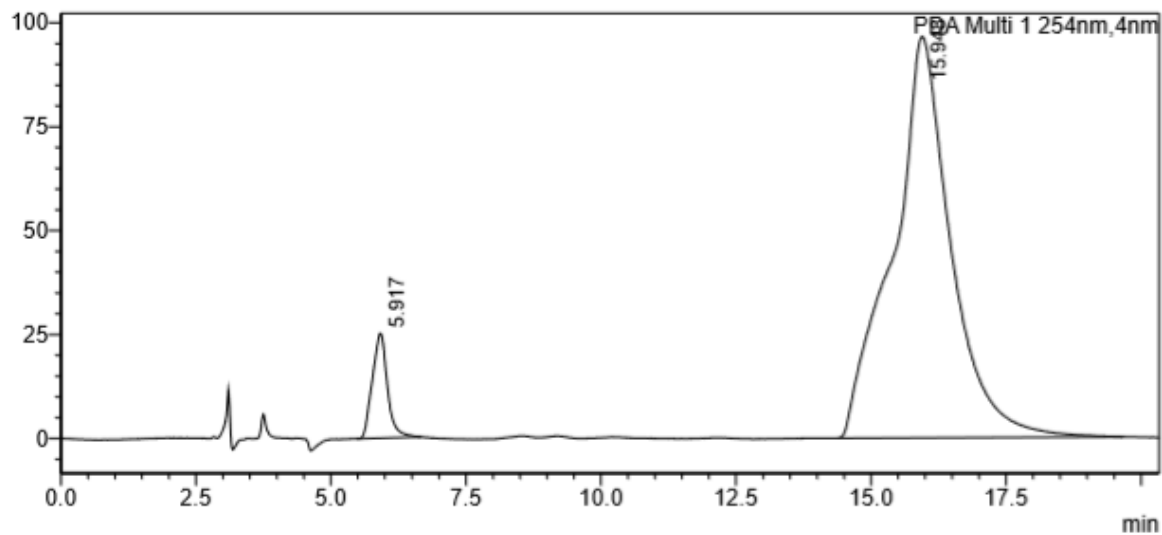


Peak Table
PDA Ch1 254nm

Ret. Time	Area%
5.782	43.036
15.479	56.964
	100.000

<Chromatogram>

mAU



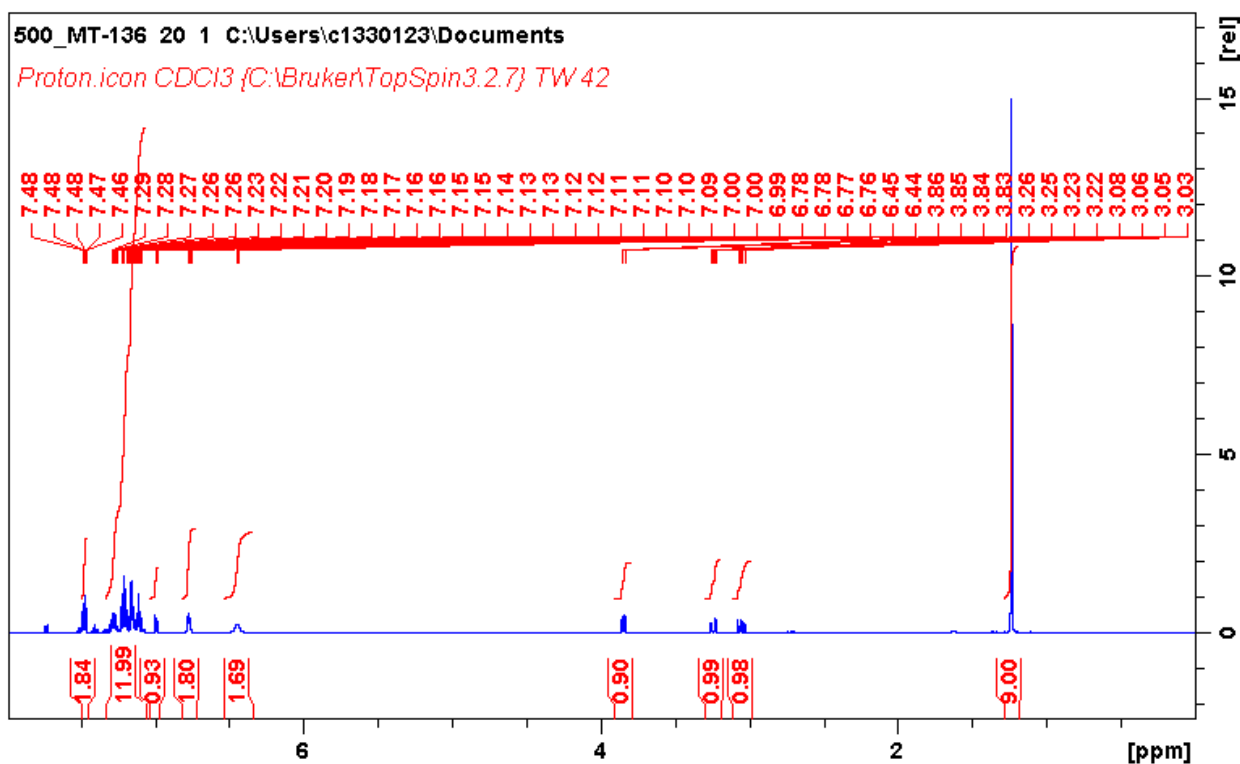
Peak Table
PDA Ch1 254nm

Ret. Time	Area%
5.917	6.367
15.948	93.633
	100.000

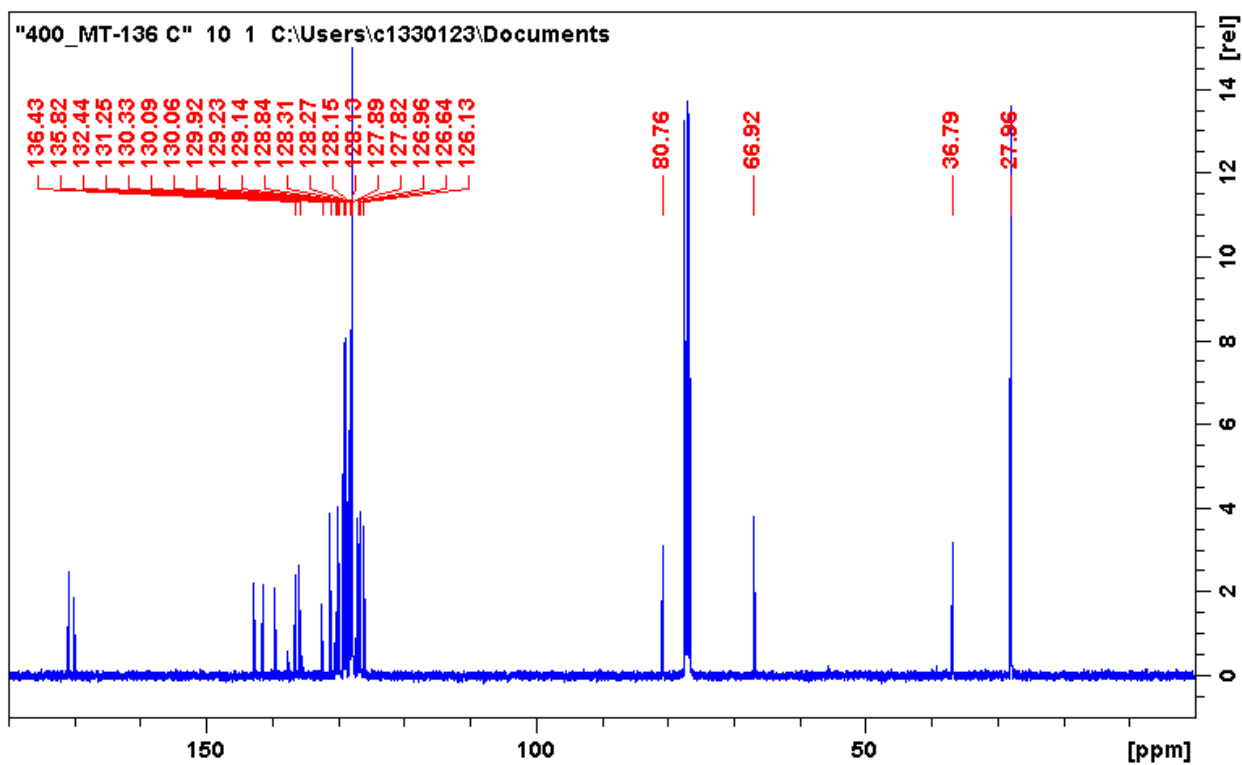
Figure 35: HPLC chromatograms for **(30)**. Racemic mixture (top), chiral catalysed mixture using catalyst **15** (bottom).

tert-butyl (*R*)-3-([1,1'-biphenyl]-2-yl)-2-((diphenylmethylene)amino)propanoate (31)

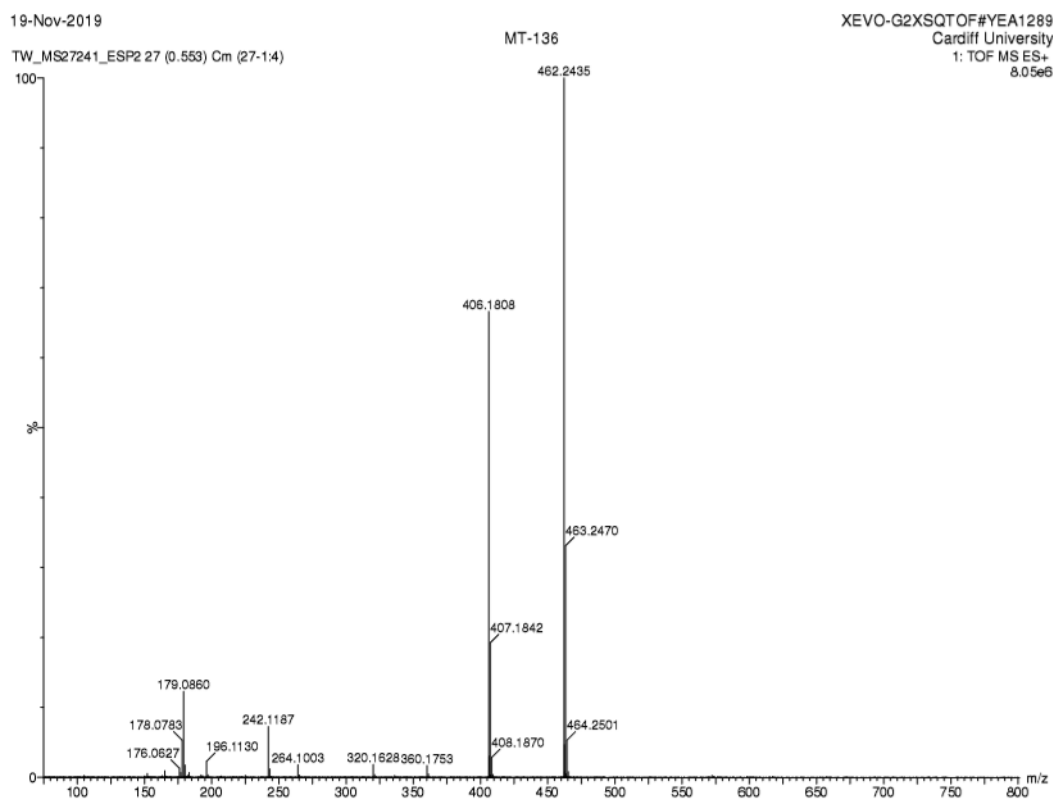
¹H NMR



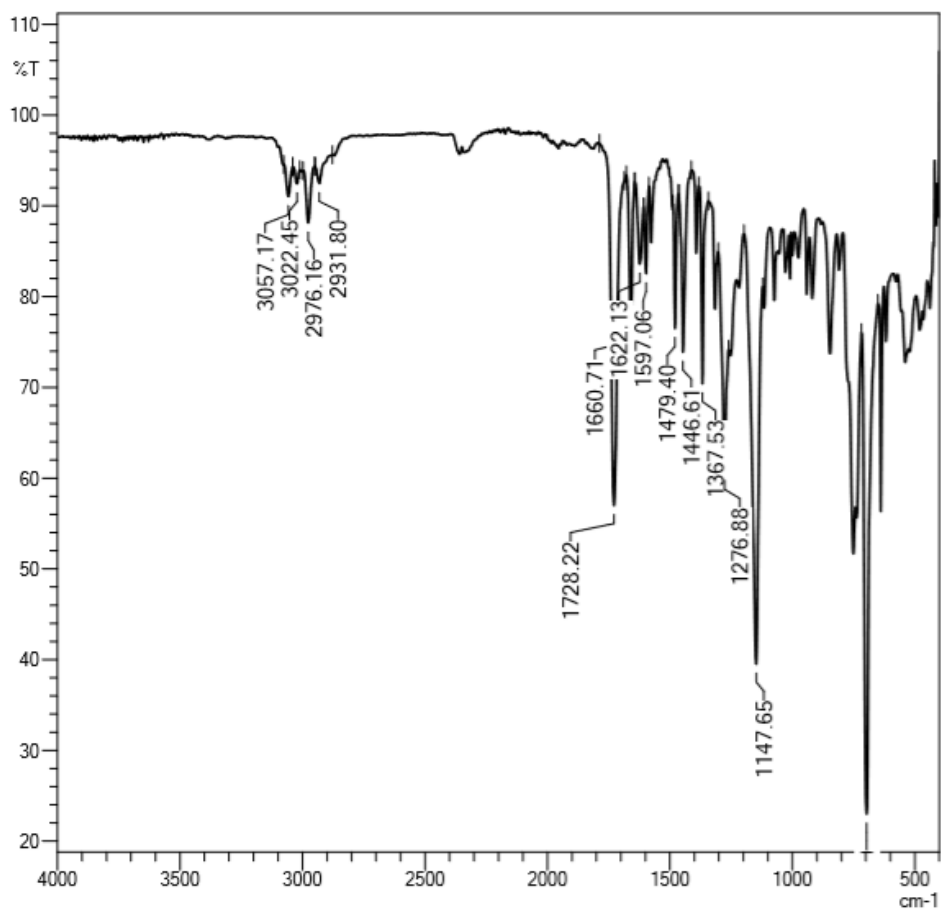
¹³C NMR



HRMS

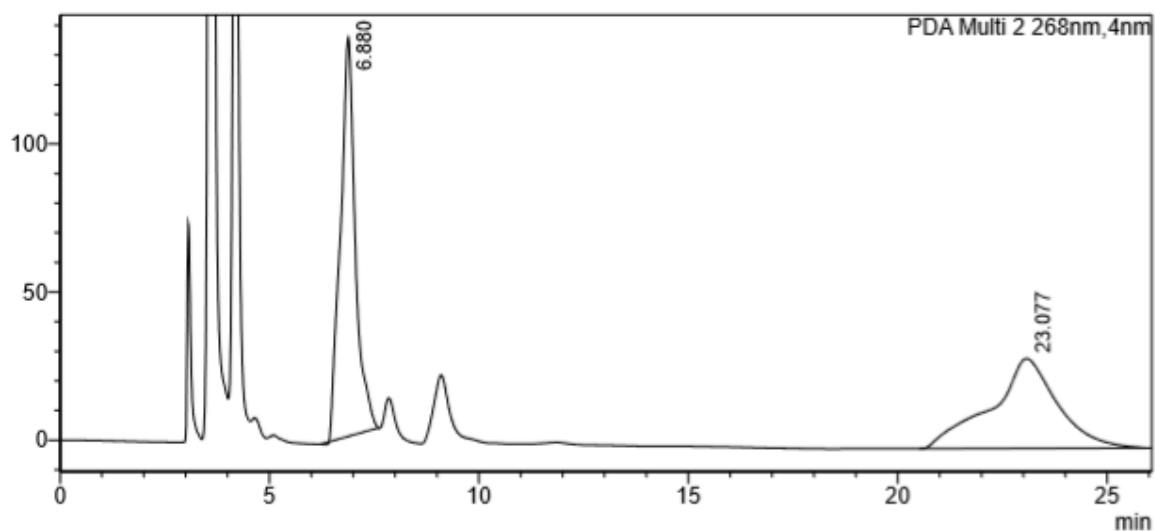


IR



<Chromatogram>

mAU

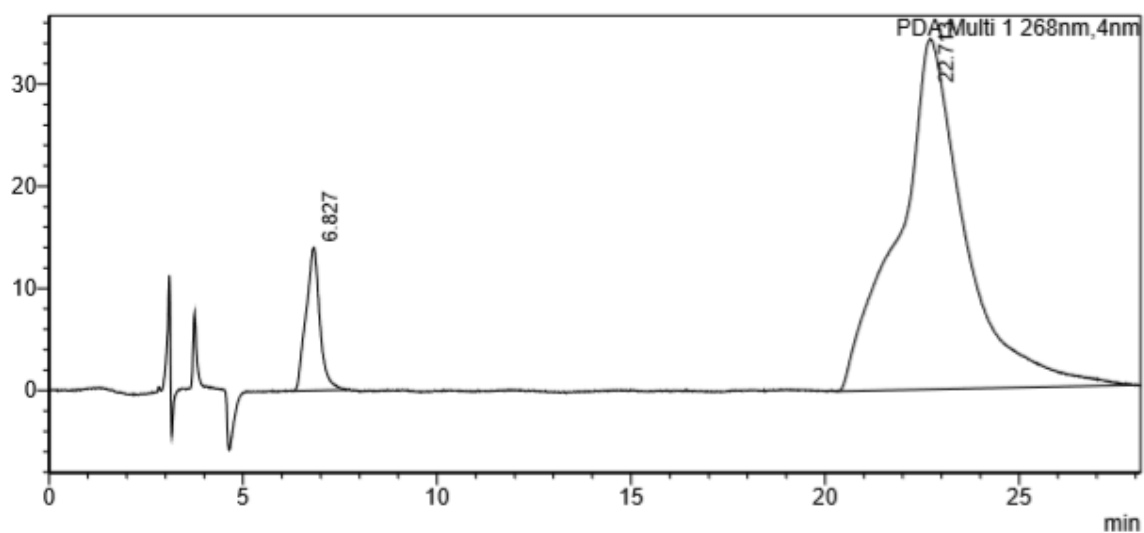


Peak Table
PDA Ch2 268nm

Ret. Time	Area%
6.880	49.976
23.077	50.024
	100.000

<Chromatogram>

mAU



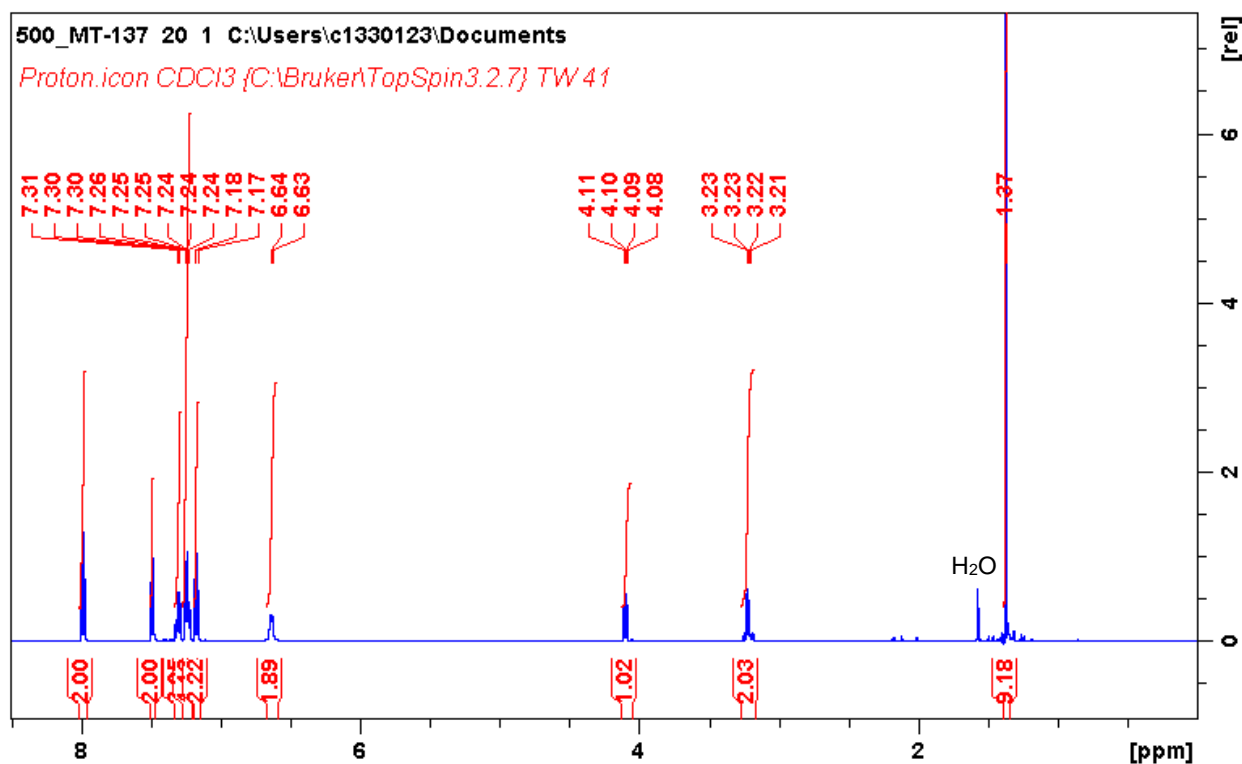
Peak Table
PDA Ch1 268nm

Ret. Time	Area%
6.827	7.793
22.713	92.207
	100.000

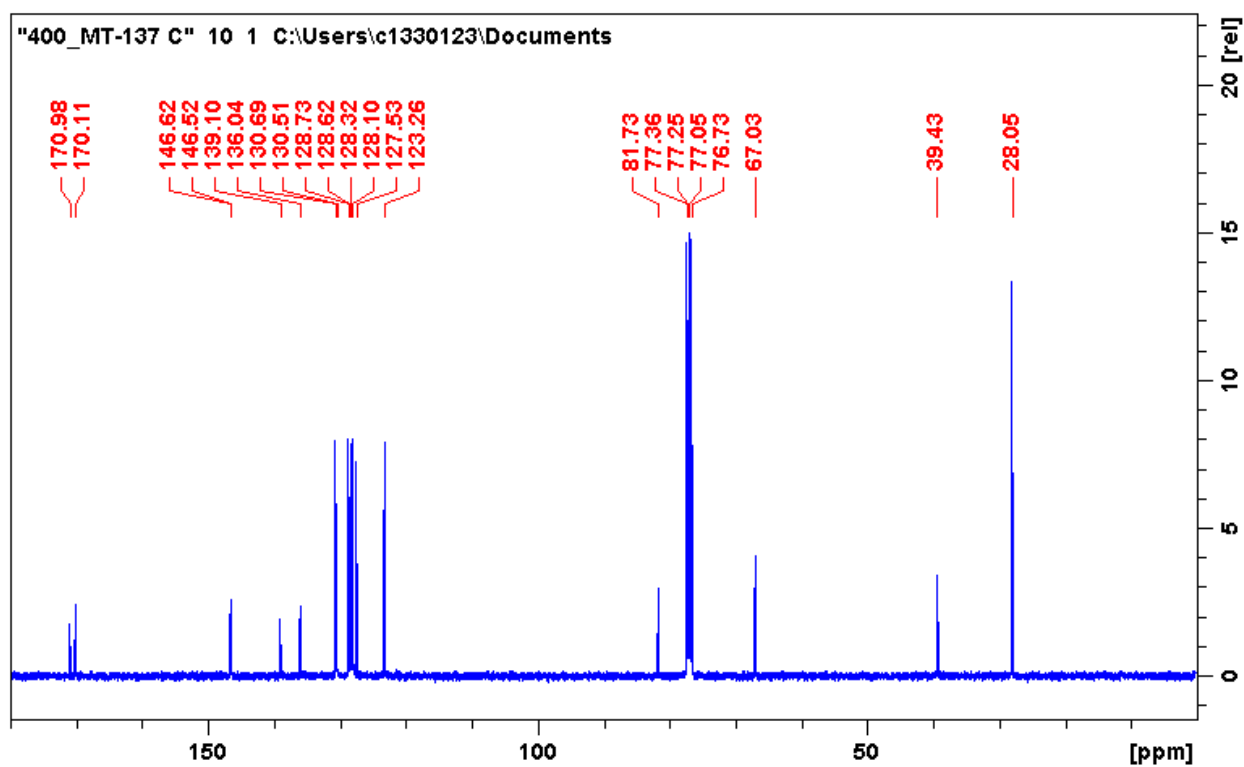
Figure 36: HPLC chromatograms for **(31)**. Racemic mixture (top), chiral catalyzed mixture using catalyst **15** (bottom).

tert-butyl (R)-2-((diphenylmethylene)amino)-3-(4-nitrophenyl)propanoate (32)

¹H NMR



¹³C NMR



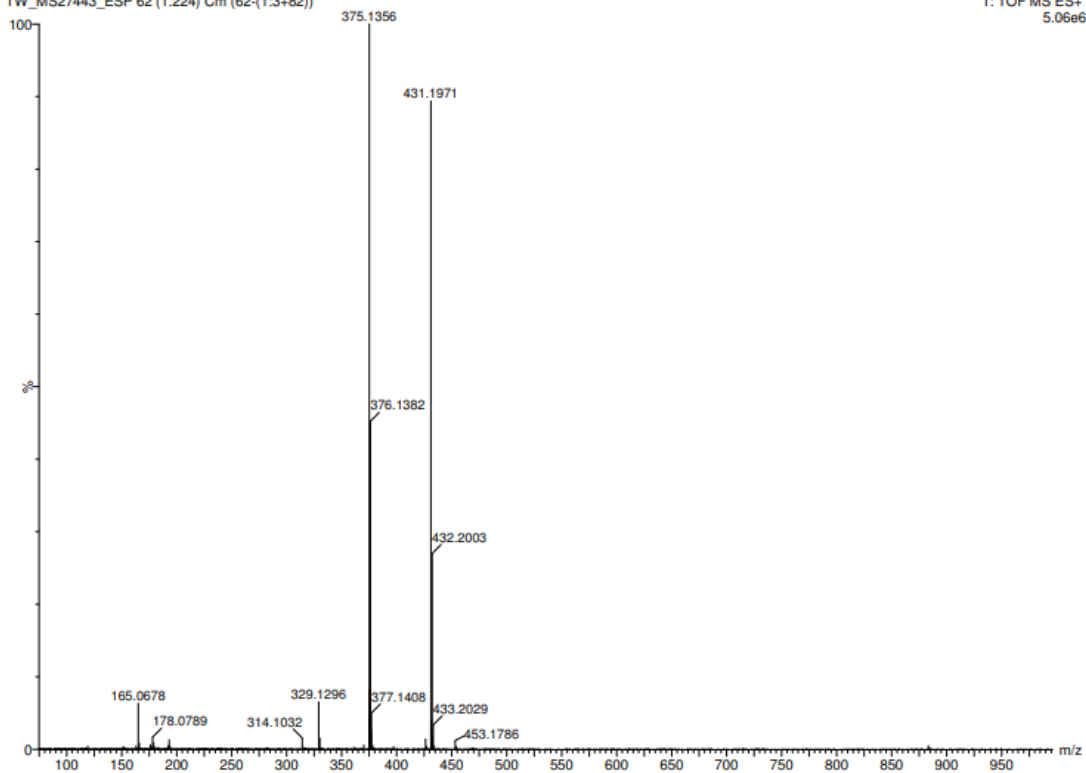
HRMS

10-Dec-2019

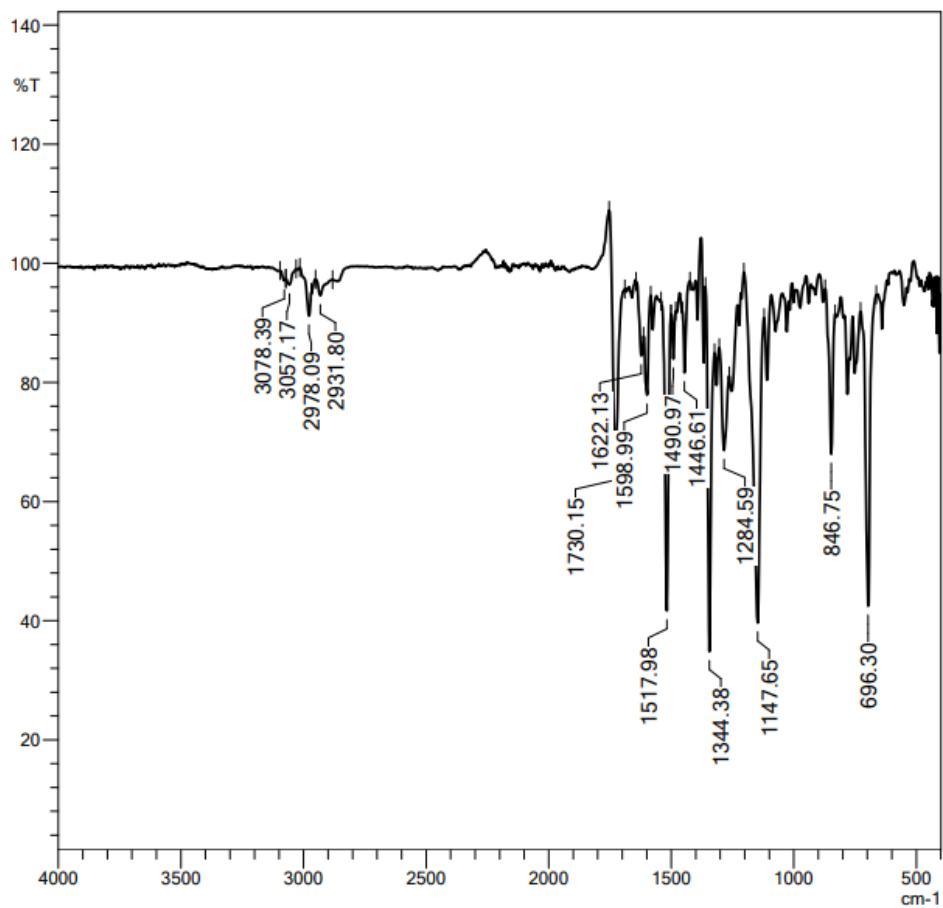
MT-NO2

XEVO-G2XSQTOF#YEA1289
Cardiff University
1: TOF MS ES+
5.06e6

TW_MS27443_ESP 62 (1.224) Cm (62-(1.3+82))

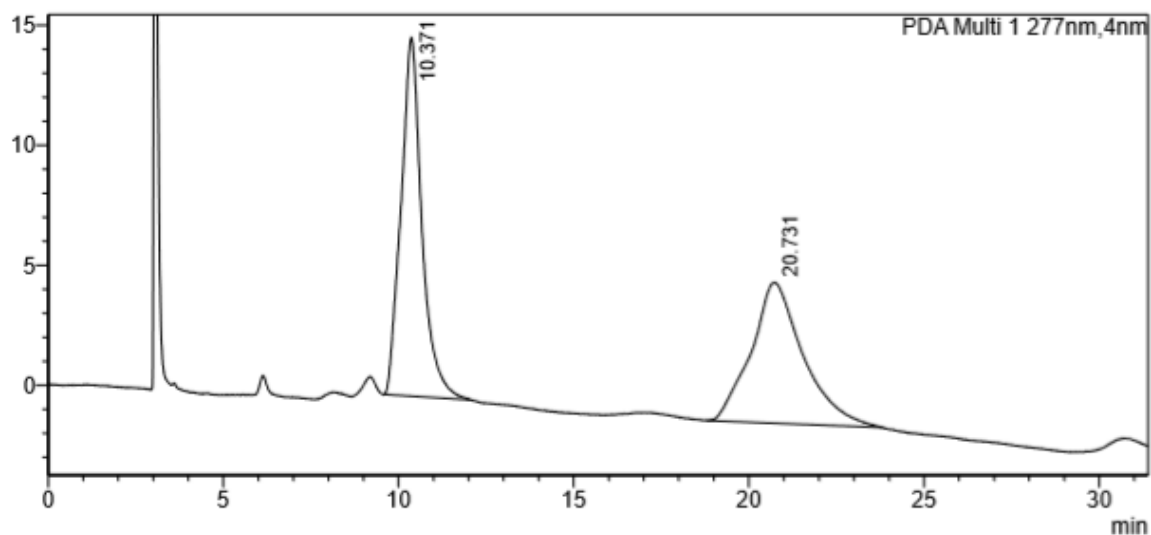


IR



<Chromatogram>

mAU

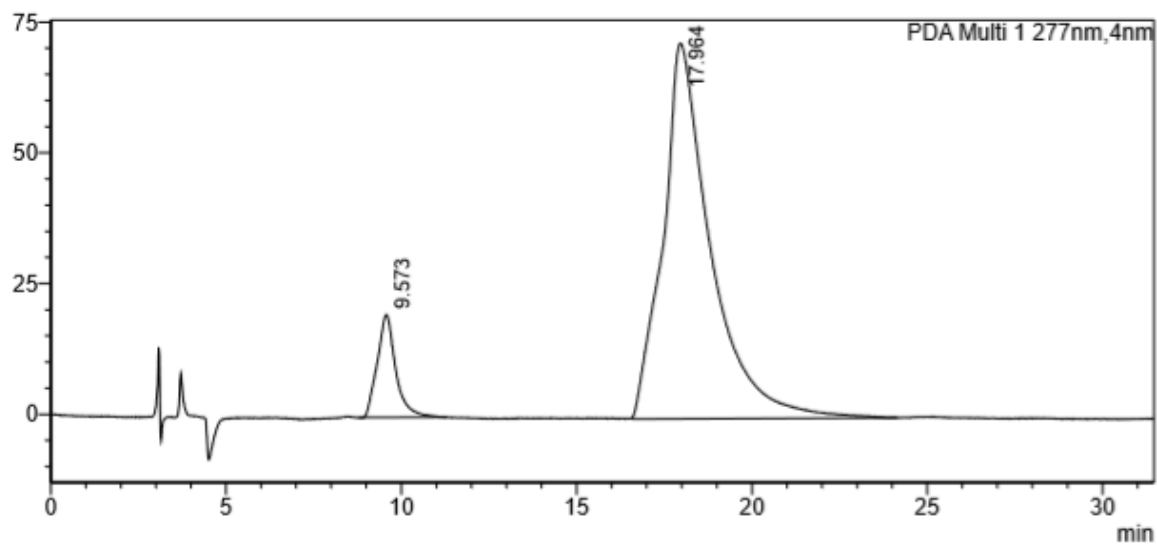


Peak Table
PDA Ch1 277nm

Ret. Time	Area%
10.371	50.506
20.731	49.494
	100.000

<Chromatogram>

mAU



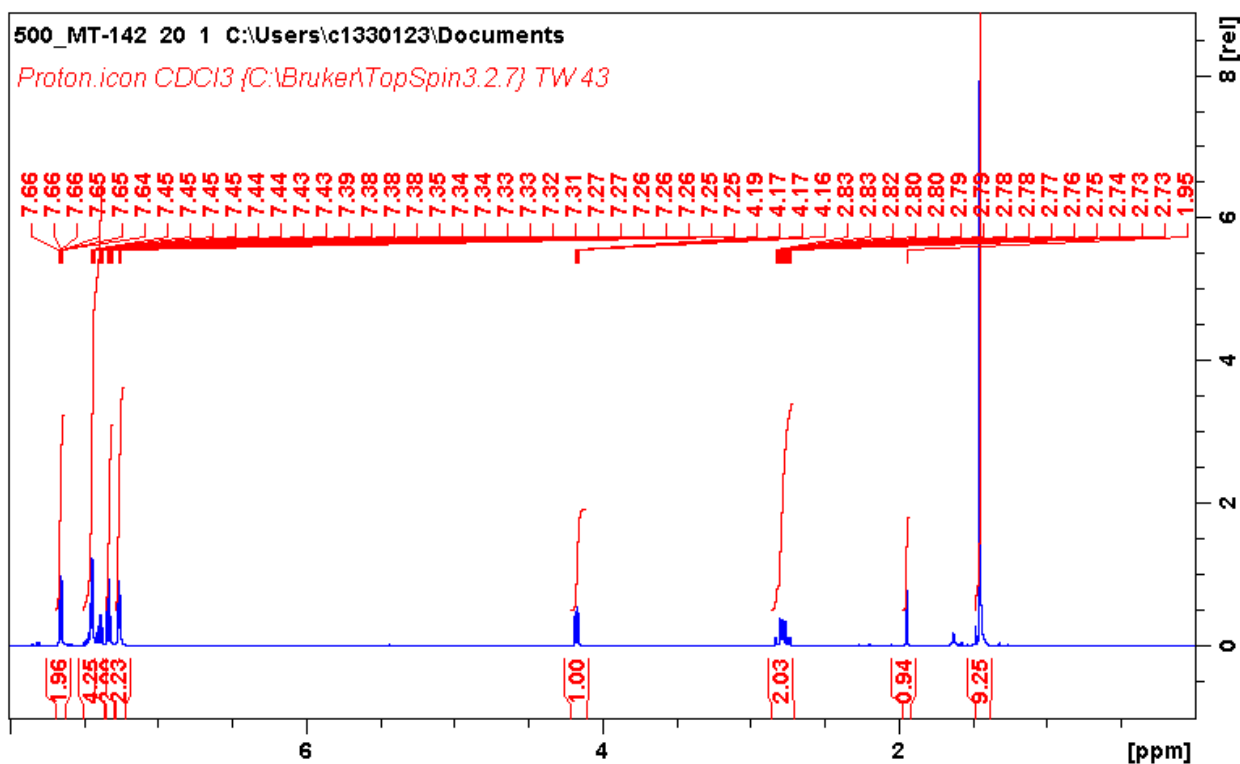
Peak Table
PDA Ch1 277nm

Ret. Time	Area%
9.573	9.657
17.964	90.343
	100.000

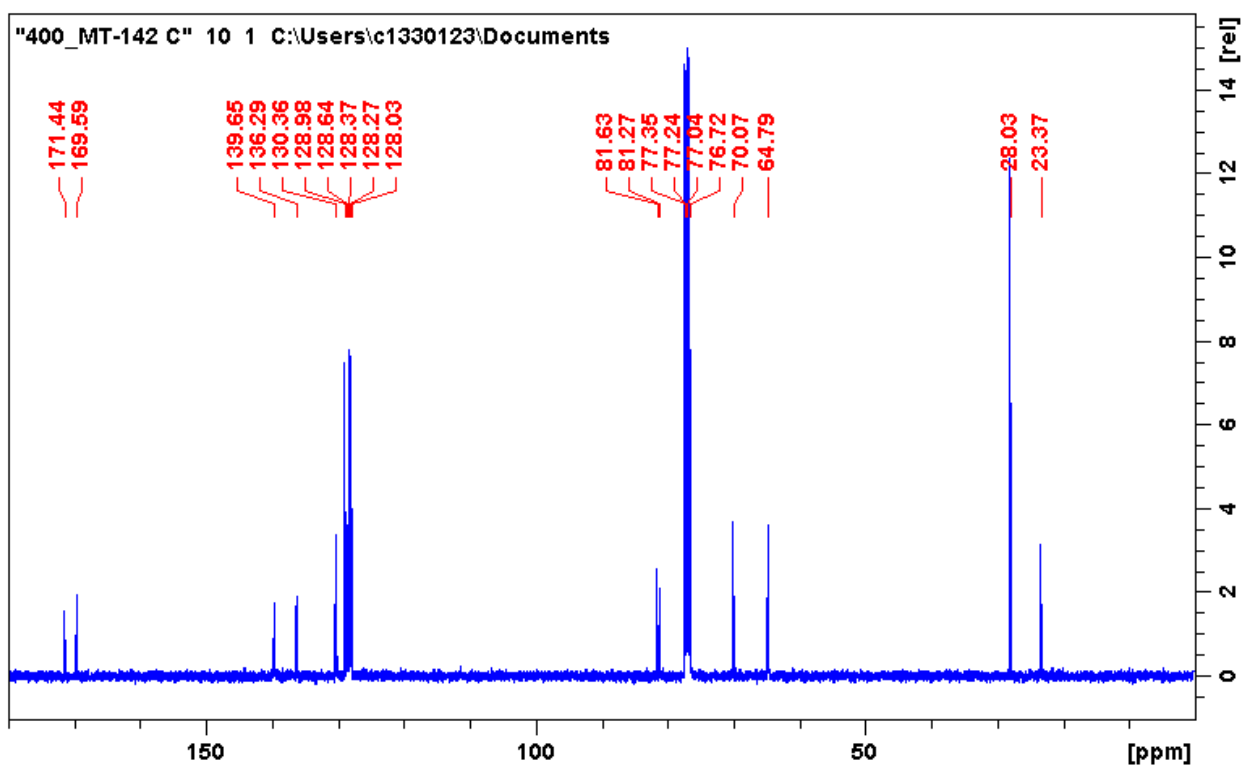
Figure 37: HPLC chromatograms for (**32**). Racemic mixture (top), chiral catalyzed mixture using catalyst **15** (bottom).

tert-butyl (R)-2-((diphenylmethylene)amino)pent-4-ynoate (33)

¹H NMR

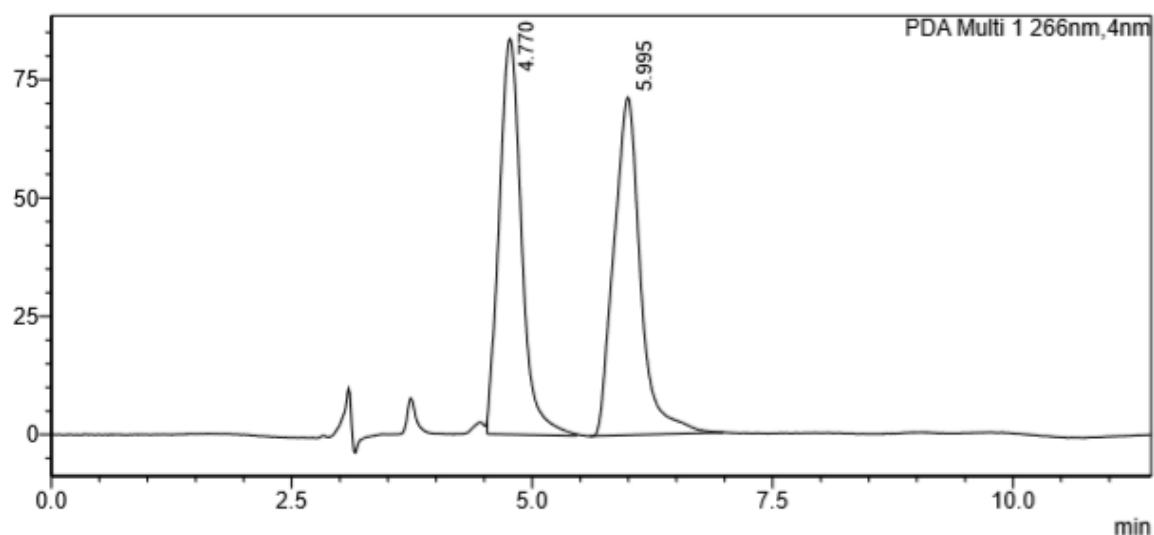


¹³C NMR



<Chromatogram>

mAU

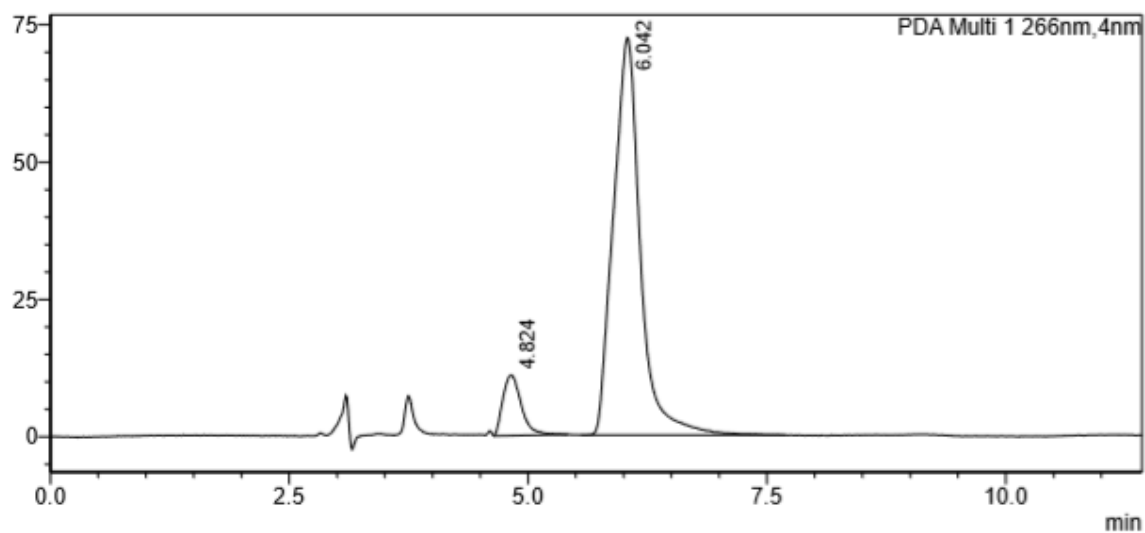


Peak Table
PDA Ch1 266nm

Ret. time	Area%
4.770	49.646
5.995	50.354
	100.000

<Chromatogram>

mAU



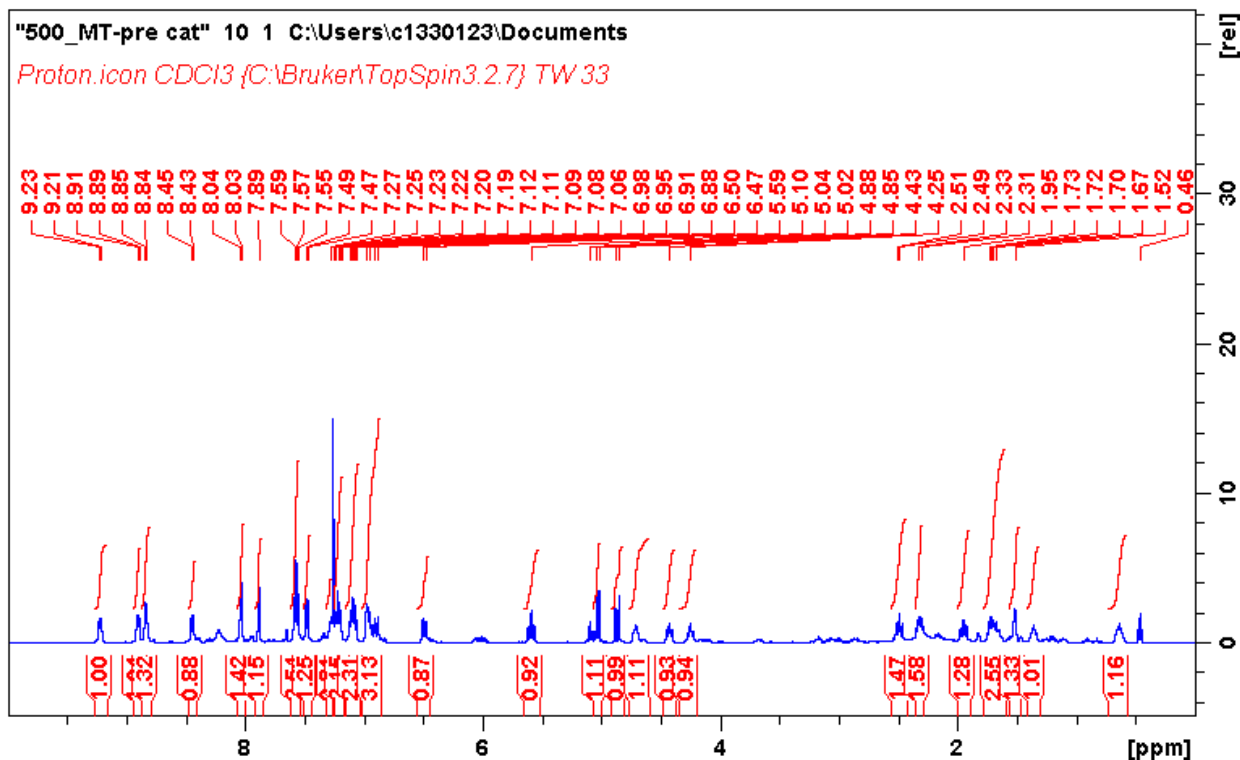
Peak Table
PDA Ch1 266nm

Ret. time	Area%
4.824	9.392
6.042	90.608
	100.000

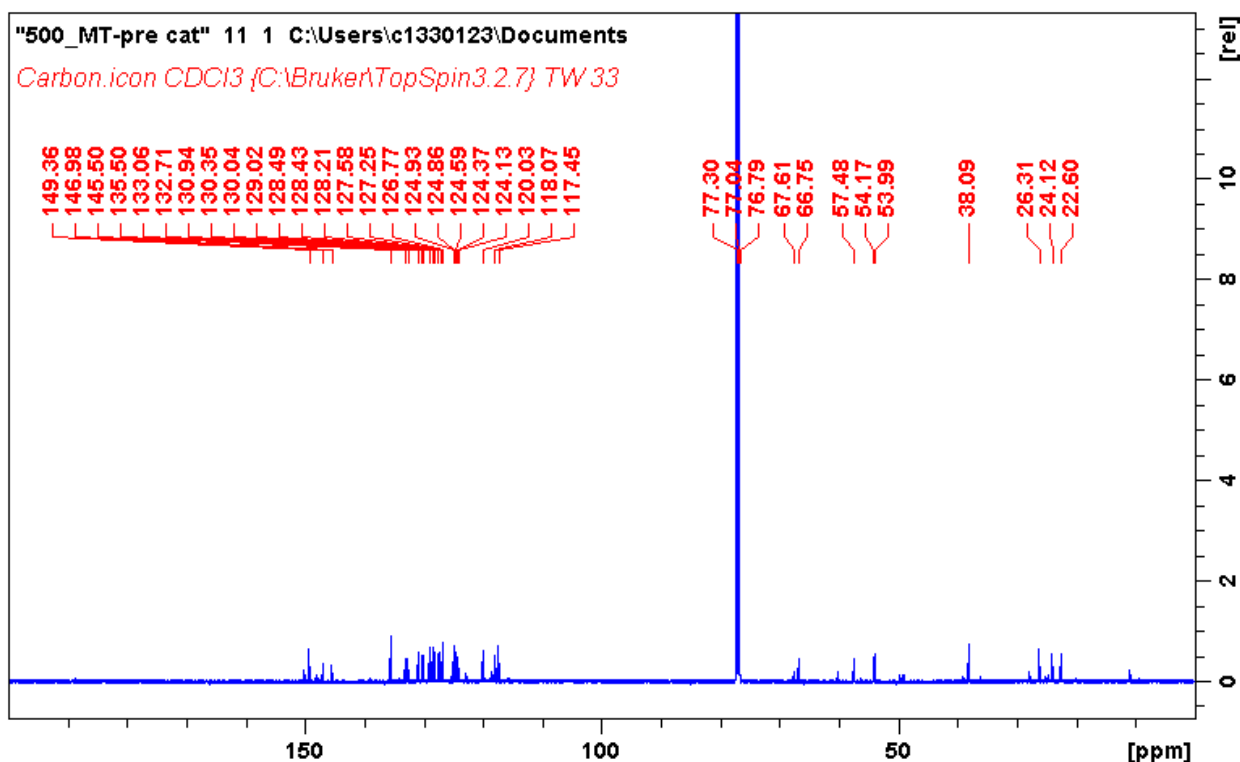
Figure 38: HPLC chromatograms for **(33)**. Racemic mixture (top), chiral catalysed mixture using catalyst **15** (bottom).

(2R, 5R, 1'S)-1-(9-anthracenyl)methyl-5-ethylene-2-[1-hydroxy-1-(quinol-4-yl)]methyl-1-azoniabicyclo[2.2.2]octane chloride (10)

¹H NMR

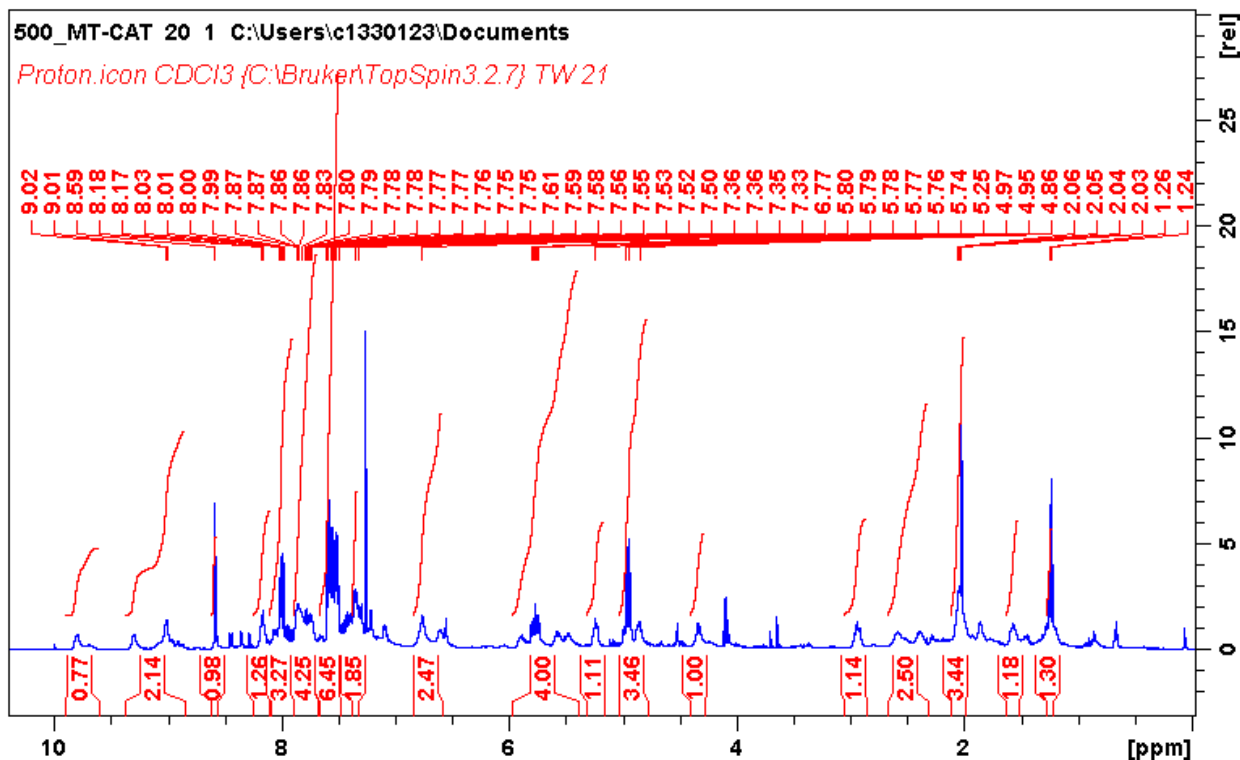


¹³C NMR

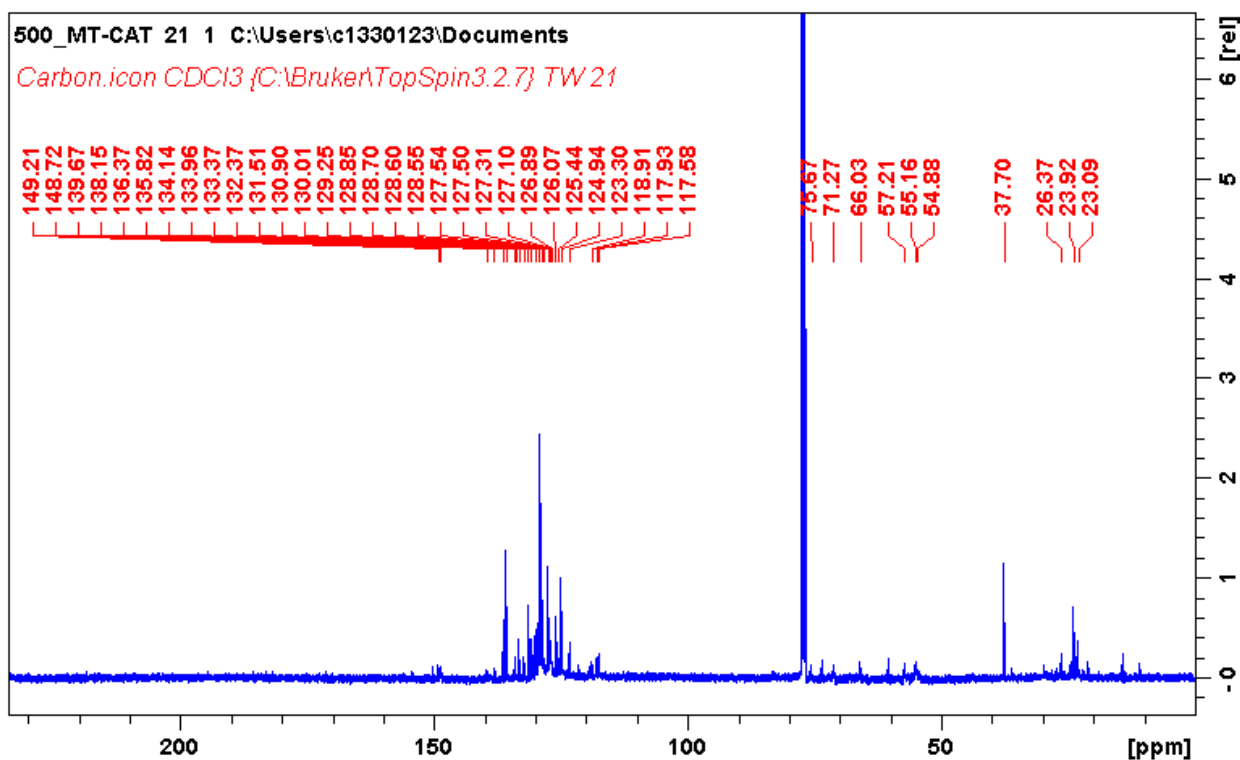


(2R, 5R, 1'S)-1-(1-anthracenyl)methyl-5-ethylene-2-[1-benzyloxy-1-(quinol-4-yl)]methyl-1-azoniabicyclo[2.2.2]octane bromide (15)

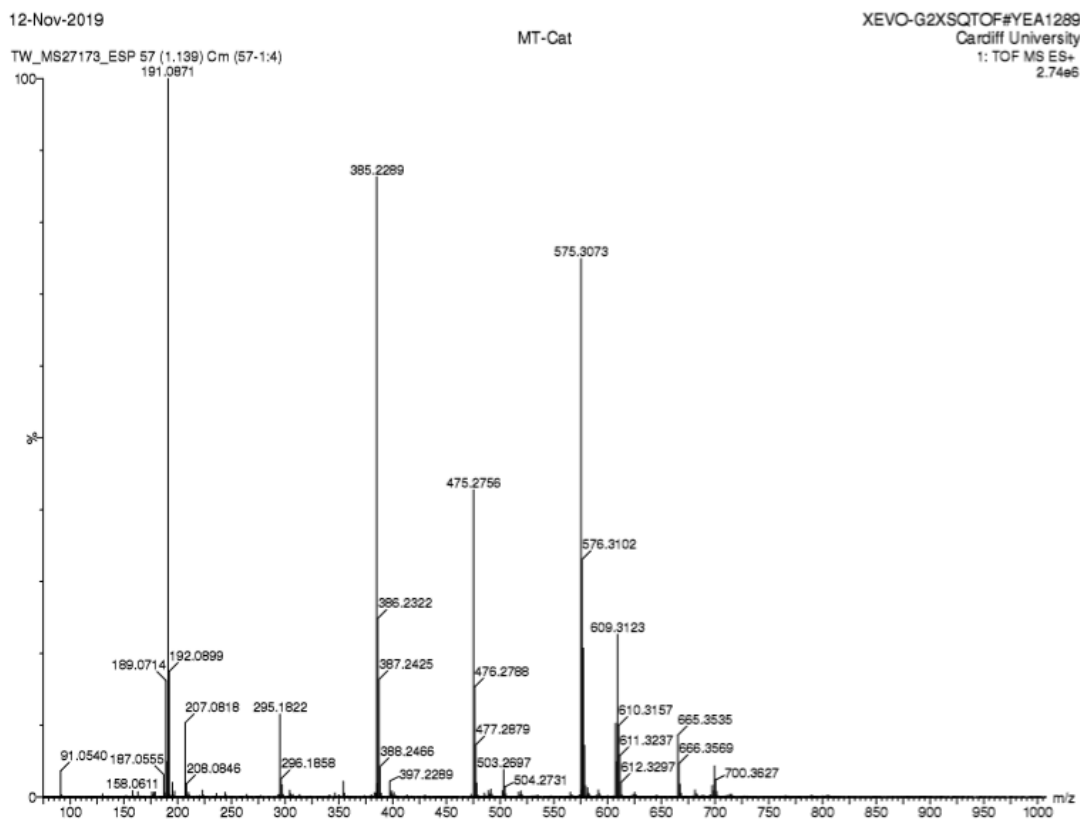
¹H NMR



¹³C NMR

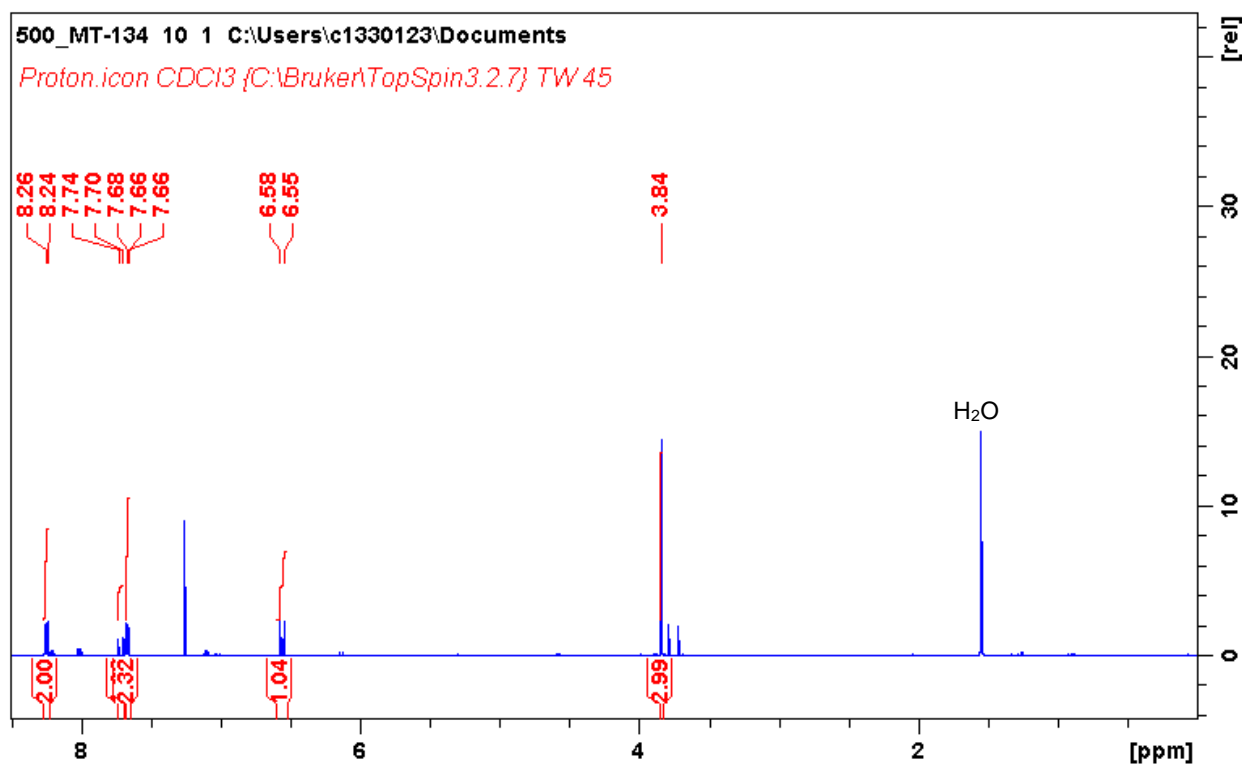


HRMS



methyl (E)-3-(4-nitrophenyl)acrylate (21)

¹H NMR



¹³C NMR

